Motion sickness and rigid body motion of a polar supply and research vessel on voyages to Antarctica and the Southern Ocean

by
Brendan Guy Boullé

Thesis presented in partial fulfilment of the requirements for the degree of Master of Engineering (Mechanical) in the Faculty of Engineering at Stellenbosch University

Supervisor: Dr. A. Bekker

March 2016

Declaration

By submitting this thesis electronically, I declare that the entirety of the work contained therein is my own, original work, that I am the sole author thereof (save to the extent explicitly otherwise stated), that reproduction and publication thereof by Stellenbosch University will not infringe any third party rights and that I have not previously in its entirety or in part submitted it for obtaining any qualification.

Date: March 2016 ....

Abstract

Motion sickness and rigid body motion of a polar supply and research vessel on voyages to Antarctica and the Southern Ocean

B.G Boullé

Thesis: MEng (Mech)

March 2016

Low frequency (0.1 Hz to 0.5 Hz) lateral and vertical motion present on ocean going vessels could cause motion sickness. ISO 2361-1 developed a means to predict motion sickness in the vertical direction, but did not propose a means on incorporating lateral motion. It was also hypothesised that motion on the SA Agulhas II is expected to be either more or less provocative depending on location. A modified six accelerometer array was developed in order to determine the lateral and vertical acceleration levels at any location on board the SA Agulhas II. Vertical acceleration was found vary along the width and length of the SA Agulhas II but was independent of height. Subjective responses of participants were collected from the personal details submission form and daily diary. It was reported that susceptibility towards motion sickness declined with age for the males. Females were found to be more susceptible than males. The percentage of motion sick participants, the percentage of vomiting participants and illness rating ($N = 32$) were correlated using Kendall's rank correlation. The percentage of motion sick participants and illness rating had the highest correlation coefficient (T) of 0.815. Participants spent most their time in the accommodation area, centred around zone D7. Daily maximum 6 h motion sickness dose values were determined at all locations on board the SA Agulhas II using vertical and lateral weighting filters for motion sickness. Illness rating correlated the best with both $MSDV_{x,6h}$ and $MSDV_{z,6h}$. Linear and multiple non-linear regression analysis was used to determine the effects each direction, at zone D7, has on motion sickness. Motion in y-axis was determined to be insignificant. However multicollinearity was identified between x- and z-axis motion, which made determining the effects of each direction impossible. The contribution of each axis was then assumed to be the same and a linear regression model was developed to predict illness rating ($R^2 = 0.417$).

Uittreksel

Rysiekte en starre liggaam beweging van 'n polêre vooraad en navorsing skip op reise na Antarktika en die Suidelike Oseaan

("Motion sickness and rigid body motion of a polar supply and research vessel on voyages to Antarctica and the Southern Ocean")

B.G Boullé

Tesis: MIng (Meg)

Maart 2016

Lae frekwensie (0.1 Hz tot 0.5 Hz) laterale en vertikale beweging teenwoordig see gaande vaartuie kon rysiekte veroorsaak. ISO 2361-1 ontwikkel 'n manier om rysiekte in die vertikale rigting te voorspel, maar nie 'n manier om laterale beweeging voor te stel en inkorporeer nie. Dit is ook veronderstel dat beweging op die SA Agulhas II na verwagting, meer of minder uitdagend sal wees, afhangende van die ligging. 'n Aangepaste ses verskeidenheid versnellingsmeter is ontwikkel om die laterale en vertikale versnelling te bepaal op enige plek aan boord op die SA Agulhas II. Daar is gevind dat die vertikale versnelling wissel langs die breedte en lengte van die SA Agulhas II, maar was onafhanklik van die hoogte. Subjektiewe responsie van deelnemers is ingesamel uit die persoonlike besonderhede voorlegging vorm en daaglikse dagboek. Dit is berig dat vatbaarheid teenoor rysiekte afneem met die ouderdom vir die mans. Vroue is gevind meer vatbaar as mans. Die persentasie van rysiekte deelnemers, die persentasie van braakinde deelnemers en siekte beoordeling ($N = 32$), is gekorreleer met behulp van Kendall se rang korrelasie. Die persentasie van rysiek deelnemers en siekte gradeering het die hoogste korrelasie koëffisiënt (T) van 0.815. Deelnemers het die meeste van hul tyd in die akkommodasie area, gesentreer rondom sone D7. Daaglikse maksimum 6 uur rysiekte dosis waardes is bepaal op alle plekke aan boord die SA Agulhas II met die gebruik van die vertikale en laterale gewig filters vir rysiekte. Siekte gradeering korreleer die beste met beide $MSDV_{x,6h}$ en $MSDV_{z,6h}$. Lineêre en verskeie nie- lineêre regressie-analise is gebruik om die efekte te bepaal in elke rigting, by sone D7, op rysiekte. Beweging in y-as is gering bepaal te wees. Maar, multikollineariteit is geïdentifiseer tussen z- en z-as beweging, wat die bepaling van die gevolge van elke rigting onmoontlik maak. Die bydrae van elke as is dan aanemende om dieselfde te wees en 'n lineêre regressiemodel is ontwikkel om siekte gradering te voorspel ($R^2 = 0.417$).

Acknowledgements

Working on the SA Agulhas II these past two years has been an honour. During the long voyages and conferences I have had the opportunity to meet various people who have made impacts in my life and contributions towards this project.

I would like to express my gratitude towards the members of the Sound and Vibration Research Group (SVRG) of Stellenbosch University for contributing towards the measurement plans, podcast videos, questionnaires and the instrumentation of the SA Agulhas II. In particular I would like to thank Keith Soal, Kim McMahon, Rosca de Waal, Hamza Omar and Fourie Gildenhuys although he was not part of the research group for their contributions towards this project. I would also like to thank my supervisor Dr Annie Bekker for her support and advice. This acknowledgement also goes out the Department of Environmental Affairs of South Africa and Smit Vessel Management Services for allowing the SVRG to participate in voyages to Antarctica and Marion Island as well as support during the instrumentation of the SA Agulhas II. I would also like to acknowledge and thank the National Research Foundation and Department of Science and Technology under the South Africa Antarctic Programme for funding the project. I would like to thank consortium members STX Finland, Aalto University, the University of Oulu, Aker Arctic, Rolls-Royce, Finish Metrology Institute, DNV and Wärtsilä. Lastly I would like to thank my my brother Anthony, my father Maurice and my mother Lindie for their support.

Dedications

This thesis is dedicated to my brother Anthony, my father Maurice and my mother Lindie.

Contents

List of Figures

List of Tables

Nomenclature

Variables

A	Acceleration
IR	Illness rating
$MSDV$	Motion sickness dose value
PV	Precent vomiting
W_f	Lateral weighting motion sickness filter
r	Position
ω	Angular velocity
α	Angular acceleration

Vectors and Tensors

$\ddot{\boldsymbol{A}}_p$	Acceleration of Point p on a fixed body
$\ddot{\boldsymbol{R}}$	Linear acceleration at the origin of a fixed body
$(\boldsymbol{a}_{P/O'})_r$	Acceleration of Point p relative to the body-fixed frame
$\boldsymbol{r}_p$	Position vector of Point p from the origin of the body-fixed frame
$(\boldsymbol{v}_{P/O'})_r$	Velocity of Point p relative to the body-fixed frame
$\boldsymbol{\omega}$	Angular velocity
$\boldsymbol{\alpha}$	Angular acceleration

Subscripts

P	Point P = 1, 2, 3, ..., n
x	x-axis
y	y-axis
z	z-axis

Abbreviations and acronyms

CF Crest Factor

CMU Central Measurement Computer

CTD Conductivity, Temperature and Depth

DC Direct Current

DCO Departmental Co-ordinator

DEA Department of Environmental Affairs

DNV Det Norske Veritas

FIR Finite Impulse Response

ICP Integrated Circuit Piezoelectric

IIR Infinite Impulse Response

IR Illness Rating

ISO International Standard Organization

MS Motion Sickness

MSDV Motion Sickness Dose Value

MSI Motion Sickness Incidence

OMA Operational Modal Analysis

PSD Power Spectral Density

PV Percentage Vomiting

RBM Rigid Body Motion

SAAII SA Agulhas II

SANAP South African National Antarctic Program

SCADAS Supervisory Control and Data Acquisition Systems

SVRG Sound and Vibration Research Group

UCTD Underway Conductivity, Temperature and Depth

UTC Coordinated Universal Time

XBT Expendable Bathy Thermograph

Chapter 1

Introduction

The Sound and Vibration Research Group (SVRG) of Stellenbosch University belongs to a consortium which consists of the following partners; Department of Environmental Affairs (DEA) of South Africa, SMIT Vessel Management Services, STX Finland, Aalto University, the University of Oulu, Aker Arctic, Rolls-Royce, Finish Metrology Institute, DNV and Wärtsilä. The aim of the consortium was to create a scientific basis for the design of ice vessels (such as the SA Agulhas II (SAAII) shown in Figure 1.1) with regards to the ship hull, propulsion, power requirements and comfort for passengers and crew members on board the SAAII. The SVRG has been involved in six full scale measurements on board the SAAII, three of these were on relief voyages to Antarctica, two were on voyages to Marion Island and one was during ice trials in the Baltic Sea.

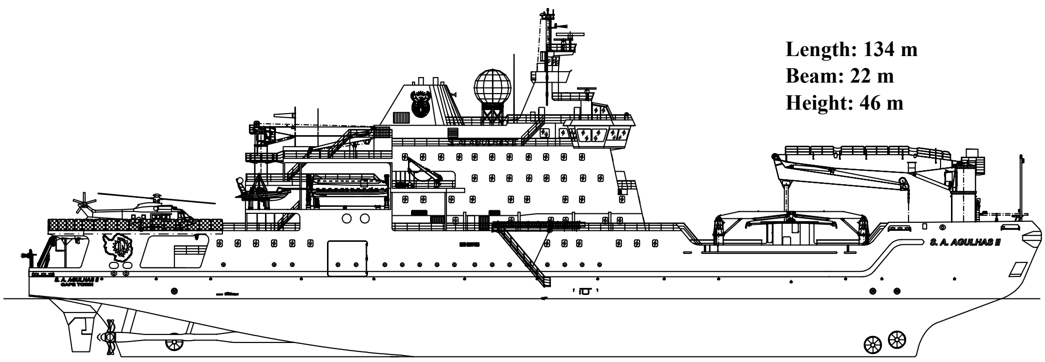

Figure 1.1: SA Agulhas II a polar supply and research vessel

The role of the SVRG was to investigate the comfort of passengers and crew members on board the SAAII. The SVRG focused its research on the effects of vibration on the effects of vibration on human comfort and later expanded to the effects of vibration on the structural integrity of the SAAII particularly in ice and open water. The evaluation of vibration is divided up into two sections according to ISO 2631-1 (1997); motion sickness (0.1 Hz to 0.5 Hz), human comfort and health (1 Hz to 80 Hz).

Motion sickness is influenced by intra- and inter-subject variability as well as various effects of motion such as; age, gender, health, history of motion sickness, frequency, direction, magnitude, duration and phase. Understanding these effects could assist engineers in reducing the occurrence of motion sickness during the design stage of ocean vessels, navigation of the ship in open water and cabin allocation of passengers or crew.

1.1 Motivation

Motion sickness has the ability to physically and psychologically affect humans and animals. Signs and symptoms, described by Griffin (1990), associated with motion sickness are; stomach awareness, nausea, vomiting, lack of motivation, depression, tension, anxiety, yawning, drowsiness, dizziness, faintness, feelings of vertigo, headaches, irregularities in breathing, sensations of warmth, sweating, aches and lower back pain. These symptoms can reduce productivity or even disable a person for a few days. Hence the motivation into investigating motion sickness on board the SA Agulhas II ship motion. Furthermore, standards such as ISO 2631-1 (1997) which assess motion sickness are limited to the vertical direction for seated and standing persons. More recent studies by Donohew and Griffin (2004) have shown that lateral motion is a contributor to motion sickness.

A field study on the SAAII creates the potential to understand if the inclusion of lateral motion with vertical motion has any significance in provoking motion sickness. Lastly, the relief voyages to Antarctica create unique environments where the SAAII is exposed to periods of open water and ice where adaptability of participants towards motion sickness can be investigated.

1.2 Scope and objectives

The objective of this study is to determine the effects that location on board the SAAII as well as lateral and vertical acceleration has on motion sickness. To determine the effects of location on the SAAII has on motion sickness;

- It is first assumed that the SAAII is rigid below 1 Hz Pisula *et al.* (2012).
- A daily diary similar to Donohew and Griffin (2004) and Pisula *et al.* (2012) was developed to determine the location passengers spent most their time in as well as which locations were the most frequented.
- An accelerometer array, similar to the array described by Padgaonkar *et al.* (1975), consisting of six Direct Current (DC) accelerometers was

developed and used to determine the angular velocity, angular and linear acceleration of the vessel. With this 6 accelerometer array the acceleration levels could be determined for any location on board the SAAII.

- The severity of motion towards motion sickness shall be determined by the variation in the r.m.s. acceleration levels along the length, height and width of the SAAII according to the methods described in ISO 2631-1 (1997), Donohew and Griffin (2004) and Pisula *et al.* (2012).

The effect of the direction of motion on the passengers and crew was determined by;

- Determining the vertical and lateral acceleration, via a six accelerometer array, at a central location where passengers spent most their time or frequented the most on the SAAII.
- Weighting the vertical and lateral acceleration according to ISO 2631-1 (1997) and Donohew and Griffin (2004).
- Determining the Motion Sickness Dose Value (MSDV) described in ISO 2631-1 (1997) for both vertical and lateral acceleration.
- Developing a daily diary similar to Haward *et al.* (2009) and Pisula *et al.* (2012) to determine whether the participants were motion sick (Motion Sickness (MS)), how ill they felt with respect to motion sickness (Illness Rating (IR)) and whether the participants vomited (Percentage Vomiting (PV)).
- The correlation between the direction of acceleration and motion sickness (MS, IR and PV).
- Multiple linear regression analysis was used to identify the effects of the direction of acceleration and motion sickness.

1.3 Document layout

The document is divided up into six main sections, namely chapters 2 to 7. Chapter 2 summaries the relevant literature that has been utilised to carry out this research and gain a broader understanding of motion sickness. Chapter 3 describes the questionnaires on a pilot study on a relief voyage to Marion Island (2014) and subsequent work on the relief voyage to Antarctica (2014/2015). Chapter 4 and 5 describe the full measurement setups on voyages to Marion Island and Antarctica respectively. A modified six accelerometer array, used in the Antarctica measurement setup, is described and tested in Chapter 6. Chapter 7 determines the relationship between the measured acceleration, using the six accelerometer array, and data obtained from the questionnaires via multiple linear regression analysis.

Chapter 2

Literature study

Various theories on how motion sickness occurs are discussed, followed by the role inter- and intra-subject variability plays with respect to motion sickness. The effects motion has on motion sickness such as, frequency, direction, amplitude, duration, rotation and phase are highlighted. Weighing filters, used to asses motion sickness, described in ISO 2631-1 (1997) and Donohew and Griffin (2004) are presented. A means to implement the weighing filters shall be presented. Motions sickness investigations on board various sea vessels are reviewed. These are often used to find correlations between the direction of motion and motion sickness. Techniques such as using accelerometer arrays to measure the rigid body motion of the vessel are also discussed.

2.1 Theories of motion sickness

The theories of motion sickness are often used to explain the role of the sensory systems known as the visual, vestibular, proprioceptive and somatosensory systems with regards to motion sickness (Griffin, 1990). Two of the most prominent theories include, *sensory conflict theory* and *postural instability theory*.

Sensory conflict theory is described by Walton *et al.* (2011) and Johnson (2005) to occur when there is a conflict between the sensory systems. Johnson (2005) further elaborates this theory in seven steps; (1) the sensory systems register motion, (2) an expected baseline motion is provided by a neural store of past patterns of sensory input, (3) the baseline motion and registered motion by the sensory systems are compared, (4) the current motion is also sent to the neural store (for updates), (5) intra- and inter-subject variability account for an individual's threshold towards the severity, incidence and adaptation to motion sickness, (6) a sustained mismatch between the baseline motion and the registered motion creates a mismatch signal, (7) lastly this mismatch signal causes motion sickness and results in adaptation towards motion sickness.

Postural instability theory was developed by Riccio and Stoffregen (1991). Riccio and Stoffregen (1991) theorized that motion sickness occurs when someone is exposed to an unfamiliar environment. An inability to maintain postural control is caused as a result of this unfamiliarity which leads to postural instability. This theory is based on a provocative motion environment and not on a conflict arising from registered sensory motion and a past experiences.

2.2 Inter- and intra-subject variability of motion sickness

Susceptibility towards motion sickness for each individual varies (Griffin, 1990). One's susceptibility to motion sickness is dependent on various inter- and intra-subject variables such as; age, gender, history of motion sickness, body posture and health. ISO 2631-1 (1997) developed a means of predicting motion sickness for a mixture of unadapted adult males and females for seated and standing persons according to the basicentric axes systems defined in Figure 2.1 (z-axis only). Later, Donohew and Griffin (2004) contributed a means for evaluating motion sickness for seated persons only (x- and y axis only).

Bos *et al.* (2007) determined the effects of age, gender and whether previous experiences of motion sickness had an effect on susceptibility. He developed an equation that describes the susceptibility that takes these effects into account;

$$S = A\left[\exp\left(\frac{a-y}{b}\right) - \exp\left(\frac{a-y}{c}\right)\right] \tag{2.1}$$

where $a = 5\,\text{years}$, $b = 40\,\text{years}$, $c = 2$, 5 or 8 (for females, mixed gender or males respectively), $A = 0.36$ or 0.72 (for passengers without and with a history of motion sickness respectively) lastly y is the age. Since S is directly proportional to A those with a history of motion sickness are more susceptible to motion sickness than those without a history of motion sickness.

Figure 2.2 shows the susceptibility of passengers without any history of motion sickness ($A = 0.36$) for females and mixture of females and males. Observations in Figure 2.2 are that females are more susceptible to motion sickness than males. Females reach their peak sensitivity to motion sickness by the age of 11 whereas males reach their peak sensitivity at the age of 21. Susceptibility towards motion sickness declines with age after one has reached their age of peak sensitivity to motion sickness. It would appear that below the age of 5 regardless of gender there is no susceptibility towards motion sickness. However, limited data for ages below 5 in the study by Bos *et al.* (2007) meant that the model could not be developed for younger ages.

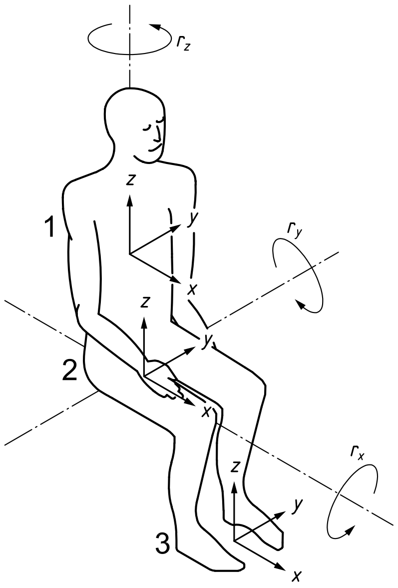

(a) Seated position

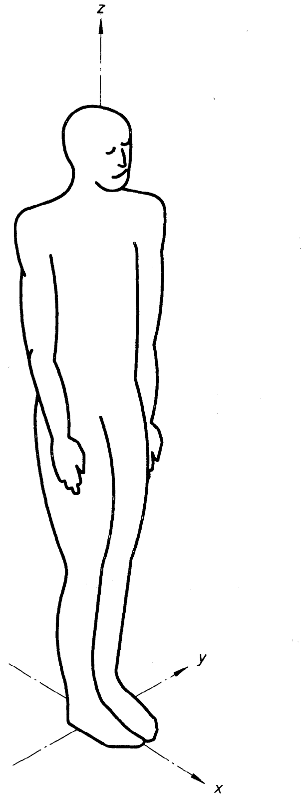

(b) Standing position

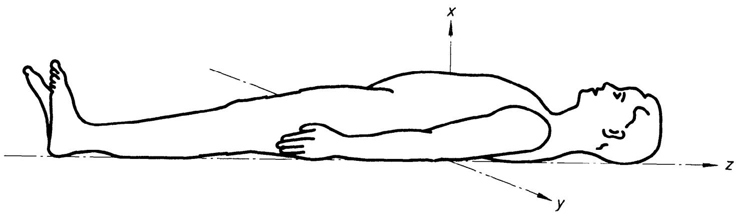

(c) Recumbent position

Figure 2.1: Basicentric axes of the human body adapted from ISO 2631-1 (1997)

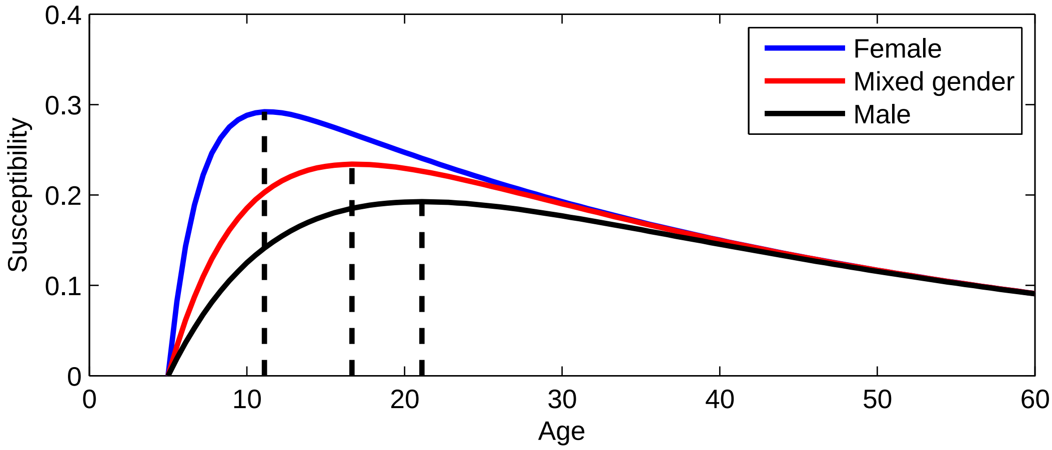

Figure 2.2: Predicted susceptibility as a function of gender based off a study by Bos *et al.* (2007)

2.3 Effects of motion on motion sickness

Many researchers have aimed to determine the effects motion has on motion sickness, these effects include; frequency, direction, magnitude, duration, phase, linear and angular motion. Understanding the attributes of these effects help better understand the environments in which motion sickness occurs.

2.3.1 Frequency, lateral and vertical acceleration

Alexander *et al.* (1947) found that the incidence of motion sickness decreased with increasing frequency (between 0.22 Hz to 0.53 Hz) for exposures times of 20 minutes. Afterwards O'Hanlon and McCauley (1973) and McCauley *et al.* (1976) investigated 25 different combinations of 10 frequencies ranging from 0.083 Hz to 0.7 Hz and magnitudes of acceleration ranging from 0.27 m/s^2 to 5.5 m/s^2 r.m.s. of vertical sinusoidal oscillation. Each subject was exposed to 2 h of oscillation while seated with their heads against a headrest in a closed cabin. A mathematical approximation to motion sickness known as the Motion Sickness Incidence (MSI) was developed from this data, which predicts the percentage of people vomiting. O'Hanlon and McCauley (1973) found that the greatest sensitivity to motion sickness was at 0.167 Hz and concluded that the frequency determined by Alexander *et al.* (1947) (0.22 Hz) should be lowered. The results from the study by McCauley *et al.* (1976) are presented in Figure 2.3.

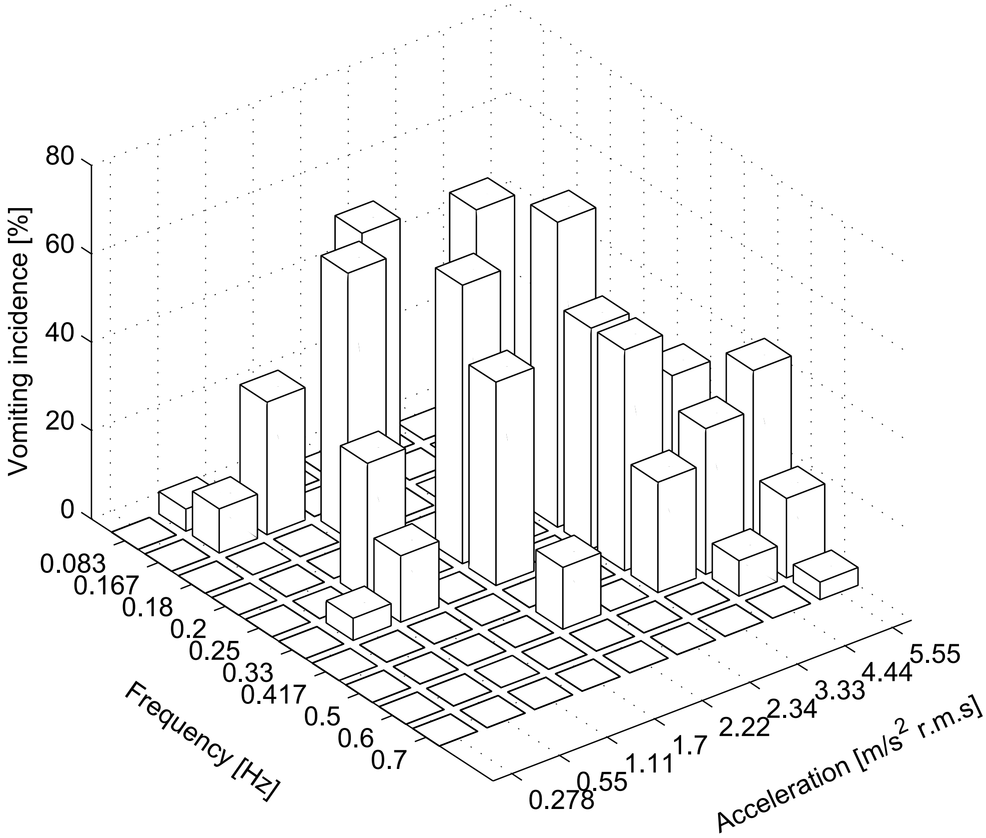

Figure 2.3: Incidence of vomiting adapted from McCauley *et al.* (1976)

Data from Lawther and Griffin (1987) and McCauley *et al.* (1976) were combined by Lawther and Griffin (1987) to create a frequency based weighting filter, which was later published in ISO 2631-1 (1997). The acceleration frequency-weighting filter developed was constant over the range of 0.125 Hz-0.25 Hz and would decrease by 6 dB/octave below 0.125 Hz and 12 dB/octave above 0.25 Hz.

The effects of linear acceleration on motion sickness are described by the weighting filters defined in ISO 2631-1 (1997) (W_f) and Donohew and Griffin (2004) (W_{dg}, notation defined for purpose of this thesis). W_f relates the frequency of vertical acceleration (z-axis) to motion sickness. The definition of W_{dg} relates lateral acceleration (x- and y-axis) to motion sickness and was published several years after the formulation of ISO 2631-1 (1997). The filter by Donohew and Griffin (2004) was developed in the context of predicting Illness Rating (IR) only. Whereas W_f was developed to predict both IR and Percentage Vomiting (PV).

Each weighting filters consist of a cascade of up to four different s-domain filters namely; a high-pass filter ($H_h(s)$), a low-pass filter ($H_l(s)$), an acceleration-velocity transition filter ($H_t(s)$) and an upward step filter ($H_s(s)$). These filters are defined in Rimell and Mansfield (2007, 2010) as follows;

$$H_h(s) = \frac{s^2}{s^2 + \frac{\omega_1}{Q_1}s + \omega_1^2} \tag{2.2}$$

$$H_l(s) = \frac{\omega_2^2}{s^2 + \frac{\omega_2}{Q_2}s + \omega_2^2} \tag{2.3}$$

$$H_t(s) = \frac{\frac{\omega_4^2}{\omega_3}s + \omega_4^2}{s^2 + \frac{\omega_4}{Q_4}s + \omega_4^2} \tag{2.4}$$

$$H_s(s) = \frac{s^2 + \frac{\omega_5}{Q_5}s + \omega_5^2}{s^2 + \frac{\omega_6}{Q_6}s + \omega_6^2} \tag{2.5}$$

where $s = j\omega$ and the parameters for the filters are found in Table 2.1.

Table 2.1: Numeric values used in equations 2.2 to 2.5, note $\omega = 2\pi f$

	H_h		H_l		H_t			H_s			
	f_1 (Hz)	Q_1	f_2 (Hz)	Q_2	f_3 (Hz)	f_4 (Hz)	Q_4	f_5 (Hz)	Q_5	f_6 (Hz)	Q_6
W_f	0.08	$1/\sqrt{2}$	0.63	$1/\sqrt{2}$	∞	0.25	0.86	0.0625	0.8	0.1	0.8
W_{dg}	0.02	$1/\sqrt{2}$	0.63	$1/\sqrt{2}$	∞	0.25	0.86	∞	1	∞	1

The cascade filters for W_f (ISO 2631-1, 1997) and W_{dg} (Donohew and Griffin, 2004) are described in equations 2.6 to 2.7.

$$W_f(s) = H_h(s)\ H_l(s)\ H_t(s)\ H_s(s) \tag{2.6}$$

$$W_{dg}(s) = H_h(s)\ H_l(s)\ H_t(s) \tag{2.7}$$

Both of the filters are show in Figure 2.4. The two low-pass filters behave similarly with a negative slope of 12 dB per octave slope between 0.25 Hz and 0.8 Hz. However the filter by Donohew and Griffin (2004) allows for a broader range of lower frequency content to pass through with positive slope of 12 dB between 0.02 Hz and 0.0315 Hz. Between 0.0315 Hz and 0.25 Hz each filter has a slope of 0 dB per octave. W_{dg} also has a filter gain of 0.55.

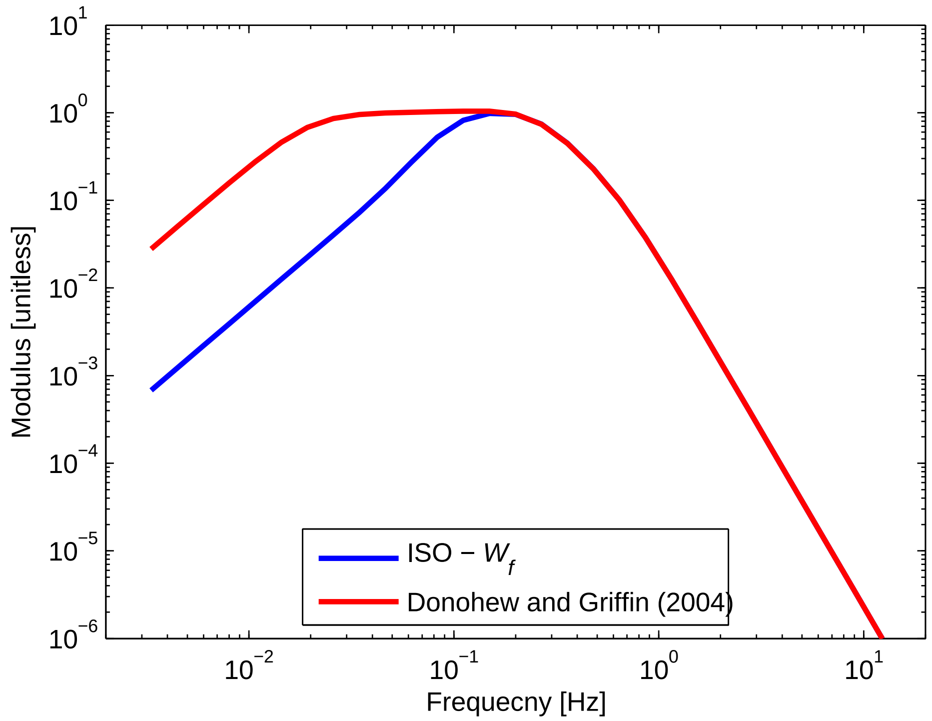

Figure 2.4: Vertical (ISO 2631-1 (1997)) and lateral weighting filters (Donohew and Griffin (2004))

2.3.2 Magnitude and duration

Studies by McCauley *et al.* (1976) and O'Hanlon and McCauley (1973) reported that there is a relationship between the incidence of motion sickness and the magnitude of low frequency vertical sinusoidal oscillation. A cumulative log-normal distribution between motion sickness incidence and exposure time was fitted to their results by McCauley *et al.* (1976). They found that during the first 80 minutes of exposure there was an increase in sickness. McCauley *et al.* (1976) determined that higher magnitudes of motion corresponds to earlier incidences of vomiting.

Data from McCauley *et al.* (1976) (Figure 2.6) and Lawther and Griffin (1988) (in Figure 2.5) suggest that below a threshold magnitude, of $0.1\,\mathrm{m/s^2}$ r.m.s, vomiting does not normally occur. Lawther and Griffin (1988) determined that there was an increase in illness rating (Figure 2.7) with increasing acceleration magnitude (r.m.s.) but there is not a lower threshold.

To relate the exposure to motion, with respect to time, and that magnitude of acceleration Lawther and Griffin (1986) formulated the motion dose;

$$motion\ dose = \left[\int a_w{}^n(t)dt\right]^n \tag{2.8}$$

Where a_w is the frequency-weighted z-axis acceleration (W_f). A good correlation was found between the motion dose value and the accumulation of motion sickness incidence during voyages when $n = 2$ or $n = 4$.

Lawther and Griffin (1987) plotted motion dose values versus vomiting incidence by combining data from Alexander *et al.* (1947), McCauley *et al.* (1976) and Lawther and Griffin (1986). With this data a linear approximation between the motion dose value, $n = 2$, and the vomiting incidence was determined;

$$PV = K \times motion\ dose \tag{2.9}$$

where the constant $K = 1/3$ for unadapted adults of mixed genders. They developed 0-3 an illness rating scale which was related motion dose values with $k = 1/50$;

$$IR = k \times motion\ dose \tag{2.10}$$

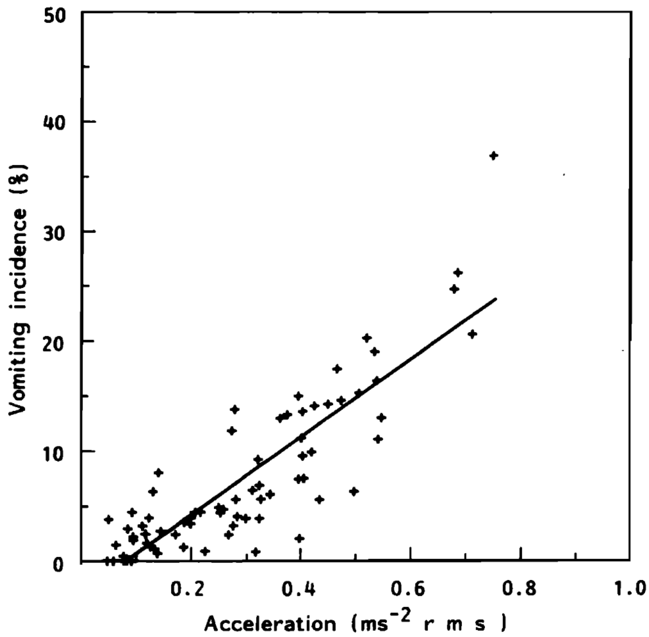

Figure 2.5: Effects of the magnitude of vertical acceleration on the vomiting incidence with a 2 h exposure at a dominant frequency of 0.2 Hz (Adapted from Lawther and Griffin (1988))

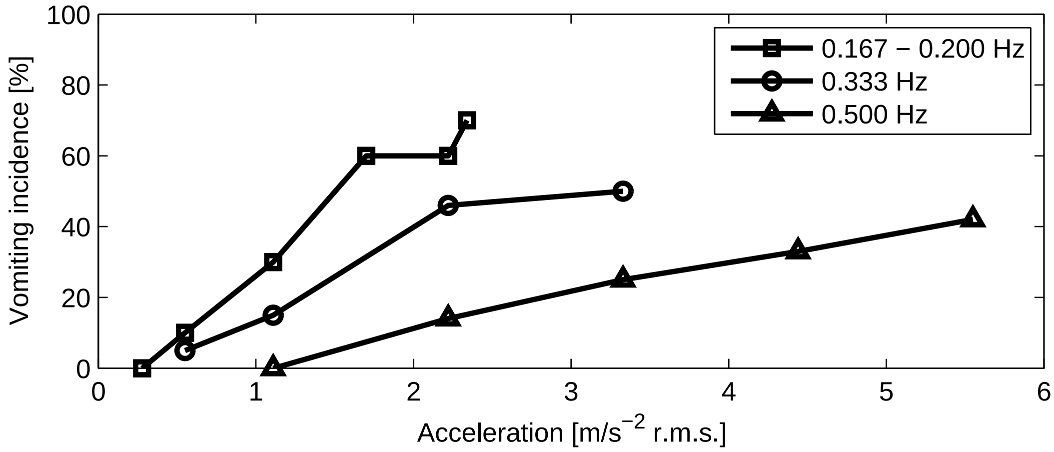

Figure 2.6: Effects of the magnitude of vertical acceleration on the vomiting incidence at three different frequencies (Adapted from McCauley *et al.* (1976))

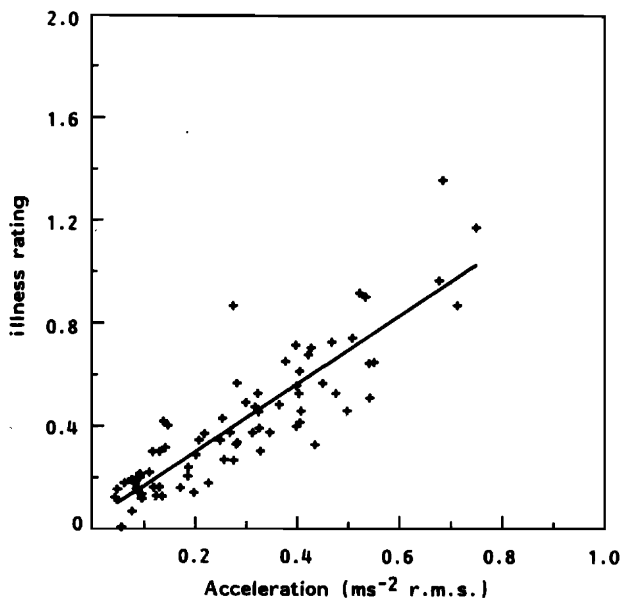

Figure 2.7: Effects of the magnitude of vertical acceleration on the illness rating with a 2 h exposure at a dominant frequency of 0.2 Hz (Adapted from Lawther and Griffin (1988))

2.3.3 Rotation and phase

Studies investigating the combined effects of lateral and rotational motion always occurred in phase with each other (Joseph and Griffin, 2007). Joseph and Griffin (2007) hypothesised that motion sickness would be dependant on the phase angle between the lateral and roll displacement. It was found, in

Figure 2.8, that the mean illness rating was greatest with 0° phase angle and decreased with a change in phase angle. The illness rating was found to be greater if the roll motion lagged the lateral motion.

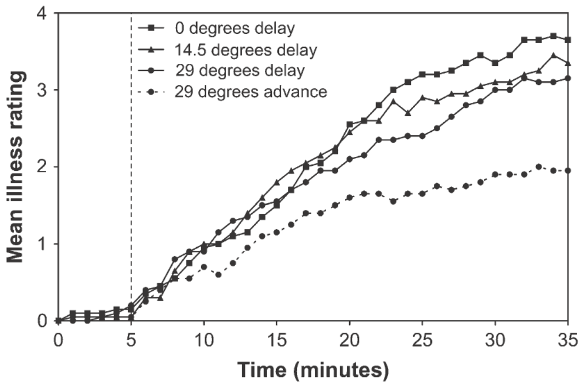

Figure 2.8: Effects on the phase angle between lateral and rotational motion on the mean illness rating (Adapted from Joseph and Griffin (2007))

2.3.4 Assessment of vertical acceleration according to ISO 2361-1

ISO 2631-1 (1997) outlines a procedure to evaluate the incidence of motion sickness. A continuous frequency-weighting filter, W_f, based on the vomiting incidence, was defined for evaluation of motion sickness in the z-axis for both standing and seated persons. Weighting the acceleration requires conversion from the time domain to the frequency domain, where it is weighted using the frequency-weighting filter, W_f. However methods of evaluating motion sickness require the weighted acceleration to be in the time domain. These methods include determining the motion sickness dose value ($MSDV_z$) in the z-axis for seated or standing persons, crest factor (CF), illness rating (IR) and the predicted percentage of participants who vomit (PV) as a result of motion sickness.

$$MSDV_z = \left[\int_0^T a_w(t)^2 dt \right]^2 \tag{2.11}$$

$$CF = \frac{a_{w,max}}{a_{w,r.m.s}} \tag{2.12}$$

$$IR = k \times MSDV_z \tag{2.13}$$

$$PV = K \times MSDV_z \tag{2.14}$$

where a_w, $a_{w,max}$, $a_{w,r.m.s}$ and T are the weighted (W_f) acceleration, the maximum weighted acceleration, the weighted r.m.s. acceleration (in m/s^2) and the duration of exposure to motion respectively. The relationships between IR, PV and $MSDV_z$ are based off 20 minute to 6 h exposures to motion. Despite all these evaluations, ISO 2631-1 (1997) does not show how to implement the weighting filter in the time domain.

2.3.5 Multi-axial vibration exposure

McCauley *et al.* (1976) determined that pitch and roll motion, either in combination or separate from vertical oscillation, had no effect on the incidence of motion sickness. They investigated the influence of roll and pitch at 0.115 Hz, 0.23 Hz and 0.345 Hz in combination with vertical oscillation of 0.25 Hz at 1.1 m/s^2 r.m.s. The magnitudes of rotation during this study were greater than generally encountered in large ships at sea; the implication of this is that roll and pitch aboard large ships are not the main cause of motion sickness. The same conclusion was made by Lawther and Griffin (1986, 1988) where motion sickness was highly correlated with the vertical acceleration and with pitch acceleration.

A means for evaluating the effects of Multi-axial vibration exposure described by ISO 2631-1 (1997). The vibration total value (a_{wt}) is determined by combining the weighted r.m.s. acceleration for orthogonal directions of motion as shown in equation 2.15. This method (described in equation 2.15) was developed for human comfort, but it does give an indication on how to combine the effects of multi-axial vibration.

$$a_{wt} = \sqrt{k_x^2 a_{wx}^2 + k_y^2 a_{wy}^2 + k_z^2 a_{wz}^2} \tag{2.15}$$

Where k_x, k_x, and k_z are the axis multiplying factors which are usually 1 for standing and seated (at the supporting seat surface) persons. The axis multiplication factors account for the variation of human sensitivity to different directions of vibration response. The weighted r.m.s. acceleration amplitudes are a_{wx}, a_{wy} and a_{wz} with in their respective orthogonal x-, y- and z-axes.

2.4 Infinite Impulse Response (IIR) weighting filters for lateral and vertical motion sickness

The s-domain mathematical definition for the weighting filter W_f is described in ISO 2631-1 (1997). This filter is able to determine the weighted acceleration in the frequency domain as well as determining the weighted r.m.s. acceleration (Mcmahon, 2014). However metrics such as the Crest Factor (CF) and Motion Sickness Dose Value (MSDV), defined in ISO 2631-1 (1997), require the weighted time domain acceleration.

Rimell and Mansfield (2007, 2010) developed discrete time domain weighting filters for whole-body vibration and motion sickness (W_f) and described the entailed methodology. The filter is defined in the discrete z-domain by means of an IIR filter. Each of the cascade filters described in equations 2.2 to 2.5 are transformed from the s-domain to the z-domain by means of a bilinear transform;

$$s \to 2\left(\frac{1-z^{-1}}{1+z^{-1}}\right) \tag{2.16}$$

A non-linear relationship exists between the analogue frequencies described in Table 2.1 and the digital frequencies in the z-domain (Rimell and Mansfield, 2007). Hence, the analogue frequencies are transformed according to the following;

$$\omega_n' \to 2\left[\tan\left(\frac{\omega_n}{2}\right)\right] \tag{2.17}$$

where $\omega_n = 2\pi f_c/f_s$ is the normalised filter design frequency (f_c, found in Table 2.1, and f_s being the centre and sample frequency respectively and $c = 1, 2, 3...6$). The z-domain cascade filters of those in equations 2.2 to 2.5 were all simplified according to;

$$H(z) = \frac{b_0 z^{-2} + b_1 z^{-1} + b_2}{a_0 z^{-2} + a_1 z^{-1} + a_2} \tag{2.18}$$

The coefficients (a_0, a_1, a_2, b_1, b_1 and b_2) for the cascade filters (H) described in equations 2.2 to 2.5 are found in Table 2.2. The coefficients are applicable to both W_f filter and the filter by Donohew and Griffin (2004) (W_{dg}).

Table 2.2: IIR coefficients for weighting filter section H_h, H_l, H_t and H_s

	H_h	H_l
a_0	$Q_1\omega_1'^2 + 2\omega_1' + 4Q_1$	$Q_2\omega_2'^2 + 2\omega_2' + 4Q_2$
a_1	$2Q_1\omega_1'^2 - 8Q_1$	$2Q_2\omega_2'^2 - 8Q_2$
a_2	$Q_1\omega_1'^2 - 2\omega_1' + 4Q_1$	$Q_2\omega_2'^2 - 2\omega_2' + 4Q_2$
b_0	$4Q_1$	$Q_2\omega_2'^2$
b_1	$-8Q_1$	$2Q_2\omega_2'^2$
b_2	$4Q_1$	$Q_2\omega_2'^2$
	H_t	H_s
a_0	$Q_4\omega_4'^2 + 2\omega_4' + 4Q_4$	$Q_5Q_6\omega_6'^2 + 2Q_5\omega_6' + 4Q_5Q_6$
a_1	$2Q_4\omega_4'^2 - 8Q_4$	$2Q_5Q_6\omega_6'^2 - 8Q_5Q_6$
a_2	$Q_4\omega_4'^2 - 2\omega_4' + 4Q_4$	$Q_5Q_6\omega_6'^2 - 2Q_5\omega_6' + 4Q_5Q_6$
b_0	$Q_4\omega_4'^2$	$Q_5Q_6\omega_5'^2 + 2Q_6\omega_5' + 4Q_5Q_6$
b_1	$2Q_4\omega_4'^2$	$2Q_5Q_6\omega_5'^2 - 8Q_5Q_6$
b_2	$Q_4\omega_4'^2$	$Q_5Q_6\omega_5'^2 - 2Q_6\omega_5' + 4Q_5Q_6$

2.5 Full scale measurements on sea vessels

Motion sickness can be found in various modes of transportation such as sea vessels, aircraft, surface vehicles, spacecraft and simulators (Golding, 2006). Field studies on sea vessels have been selected because of their relevance to this thesis. Field studies on trains are highlighted to motivate the importance of motion in other directions besides the z-axis. Multiple field studies were done on sea vessels such as ships, ferries and oil rigs; such studies were done by Lawther and Griffin (1986, 1988); Lewis and Griffin (1997); Haward *et al.* (2009); Khalid *et al.* (2011); Pisula *et al.* (2012).

Haward *et al.* (2009) studied the motions of an offshore oil production and storage vessel. They measured continuously for a five month period and reported ship motions in all six axes (fore-aft, lateral, vertical, roll, pitch and yaw). 66 to 78 % of 47 crew members (male and mostly adapted to the seafaring environment) filled in a total of 1704 daily diary entries detailing crew performance, health, sleep and motion sickness. A low vomiting incidence of 3.1 % was determined and compared with the predicted vomiting incidence of 9.3 % (according to ISO 2631-1 (1997)) for an unadapted mixed population of adults. The motion sickness symptoms most strongly influenced by the magnitude of the ship motions were stomach awareness and dizziness and not vomiting.

Gahlinger (2000), Riola and García de Arboleya (2006) and Golding (2006) agree that the dominant frequency of motion, in the z-axis (vertical), of a ship is around 0.2 Hz, where it is believed that human sensitivity to motion sickness is a maximum. In several studies Lawther and Griffin (1986, 1987, 1988) determined that motion sickness incidence was highly correlated with the vertical motion and the pitch of the ship.

Motion sickness is found in trains but is especially prominent in tilting trains. Unlike ships the principle cause of motion sickness on trains is not vertical acceleration, but roll. Förstberg (2000) studied the effects of roll compensation on tilting trains and via regression analysis found a strong correlation between motion sickness and roll motion. From the study there was no clear means to separate the combined effects of roll and vertical acceleration. They did not measure yaw acceleration, which meant that the effects of curvature radius could not be investigated explicitly.

Persson (2008) hypothesized that combinations of translation and rotation, which is recognised as an effective means of causing motion sickness, are possible causes of motion sickness in tilting trains. It was reported that lateral acceleration in non-tilting trains was higher than in tilting trains.

2.6 Theory of accelerometer arrays to determine rigid body motion

Various accelerometer arrays documented to define the kinematics of a rigid body. Padgaonkar *et al.* (1975) defined a six accelerometer and nine accelerometer array along with their associated advantages and disadvantages. These arrays require that the measurement points are either in-plane or perpendicular to each other.

Padgaonkar *et al.* (1975) states that the rigid body motion of an object is completely defined when the unknown angular acceleration, angular velocity and translational accelerations are determined. Also five accelerometers are required to determine the angular acceleration and velocity of an object, an additional linear accelerometer is needed to determine the translational acceleration of a rigid body.

A rigid body (Figure 2.9) is a solid system of particles where the distances between these two particles remain the unchanged (Meriam and Kraige, 2008). It describes the overall motion of many machines, sea vessels, vehicles, spacecraft and even animals. Each particle is assigned a point name.

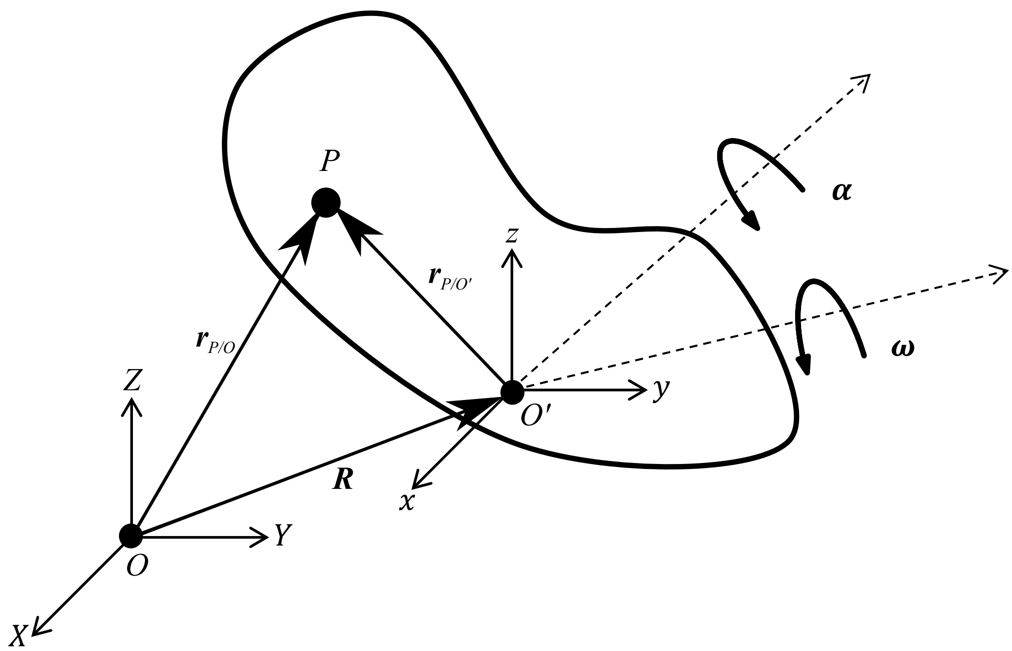

Figure 2.9: 6 Degree of freedom rigid body

Since a rigid body is a system of particles, equations of motion for individual points can be extended to an entire body. The three-dimensional translational acceleration of any Point P (where $P = 0, 1, 2, ..., n$), on a body is defined by;

$$\boldsymbol{a}_P = \ddot{\boldsymbol{R}} + (\boldsymbol{a}_{P/O'})_r + 2\boldsymbol{\omega} \times (\boldsymbol{v}_{P/O'})_r + \boldsymbol{\omega} \times (\boldsymbol{\omega} \times \boldsymbol{r}_P) + \boldsymbol{\alpha} \times \boldsymbol{r}_P \tag{2.19}$$

Where;

$\ddot{\boldsymbol{R}}$ = acceleration of the body-fixed frame (xyz) with respect to the inertial reference frame (XYZ)
$(\boldsymbol{a}_{P/O'})_r$ = acceleration of the Point P, relative to the body-fixed frame
$\boldsymbol{\omega}$ = angular velocity of the body
$\boldsymbol{\alpha}$ = angular acceleration of the body
$(\boldsymbol{v}_{P/O'})_r$ = velocity of Point P relative to the body-fixed frame
$\boldsymbol{r}_P$ = position vector of the Point P from the origin of the body-fixed frame

Assuming that a body is rigid, simplifications such as $(\boldsymbol{a}_{P/O'})_r = \boldsymbol{0}$ and $(\boldsymbol{v}_{P/O'})_r = \boldsymbol{0}$ reduces equation 2.19 to;

$$\boldsymbol{a}_P = \ddot{\boldsymbol{R}} + \boldsymbol{\omega} \times (\boldsymbol{\omega} \times \boldsymbol{r}_P) + \boldsymbol{\alpha} \times \boldsymbol{r}_P \tag{2.20}$$

The derivations of both equations 2.19 and 2.20 are found in Appendix A.

2.6.1 Six accelerometer array

The configuration of a six accelerometer array presented in Figure 2.10, was described by Padgaonkar *et al.* (1975). The array consists of three points on a rigid body which consists of a tri-axial accelerometer setup, one single axis accelerometer and one bi-axial accelerometer at Points 0, 1 and 2 respectively. Both Haward *et al.* (2009) and Pisula *et al.* (2012) used this array to determine the translational r.m.s. acceleration along the length, width and height of a vessel in their respective motion sickness studies.

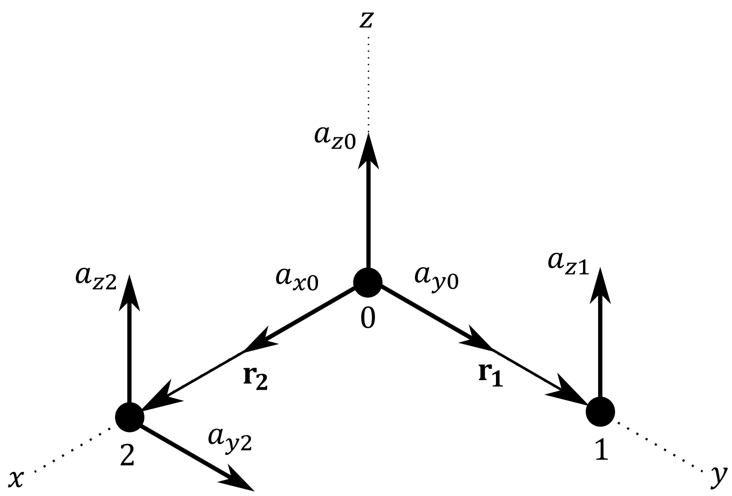

Figure 2.10: Six accelerometer array

The following properties were determined from the accelerometer array;

$$\ddot{\boldsymbol{R}} = a_{x0}\mathbf{i} + a_{y0}\mathbf{j} + a_{z0}\mathbf{k} \tag{2.21}$$
$$\boldsymbol{r}_1 = 0\mathbf{i} + r_{y1}\mathbf{j} + 0\mathbf{k} \tag{2.22}$$
$$\boldsymbol{r}_2 = r_{x2}\mathbf{i} + 0\mathbf{j} + 0\mathbf{k} \tag{2.23}$$
$$\boldsymbol{r}_0 = 0\mathbf{i} + 0\mathbf{j} + 0\mathbf{k} \tag{2.24}$$

Applying equation 2.20 to both Point 1 and Point 2 the angular acceleration can then be determined by (for the derivation of these equations refer to Appendix A);

$$\alpha_x = (a_{z1} - a_{z0})/r_{y1} - \omega_y\omega_z \tag{2.25}$$
$$\alpha_y = -(a_{z2} - a_{z0})/r_{x2} + \omega_x\omega_z \tag{2.26}$$
$$\alpha_z = (a_{y2} - a_{y0})/r_{x2} - \omega_x\omega_y \tag{2.27}$$

Where;

a_{mn} is the lateral acceleration along either the x, y or z-axis (m/s^2)

r_{mn} is the either the x, y or z coordinate of Point 0, 1 or 2 (m)

α_m is the angular acceleration about either the x, y or z-axis (rad/s^2)

ω_m is the angular velocity about either the x, y or z-axis (rad/s)

and the first subscript (m) denotes the direction of measurement and the second subscript (n) denotes the location of measurement.

Solving equations 2.25 to 2.27 requires knowledge of the angular velocity. Since the angular velocity is unknown Padgaonkar *et al.* (1975) suggested solving these non-linear equations numerically and applying stepwise integration of angular acceleration to determine the angular velocity. This method requires that the distances between points are known to high degrees of accuracy, errors in the measured acceleration usually result in the accumulation of error during the stepwise integration of $\boldsymbol{\alpha}$ which affects $\boldsymbol{\omega}$.

2.6.2 Nine accelerometer array

Padgaonkar *et al.* (1975) proposed the nine accelerometer array to eliminate the need for any numerical integration, thus preventing the accumulation of errors in $\boldsymbol{\alpha}$. Ideal conditions for the nine accelerometer array include;

- The instrumented body experiences a direct impact on a hard surface
- The accelerometer used has a low sensitivity which cannot accurately predict acceleration during impact conditions or if the body experiences high levels translational and linear acceleration.

- The accelerometer has significant cross-axis sensitivity which results in a large error with the six accelerometer array.

As shown in Figure 2.11 there are three additional accelerometers added to the six accelerometer array discussed in Section 2.6.1, two of them are added to Point 3 and an additional one is added to Point 1.

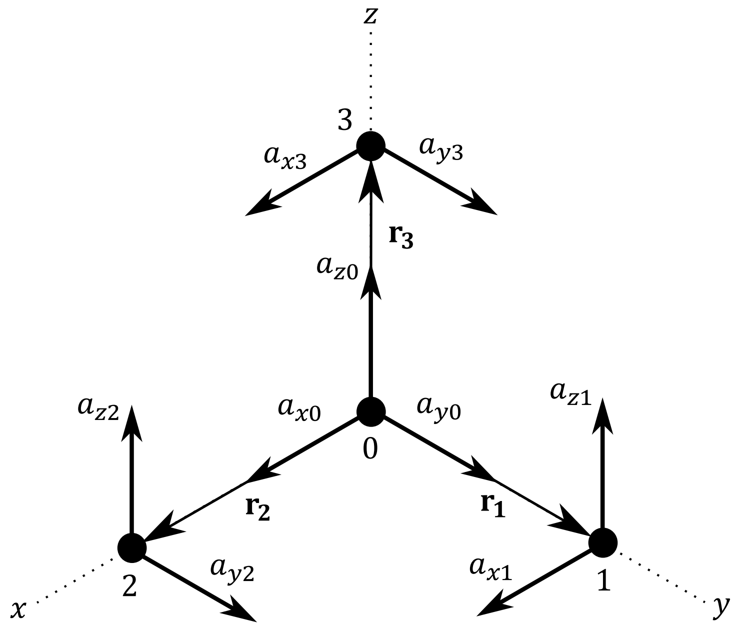

Figure 2.11: Nine accelerometer array

This configuration enables the determination of the angular acceleration of the rigid body through;

$$\alpha_x = -(a_{y3} - a_{y0})/r_{z3} + \omega_y \omega_z \tag{2.28}$$
$$\alpha_y = (a_{x3} - a_{x0})/r_{z3} - \omega_x \omega_z \tag{2.29}$$
$$\alpha_z = -(a_{x1} - a_{x0})/r_{y1} + \omega_x \omega_y \tag{2.30}$$

Equations 2.25 to 2.30 are combined to eliminate the cross products in the angular acceleration which results in;

$$\alpha_x = (a_{z1} - a_{z0})/2r_{y1} - (a_{y3} - a_{y0})/2r_{z3} \tag{2.31}$$
$$\alpha_y = (a_{x3} - a_{x0})/2r_{z3} - (a_{z2} - a_{z0})/2r_{x2} \tag{2.32}$$
$$\alpha_z = (a_{y2} - a_{y0})/2r_{x2} - (a_{x1} - a_{x0})/2r_{y1} \tag{2.33}$$

These equations can be solved directly without any stepwise numerical method. However, $\boldsymbol{\alpha}$ needs to be integrated with respect to time in order to determine $\boldsymbol{\omega}$.

2.7 Discussion

It was shown that humans are most susceptible to motion sickness between 0.125 to 0.25 Hz with decreasing susceptibility below 0.125 Hz and above 0.25 Hz for vertical oscillation. The frequency-weighting filter W_f, stipulated in ISO 2631-1 (1997), was developed to account for susceptibility for vertical motion. A lateral frequency-weighting filter was developed recently and is currently not found in any known standards. W_f is based off the number of people vomiting and the lateral frequency-weighting filter is based off the illness rating of the subjects as vomiting did not occur. W_f can be used to predict the illness rating or the percentage of people who will vomit. In order to combine the effects of vertical and lateral displacement the illness rating must be used as the lateral frequency-weighting filter is based off the illness rating. The final result would be something similar to evaluating the overall comfort level of a seated or standing person.

Motion sickness is highly correlated with vertical motion, but can still occur with translation and oscillation about other axes. It has been theorised on tilting trains that the combination vertical and roll motion is the potential cause of motion sickness. There is a strong correlation on large ships where vertical motion is reported as the principle cause of motion sickness. This highlights the importance of studying translation and oscillation and the combination thereof. Currently such effects are studied on sea vessels and trains but it is difficult to determine the principal cause of motion sickness using correlations between motion of the environment and motion sickness. Some studies have been done in laboratories but the amplitudes used are larger than those measured on trains.

To account for the effects of duration and frequency has on motion sickness the MSI was developed, a simpler method was developed later on. A motion sickness dose value ($MSDV_z$) of the frequency-weighted acceleration in the vertical direction was suggested and is now used in ISO 2631-1 (1997). A linear relationship was found between the motion dose value and the percentage of people that would vomit as well as the illness rating. It was recently found, by (Joseph and Griffin, 2007), that motion sickness is dependent on the phase angle between the lateral and roll motion.

Chapter 3

Questionnaires

This section discusses the design and development of motion sickness questionnaires on voyages to Marion Island 2014 and Antarctica 2014/2015 as well as the demographics of the passengers and preliminary results. Questionnaires were developed in order to correlate Percentage Vomiting (PV), Illness Rating (IR) and Motion Sickness (MS) experienced by passengers to location and ship translation. These questionnaires were designed to be filled in daily. Lessons learnt were incorporated into the design for the questionnaires used during the 2014/2015 voyage to Antarctica.

3.1 Marion Island 2014 voyage

No researchers from the Sound and Vibration Research Group (SVRG) were present on the voyage which meant that the questionnaire was administered by someone without explicit understanding of the research results. A podcast video was created by the SVRG, using Camtasia Studio 8, to present our studies and explain the purpose of the motion sickness studies and how to fill in the questionnaires. Questionnaires and a copy of the podcast video were handed over to the South African National Antarctic Program (SANAP) director of the Department of Environmental Affairs (DEA) and Departmental Co-ordinator (DCO), whom were on board the ship during the voyage. The questionnaires were handed out to the passengers during the first day of the voyage, in the auditorium, while a podcast video was presented. During the voyage no reminders were communicated to the respondents.

3.1.1 Questionnaire

The methods defined in ISO 2631-1 (1997) only predict passenger responses to motion sickness. In order to capture the actual passenger responses to motion sickness, questionnaires were handed out to each passenger. The questionnaires consisted of three sections (presented in Appendix B); a once-off *passenger details* section, a once-off *motion sickness susceptibility* questionnaire adapted from Griffin and Howarth (2000) and a *daily diary* which was to be filled in daily. The design of the questionnaire was adapted from a study by Howarth and Griffin (2009) where numerous surveys were conducted over a period of 5 months and a total of 1704 daily diary entries were completed, each survey lasting approximately two weeks.

All passengers were made aware that the questionnaire was anonymous and the data collected from the survey would be treated as such. Passengers were encouraged to participate in the questionnaire, which was entirely voluntary, and could be discontinued participation at any time without providing a reason.

Each questionnaire, found in Appendix B, was bound in a booklet consisting of;

- A *front cover* which included a participation number.
- A *ship diagram* dividing the ship into zones for reference in the rest of the questionnaire.
- A page of *definitions and instructions* for the questionnaire.
- A *personal details questionnaire.*
- A *motion sickness susceptibility questionnaire* (adapted from Griffin and Howarth (2000)).
- A three page *daily diary* for every day (based off Haward *et al.* (2009)).

The *front cover* included the project title and participation number which allowed the questionnaire to be identifiable, yet anonymous. The *ship diagram* attempted to determine the location of passengers on the ship. The ship was divided up into zones, which were defined according to the likelihood of variation in motion sickness exposure. A page of *definitions and instructions* was included to assist participants in understanding key concepts by defining motion sickness. Instructions detailed when to fill in the questionnaires and where to deliver them.

The *motion sickness susceptibility* questionnaire determined the susceptibility of participants to motion sickness and transport that is most effective in causing motion sickness. Various modes of transport such as cars, buses, coaches, small boats, ships, aeroplanes and trains were included in the questionnaire.

The once off *passenger details questionnaire* was designed to investigate the effects of intra- and inter-subject variability by determining; the age, gender, body weight, stature, voyage experience, whether motion sickness medication was taken and when a participant was on board the ship. On the first day of the voyage the passengers were asked to fill in the personal details questionnaire.

The *daily diary* questionnaire was designed for various studies for the purpose of; task performance and motion sickness similar to Haward *et al.* (2009), environmental factors, tiredness and sleep, lastly on wave slamming and its effects on people and equipment (which is the topic of another masters study within the SVRG). The questionnaire was to be filled at the end of each day or the beginning of the following day, documenting the participants experiences for the past 24 hours. The section on motion sickness was aimed to determine the illness rating associated with the signs and symptoms of motion sickness and location of each participant. The *daily diary* was designed to determine several experiences of respondents, including;

- The effects of cognitive and physical work on task performance on leisure and work activities.
- What activities were performed, which location of the ship these activities were performed and how long each activity took.
- The effects of motion sickness on task performance.
- The common symptoms of motion sickness along with the illness rating.
- Whether a passenger or crew member was motion sick.
- The illness rating of a passenger and crew member.
- Whether a passenger vomited.
- Whether a passenger took motion sickness medication, along with its type and dosage.
- Whether any problems were experience due environmental factors such as noise, vibration, temperature, lighting and air quality.
- Whether their sleep had been effected and how long they slept.

3.1.2 Demographics

During the various legs of the voyage the population size of the passengers on the vessel changed, whereas the population size of the crew remain unaffected. During the voyage planning meetings the initial population size of the voyage (during the departure leg) was 100 passengers and 50 crew members with a mixture of males and females.

Towards the end of the departure leg, at Marion Island, a number of the passengers disembarked the ship and remained on Marion Island for the oceanographic leg. The population size changed during for the oceanographic leg, but the population size could not be determined since the voyage was unmanned. It was neglected to provide instructions to the administrators to record the change in population size.

After the oceanographic leg of the voyage was completed the passengers that remained on Marion Island would board the SA Agulhas II (SAAII), thus changing the population size on board the ship. The previous over-wintering team boarded the ship, leaving the new over-wintering team on the island for a whole year. This meant that a new set of passengers were on board the ship, questionnaires were not handed to them as only 100 were printed. Of the 100 questionnaires handed out a total of 43 passengers responded to the questionnaire; however crew members did not participate in this questionnaire.

3.1.3 Results

All questionnaires were filled in by hand and the information contained within them was manually transferred into an Excel spreadsheet. Information such as the illness rating, whether the passenger had motion sickness and whether the passenger vomited was transferred. Response rates for the questionnaires were 43 % on Day 1 with a confidence interval of 9.23 %, dropping to a response rate of 11 % within 10 days at a confidence interval of 27.9 %.

The response rates for the questionnaire can be seen in Figure 3.1 for the locations, signs and symptoms as well as the associated illness ratings. The highest response rate was 43 % with a confidence interval of 9.23 %. The response rate reduced to 11 % by Day 10 and to 3 % by Day 16 where the confidence interval was 52.8 %. The effect of the confidence interval is shown in Figure 3.2. The reduction in the response rate increased the confidence interval, which increased the error in estimating the percentage of all motion sick passengers. The lack of responses therefore reduces the reliability of the conclusions that can be drawn from the study of questionnaire responses.

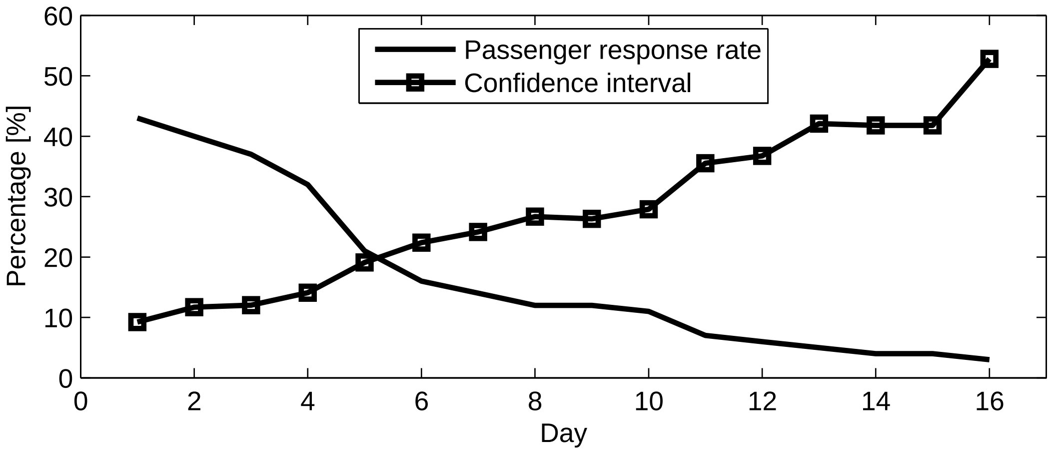

Figure 3.1: Confidence interval and passenger response rate - Marion

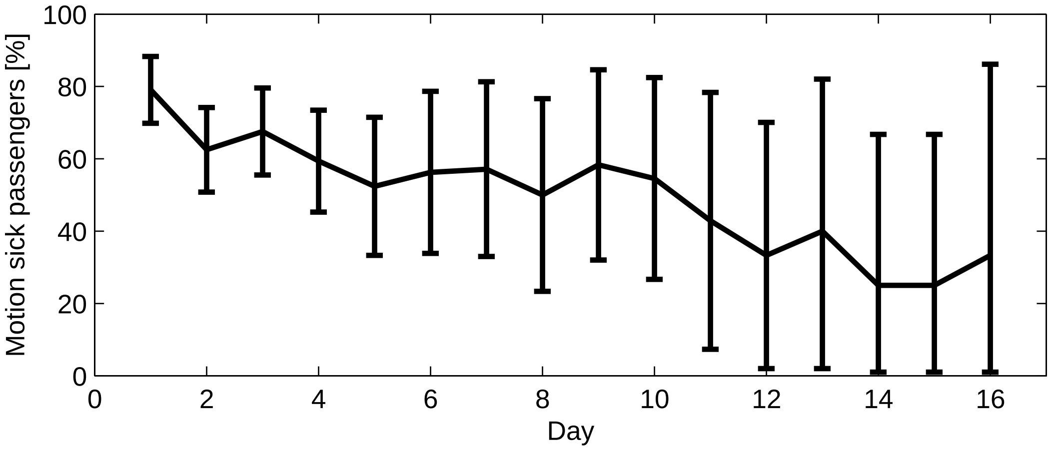

Figure 3.2: Effect of confidence interval on the percentage of motion sick passengers - Marion

The study by Haward *et al.* (2009) had a participation rate of 66 to 78 %. Their study lasted five months, but consisted of two week voyages for a crew size of 47. The lack of reponses to this survey is attributed to a number of factors such as; long and complicated daily diary questionnaires or lack of personnel to oversee the administration of the questionnaire during the voyage.

Although the confidence interval deteriorated rapidly, there appears to be a decline in the percentage of motion sick passengers (Figure 3.2). This indicated that adaptation could be taking place for the respondents. However, due to the low response rate the same cannot be said for all passengers.

3.1.4 Discussion

The questionnaires from the Marion 2014 voyage yielded a low response rate which resulted in unreliable data. It is speculated that the low response rate occurred due to the following;

- The questionnaire being too long and complicated, and perhaps aimed at determining too many influences of ship motion passengers
- No researchers from the SVRG were able to administer the questionnaires and presentation thereof personally to answer questions or explain unclear instances within the questionnaire
- Passengers were not motivated or encouraged to fill their questionnaires on a regular basis.

In order to increase the success of the questionnaire it was decided that a member of the SVRG is required to be on board on the SAAII. The member would be able to administer the questionnaire effectively, motivate passengers and distribute reminders across the SAAII. Additionally the questionnaire should be simplified to reduce the burden of filling out the questionnaire on a daily basis.

3.2 Antarctica 2014/2015 voyage

The aim for this voyage was to determine the motion sickness incidence and whether location on board the SAAII and direction of motion played a role in motion sickness. Since the survey for the Marion voyage was unsuccessful the questionnaires were improved and simplified by;

- Eliminating the *motion sickness susceptibility questionnaire* to reduce the length of the booklet.
- Improvements were made to the *personal details questionnaire* to be able to categorise participants into ship crew members, land based personnel, ship based scientists and land based scientists.
- Reducing the *daily dairy* from three pages per day to half a page per day by focusing on questions tailored for motion sickness.
- Having a researcher on board to administer the survey.

The SAAII was in the harbour during the first day (4 December 2014) of the voyage and the questionnaires were handed over to the passengers on the second day. The first mate of the SAAII received the questionnaires for the crew members the same day, and was responsible for distributing the questionnaires to crew members. Throughout the voyage passengers would leave the vessel and new passengers would board the vessel, these passengers would also receive a questionnaire.

Each questionnaire was given a unique number (Ant#) so that participants would be able identify their own questionnaires whilst maintaining anonymity. These numbers were used to identify questionnaires and to categorise participants according to the information contained in their personal details submission form. Passengers were designated numbers Ant 1 to Ant 100 as well as Ant 151 and above, crew members were assigned questionnaires Ant 101 to Ant 150.

3.2.1 Questionnaire

As the $MSDV_z$ is applicable to unadapted adults (male and female) it is necessary to determine the intra- and inter-subject variability. Various intra-subject and inter-subject variables play a role in motion sickness such as age; gender and experience (ISO 2631-1, 1997).

The *personal details questionnaire* in Figure 3.3 aimed to;

- Identify the age and gender of the subject
- Identify ship based and land based passengers as well as crew members
- Determine the number of voyages and time spent at sea of the the subject (sea experience)
- Determine whether the subject took medication to combat motion sickness.

The *daily diary* in Figure 3.4 aimed to correlate motion sickness variables such as; illness ratings, percentage of motion sick subjects and the percentage of subjects who vomited to locations (known as zones) on the ship and direction of linear acceleration.

Lawther and Griffin (1986) and Lawther and Griffin (1988) considered to only determine the acceleration levels in the lounges of the ship in their studies. Whereas, Haward *et al.* (2009) considered the acceleration levels at the accommodation area of an offshore oil rig. However Pisula *et al.* (2012) divided their ship, of 79.5 m in length and 33 m in height, into fifteen non-equispaced zones of three rows and five columns. Figure 3.5 shows that SAAII was divided into seventy eight zones (used in the *daily diary*) in a similar fashion as Pisula *et al.* (2012). A list was attached to the survey, which provided a guide for the participants to identify which zones that they were in. The participants were asked to fill out which zones they spent the most hours in.

1. Demographics

Age group					Gender	
20-30	30-40	40-50	50+		M	F

Please circle the most appropriate term that describes you			
Ship based scientist	Land based scientist	Land based personal*	SA Agulhas II crew member

* Land based personal includes everyone staying over at SANAE that is not a scientist

2. Experience at sea

Time spent at sea	Days		Weeks		Months	
Number of voyages	1st	2nd	3rd	4th	5th	6+

3. Motion sickness

Do you take motion sickness tablets?		*Do you use any other means to prevent motion sickness?*		*What medication or means to you use to combat motion sickness?*
Yes	No	Yes	No	

Figure 3.3: Personal details questionnaire - Antartica 2014/2015

Daily questionnaire: Day 64, Friday 05/02/2015

1. Motion sickness

Did you get motion sick?		*Did you vomit?*		*What is your illness rating on a scale of 0-3?* *(0 = nothing, 1 = slight, 2 = moderate, 3 = dreadful)*			
Yes	No	Yes	No	0	1	2	3

2. Three locations where you spent the most time today

	Zone	*Horizontal location*			*Hours spent*
1		Port	Middle	Starboard	
2		Port	Middle	Starboard	
3		Port	Middle	Starboard	

3. Slamming

Encountered slamming	No			Occasionally			Regularly		
Worst slamming incident rating *(1= nothing, 3 = slight, 10 = severe)*	1	2	3	4	5	6	7	8	9	10
Activity/equipment affected by slamming *(tick all the appropriate boxes)*	No			Typing/writing			Visual tasks (reading/TV)		
	Equipment use			Equip. damage			Sleeping		
Comments:									

Figure 3.4: Daily dairy questionnaire - Antartica 2014/2015

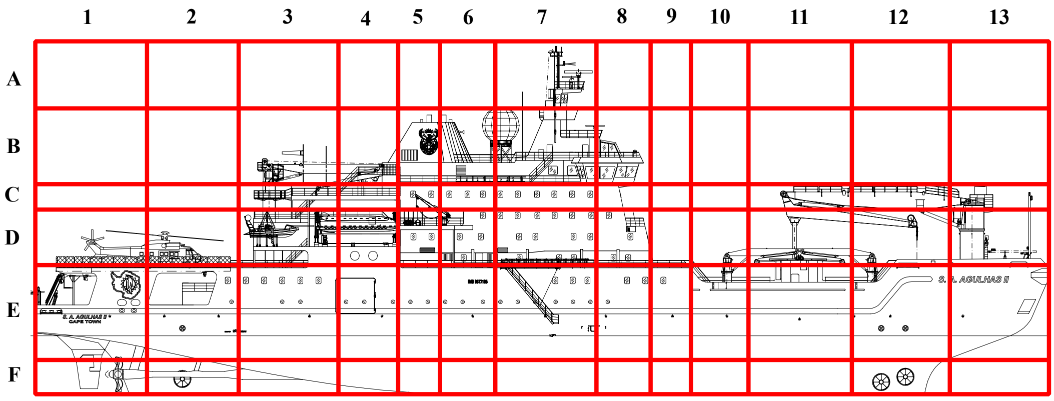

Figure 3.5: 78 Ship zones of the SAAII - Antartica 2014/2015

3.2.2 Results

A total of 98 passengers and 44 crew members were on board the ship at the start of the voyage, with a total of 7 crew members and 53 passengers responding. A total of 16 females, 30 males and 14 unknowns (aged between 20 to 60 with a mean age of 34 years old) participated in this questionnaire. 26.4 % of the respondents took motion sickness medication while 9.4 % used other means to combat motion sickness such as going outside, consuming ginger products or meditating, no wrist bands were used. See Figure 3.6 for details on the change in ship population size and number of respondent for the duration of the voyage.

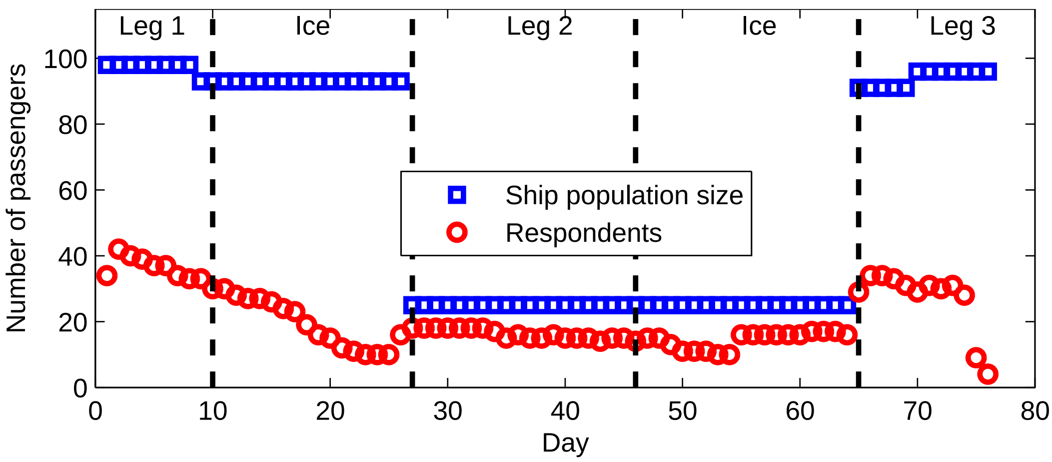

Figure 3.6: Number of respondents and passenger population size - Antartica 2014/2015

Collection of the questionnaires began at the end of Day 74 and continued to Day 76. The reponse rate of the questionnaire improved and ranged between to 29 % to 72 %, during open water. This resulted in confidence intervals between

0 % and 13 % compared to the Marion voyage which was between 9 % and 52 % (Refer to Figure 3.7).

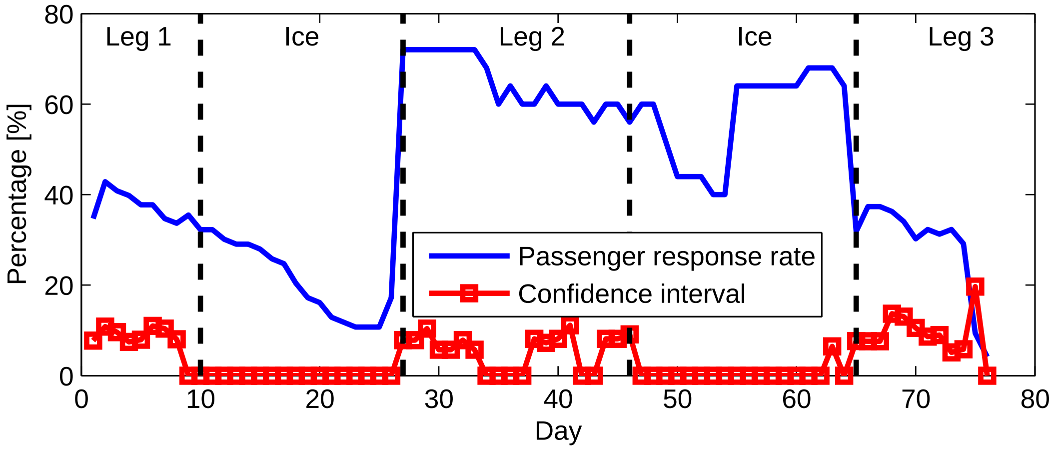

Figure 3.7: Confidence interval and passenger response rate - Antartica 2014/2015

Females were found to be more susceptible to motion sickness than males, see Figure 3.8. For 75 % of the daily motion sickness observations females reported more motion sickness than the male respondents. It can be seen, in Figure 3.9, that there is a trend where older males are less susceptible to motion sickness than younger males. Females tend to become more susceptible with increasing age, but since they only spanned over two age groups (in the *personal details questionnaire* there were five age groups ages 20-30, 30-40, 40-50 and 50+) there is insufficient data to make a conclusion. In other words there were no females above the age of 40.

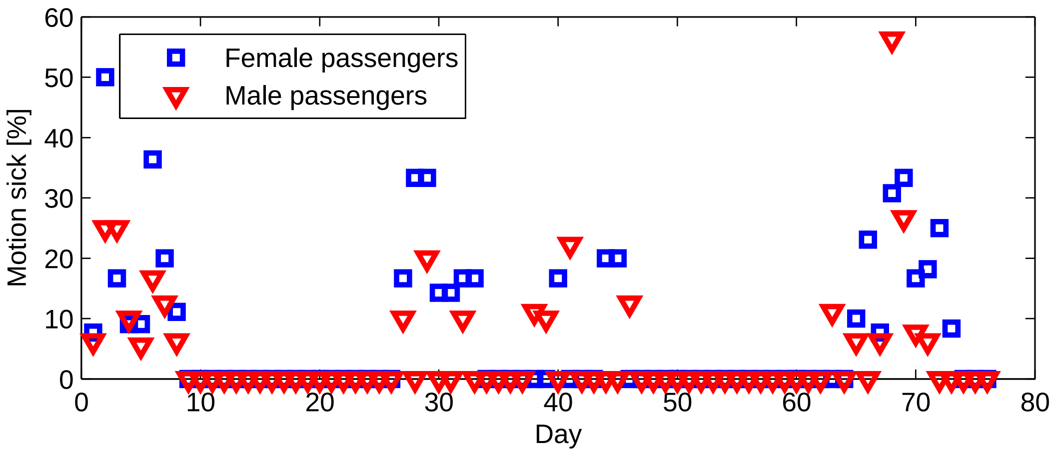

Figure 3.8: Inter-subject variability: Gender

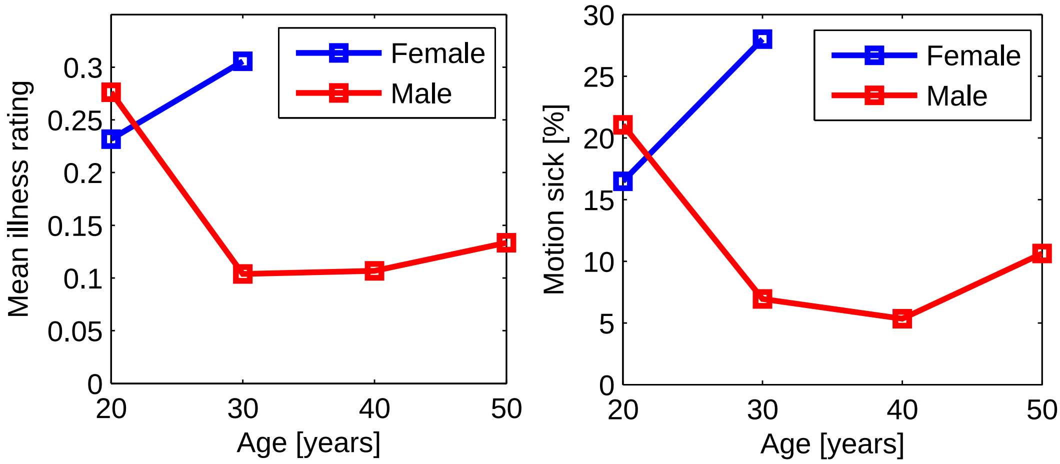

(a) Mean illness rating (b) Percent motion sick

Figure 3.9: Inter-subject variability: Age and gender

The ten locations most frequented according to survey responses are presented in Figure 3.10. Figure 3.10 (a) shows the time cumulatively logged by participants, spent in the top ten locations on board the ship. The first seven locations are focused around the accommodation area of the ship, location D5 to D8 are where passenger cabins are located. The frequency (number of times) logged for each location is shown in Figure 3.10 (b), the top three locations indicate that the accommodation area is the most frequently used followed by the monkey island / bridge (B8) and the laboratory area (E1) of the SAAII. Based on Figures 3.10 (a) and (b) passengers spent most their time in the accommodation area, especially on Decks 6 and 7 (locations D5 to D8). Some participants did not refer to a ship zone, but rather filled out question 2 (in the *personal details questionnaire*) with cabin, lounge or labratory.

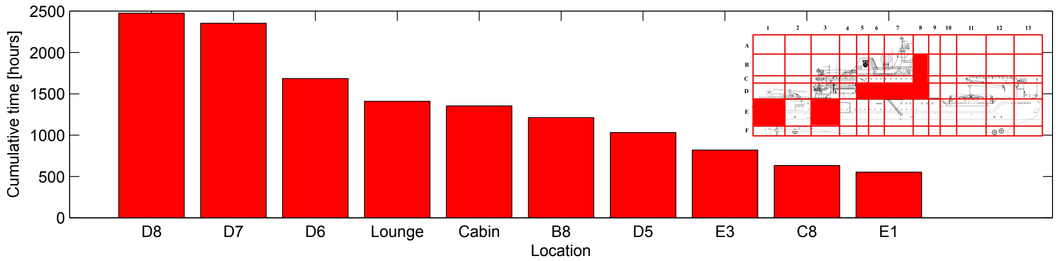

(a) Cumulative time logged at each location

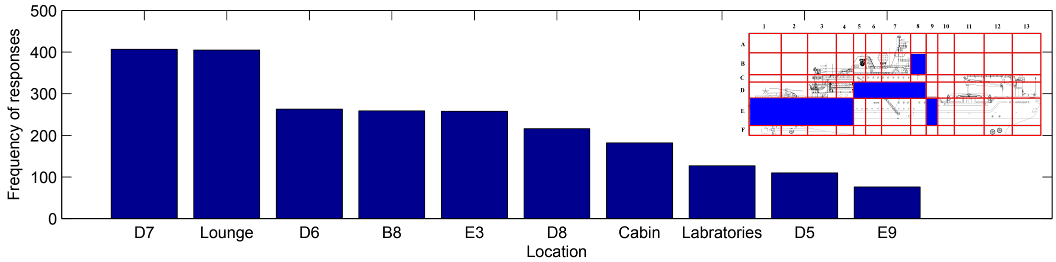

(b) Frequency of responses per location

Figure 3.10: Popular ship zones - Antarctica 2014/2015

No motion sickness was reported in ice except on Day 63 when an over-winter member from SANAE felt slightly ill on their first day on board the SAAII while the ship was stationary at the Antarctic ice shelf (refer to Point (a) in Figure 3.11). Figure 3.11 indicates that there is an increase in motion sickness within the first few days of each leg and a drop afterwards as the passengers adapt to motion sickness. The percentage of passengers who were motion sick reduced during Leg 2. During Leg 3 the percentage of passengers who were motion sick rose to higher levels than Leg 1. This could potentially mean that higher levels of acceleration occurred during Leg 3, this will be investigated in Chapter 6 where the daily $MSDV_z$ and r.m.s. accelerations will be plotted versus time.

Figure 3.12 indicates that there are similar levels of motion sickness during Leg 1 and 3. However during Leg 3 there was a higher level of motion sickness in the land based passengers than the ship based passengers, which could indicate that the passengers have adapted to motion sickness as a result of being on the ship for the duration of the voyage.

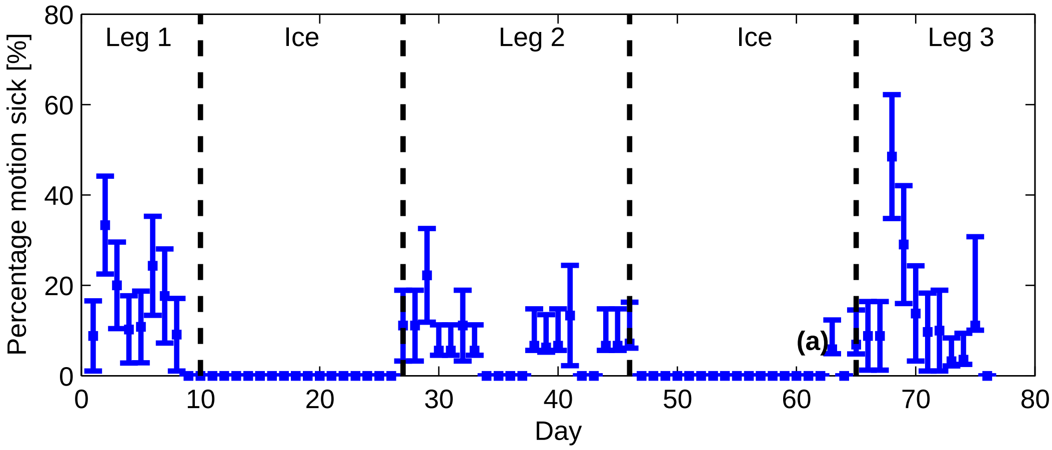

Figure 3.11: Effect of confidence interval on the percentage of motion sick passengers - Antarctica 2014/2015

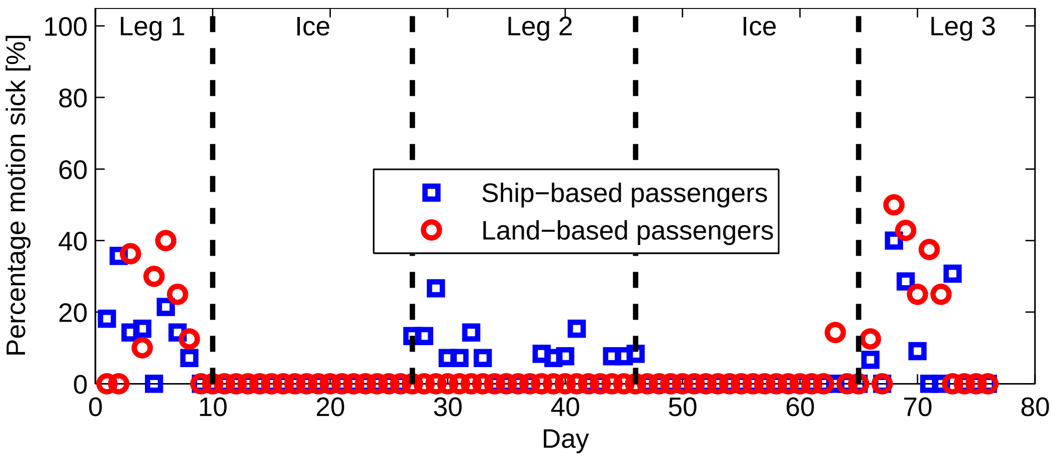

Figure 3.12: Comparison of ship based and land based passengers - Antarctica 2014/2015

Chapter 4

Full scale measurements: SA Agulhas II voyage to Marion (2014)

Full scale measurements were conducted on board the SA Agulhas II during its 35 day annual relief voyage to Marion Island from the 2 April to 6 May 2014. The ship operated in open water during this voyage which comprised of three legs; the departure leg, an oceanographic leg and the return leg to Cape Town. This full scale measurement served three separate projects, each project investigated by a member of the Sound and Vibration Research Group (SVRG) of Stellenbosch University.

The first project, which is the focus of this thesis, was to determine;

- The magnitude and direction of low frequency motion of the ship.
- The effect this motion has on the motion sickness incidence of occupants.
- Whether different locations on board the ship has an effect on the motion sickness incidence.

The second project was to determine the effects of slamming on human comfort, equipment and the structural integrity of the ship. The third project was to determine the operational mode shapes of the ship, the relationship between levels of vibration and operational conditions of the ship.

Logistical arrangements, such berth as allocation, for the voyage were planned and allocated by the Department of Environmental Affairs (DEA). The SVRG was involved during the later stages of the planning of the voyage as a result no berths were allocated to the group. This was accounted for during the implementation of these projects.

4.1 Voyage description

The 2014 annual relief voyage to Marion Island was dedicated to logistics and science. During logistical operations passengers, cargo and luggage are flown from the ship to Marion Island. These passengers mostly included the Marion Island relief team, engineers, Department of Public works, mammologists and geologists. Passengers staying on board the ship mostly included marine biologists, geochemists and oceanographers.

The voyage, described using the GPS coordinates shown in Figure 4.1, is summarised as follows;

- The ship departed from Cape Town (A) on 2 April.
- Between 2 April and the 5 April, was the Cape Town (A) to Marion Island (B) leg of the voyage. During this leg various oceanographic science experiments were conducted. These scientific experiments ranged from measuring ocean water conductivity, temperature and depth by using various instruments such as; Conductivity, Temperature and Depth (CTD), Underway Conductivity, Temperature and Depth (UCTD) and Expendable Bathy Thermograph (XBT).
- Logistical activities began upon arrival at Marion Island (B) from 6 to 9 April. Logistics include cargo deployment, helicopter flights to transport passengers and luggage to Marion Island. This reduced the overall population size of the passengers staying on board the ship.
- The ship departed for the oceanographic leg of the voyage between 10 April and 25 April, as shown in Figure 4.1 (Points B to C). CTD's, UCTD's and XBT's were deployed for the duration of this leg.
- The ship returned to Marion Island (D) on 26 April and began logistical operations which lasted until 30 April. The 2013 overwintering team was relieved and all other passengers were flown onto the ship, which increased the overall population size.
- The return leg to Cape Town began on 1 May and ended upon arrival at Cape Town (E) on 6 May. During this leg CTD's, XBT's and UCTD's were deployed.

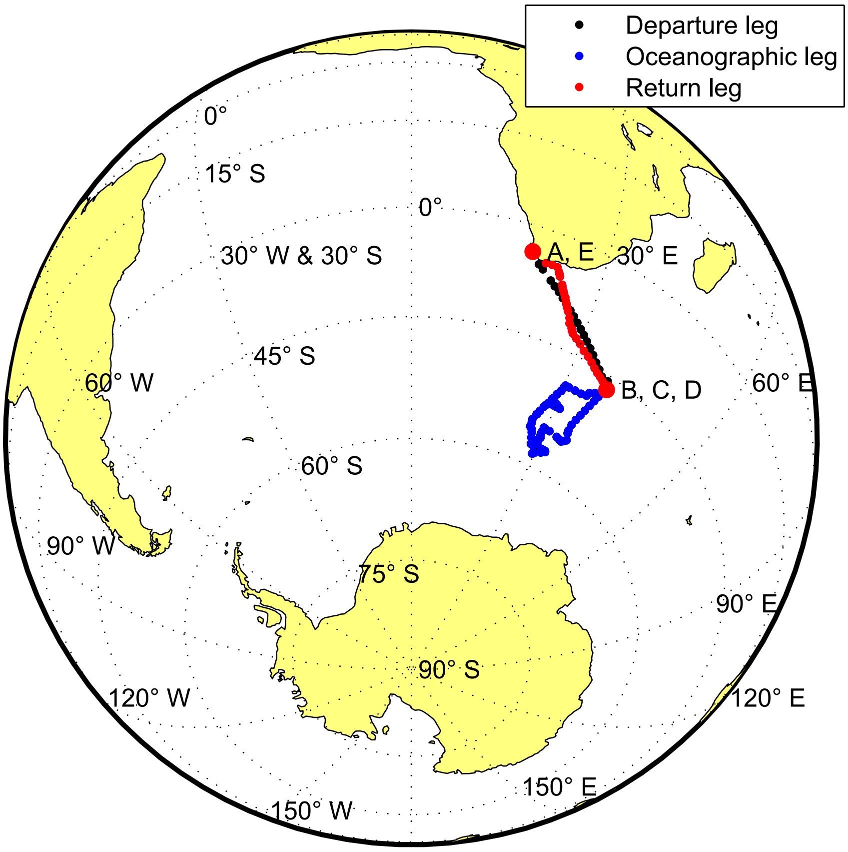

Figure 4.1: GPS Coordinates - Marion 2014

4.2 Measurement software and hardware

A total of 19 measurement channels were used and consisted of; 7 Direct Current (DC) accelerometers, 3 seismic accelerometers and 9 Integrated Circuit Piezoelectric (ICP) accelerometers. Accelerometers were placed in the same or similar positions as done in previous work by Soal (2014) on board the SA Agulhas II. Three LMS Supervisory Control and Data Acquisition Systems (SCADAS) were distributed throughout the ship each with a limited amount of channels for the measurement of acceleration. Each accelerometer was connected to the SCADAS via low noise co-axial teflon cables.

The software used to measure and save the data for the duration of the voyage was LMS Test.Lab 13A Turbine Testing. This software is capable of capturing multi-channel measurements continuously throughout the voyage. A sample rate of 2048 Hz was selected and measurements were coordinated by setting the computer clock time to Coordinated Universal Time (UTC). Every 5 minutes data was stored in a LDSF file format. The measurement system started to record the day before the departure of the SA Agulhas II (SAAII), since the day of departure passengers were only allowed on board the SAAII.

Since no team member from the SVRG were allocated berths on board the ship for the Marion voyage, a crew member from Smit Amandla was trained to operate the measurement system. An instruction manual was placed on the desktop of the computer with instructions on how to restart the system in the event of a system crash. The crew member was instructed to check on the system to see if it was still running at his convenience.

4.3 Measurement setup

The SAAII was instrumented with seven single axis PCB 3711B1110G DC accelerometers, with a nominal sensitivity of $20.4\,\mathrm{mV/(m/s^2)}$, measurement range of $98.1\,\mathrm{m/s^2}$ and a frequency range of 0 kHz to 1 kHz. To determine the rigid body motion of the ship which includes the angular velocity, translational and angular acceleration about all three axes, a six accelerometer array was used (slightly different from that discussed in Chapter 2). The array shown in Figure 4.2 is located on Decks 2 and 4 where x-,y- and z represent an accelerometer as well as its direction of measurement. The array consists of three points namely, Points 0, 1 and 2. Point 3 did not form part of the array but served to analytical solutions of the rigid body motion of the ship.

The ship is assumed to be rigid below 1 Hz (Pisula *et al.* (2012)). Soal (2014) and STX Finland (2010) determined the first resonant frequency to be 2.60 Hz and 1.94 Hz respectively which is associated to the first bending mode about the y-axis.

ISO 2631-1 (1997) states that the Motion Sickness Dose Value (MSDV) is to be determined on the surface where occupants are located. But the placement of these seven accelerometers were far from any accommodation area, however using the rigid body assumption acceleration levels could then be determined at frequently used passenger locations, such that MSDV along with the Percentage Vomiting (PV) can be predicted. It should be noted that the placement of the accelerometers were limited to cable routing already in place.

All surfaces were cleaned with acetone and accelerometers were glued to mounting blocks, using super glue. The mounting blocks were glued to rigid surfaces or the frame of the ship to ensure that local deformation is negligible. All accelerometers and cables were checked to determine whether they function correctly in the Structural Laboratory of the Department of Mechanical and Mechatronic Engineering of Stellenbosch University. A summary of the equipment is presented in Appendix C.

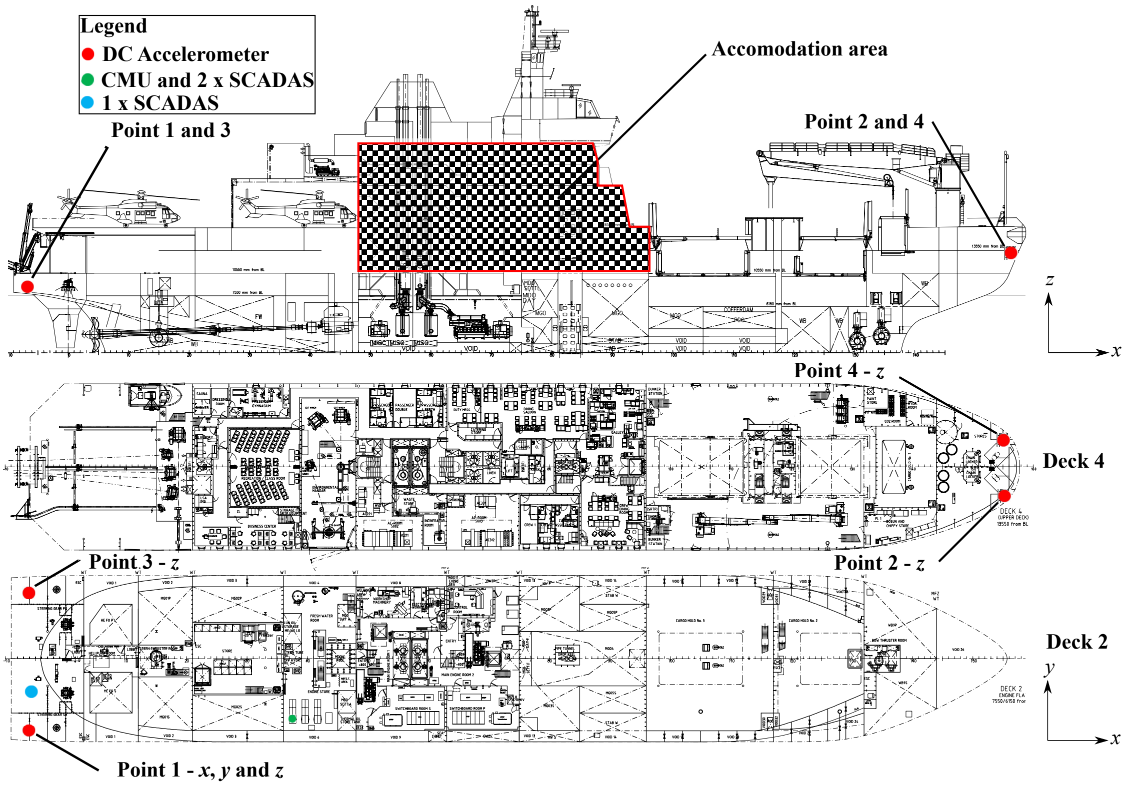

Figure 4.2: Measurement setup - Marion 2014

4.4 Vibration analysis

A total of 5939 files (20.6 days worth of measurements) were generated during the voyage. Each file was saved as LDSF format. This indicates that a total of fifteen days worth of data were not captured successfully. An Excel macro, written by LMS (a Siemens business), was used to convert the LDSF files to .mat files. Each .mat file contained data for every channel. Each channel was stored as a structure format. The structure stores vital information about each channels such as; the sample time, units of measurement, channel type, channel number, direction, sample size and the time the measurement began (creation time).

To verify whether the data measured was reliable, the absolute unweighted maximum acceleration values from each 5 min .mat file was determined for all seven accelerometers in the array. These maximum values were plotted against time to identify peak values for each 5 min interval. These peak values were then check for overloads, which were identified if the accelerometer exceeded its measurement range (clippling) or saturated.

Points 2 and 3 in Figure 4.2, were determined to be unreliable as they frequently overloaded. Both these Points were vital in validating the six accelerometer array and determining rigid body motion. Since these channels were unreliable, determining the angular velocity, lateral and angular acceleration of the ship was not possible. The crest factors and weighted (W_f for vertical and W_{dg} for lateral acceleration) r.m.s. acceleration for both points are displayed in Figures 4.3 to 4.4 (for each measurement file), the remaining crest factors and r.m.s. are presented in Appendix D.

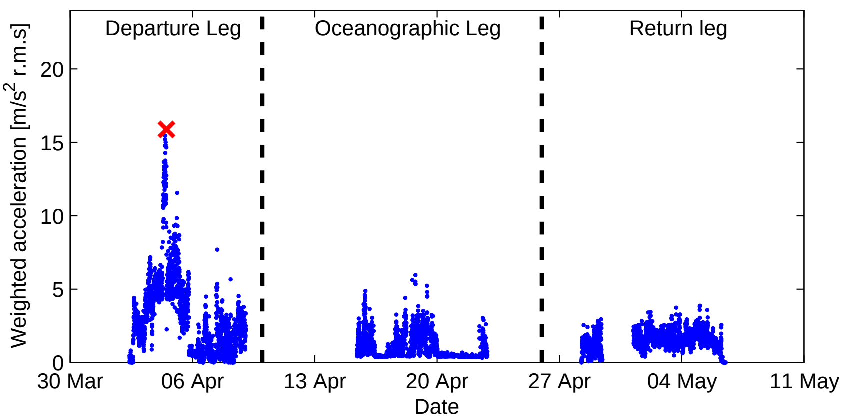

(a) Point 2 - y direction

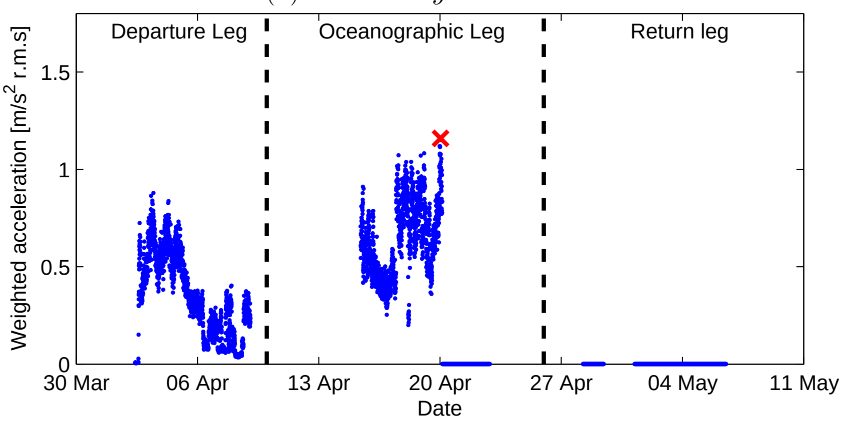

(b) Point 3 - z direction

Figure 4.3: Weighted (a) vertical (W_f) and (b) (W_{dg}) lateral r.m.s. acceleration - Marion 2014

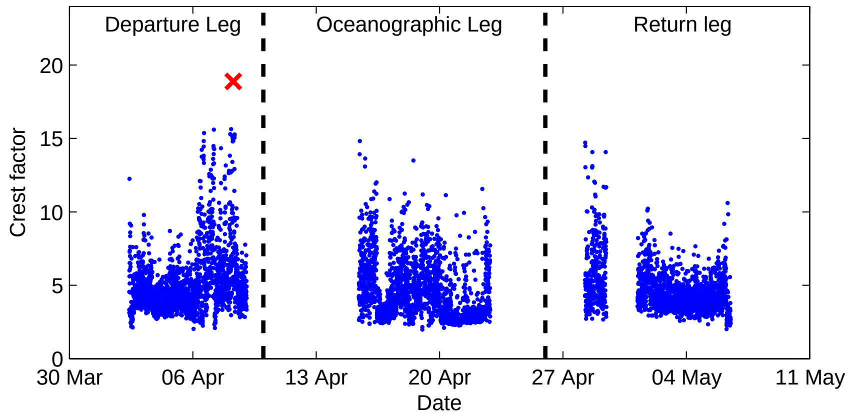

(a) Point 2 - y direction

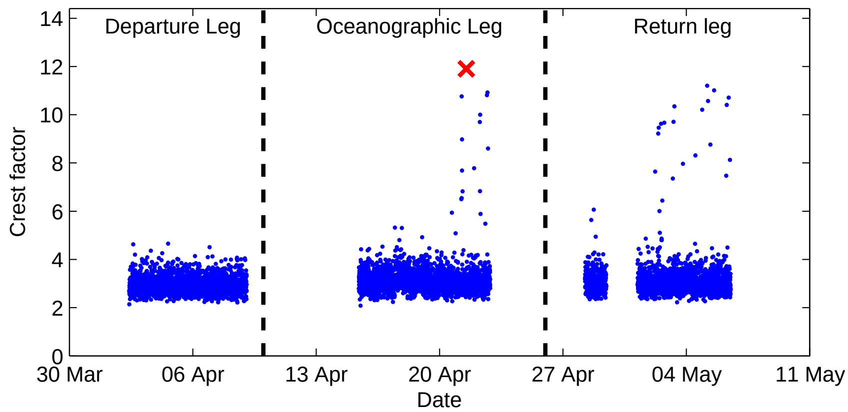

(b) Point 2 - z direction

Figure 4.4: Weighted (a) vertical (W_f) and (b) (W_{dg}) lateral crest factor - Marion 2014

4.5 Discussion

A crew member was instructed only on how to restart the measurement computer and not how to identify problems with the data acquisition system and sensors. Even if a crew member was trained it required a dedicated person to troubleshoot problems with the sensors, since the crew member was only able to check the system at his own convenience (since crew members are extremely busy with their own work). The system is at risk of being neglected and any problems with the sensors would not be resolved. As a result 15 days worth of data was not recorded and 2 channels were unreliable for data analysis.

Determining acceleration levels at any position on the ship via rigid body simulation was no longer possible thus; the motion sickness dose values, PV, and Illness Rating (IR) could only be determined at the bow and stern of the ship.

These locations are not likely to be frequented by human occupants. To reduce the risk of unreliable channels the system needed to be supervised twice daily by a dedicated, experienced member from the SVRG. Therefore the success of the relief voyage to Marion Island (2014) was limited by the lack of researchers on board to administer the measurement system.

Chapter 5

Full scale measurements: SA Agulhas II voyage to Antarctica (2014/2015)

Full scale measurements were conducted on the SA Agulhas II (SAAII) during the Antarctica 2014/2015 relief voyage. The voyage began on 4 December and ended on 17 February 2015. This chapter describes the voyage, measurement software and hardware, measurement setup and vibration analysis according to ISO 2631-1 (1997).

5.1 Voyage description

The SAAII's voyage to Antarctica lasted 76 days and was divided up into three open water legs and two ice legs. For the purposes of this study only data from the three water legs (Leg 1, Leg 2 and Leg 3) were used. Refer to Figure 5.1 in conjunction with the following voyage description;

- 4 December: The SAAII was in the harbour, at the V&A Waterfront (a), as a result of delays and strong winds.
- 5 December to 13 December: Leg 1 (a-c) was under way. On Day 2 the questionnaires were handed out to passengers and crew members. A team of scientists were dropped off at Bouvet Island (b) on Day 9. Various oceanographic science experiments were underway, with the purposes of measuring ocean temperature, depth, conductivity and iron concentration in the ocean.
- 14 December to 29 December: The first leg in ice (c-d) where the land-based personnel are flown to SANAE and various logistical operations were undertaken such as flying small cargo to SANAE and offloading

large cargo on the ice shelf. On Day 26 a reminder to fill in the questionnaires was posted on the information boards around the SAAII. The new over-wintering team and various other passengers departed from the SAAII, to either return to Cape Town via a flight or the following Antarctica voyage. Two new passengers, which flew in from Cape Town, boarded the ship.

- 30 December to 18 January: Leg 2 (d-f) known as the "buoy run" was under way. The various oceanographic science experiments were the same for Leg 1. The SAAII arrived at South Georgia (e) on Day 34, where passengers spent approximately 6 hours on land.

- 19 January to 6 February: The second ice leg (f-g) began, logistical operations continued. Land based personnel, except for the nine new over-wintering team boarded the SAAII.

- 7 February to 17 February: This was the third and last leg (Leg 3) of the voyage (g-i). The scientists on Bouvet (h) boarded the SAAII on day 70 and oceanographic science continued as per Leg 1 and 2.

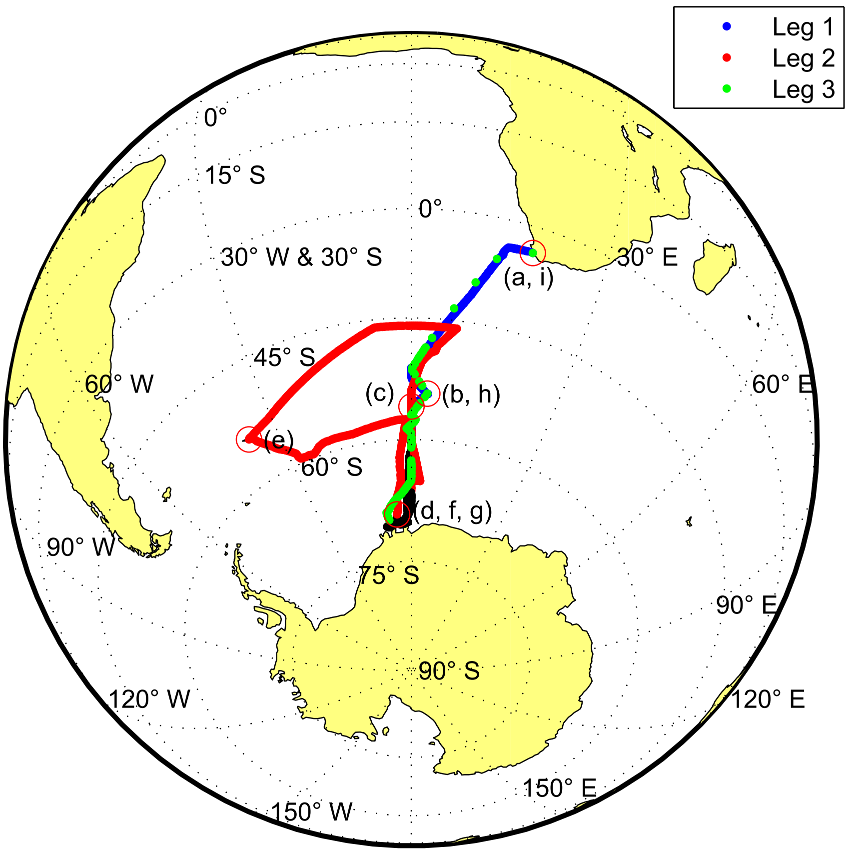

Figure 5.1: GPS Coordinates - Antarctica 2014/2015

5.2 Measurement software and hardware

The measurement software and hardware for the instrumentation of the vessel is summarised in Table 5.1. Acceleration was measured in five different locations on the SAAII as described in Section 5.3.

Table 5.1: Key measurement equipment

Equipment	Description
2 x LMS SCADAS	16 Channel
1 x LMS SCADAS	12 Channel
8 x PCB DC accelerometers	20.4 mV/(m/s^2) nominal sensitivity, 0 kHz to 1 kHz frequency range, ±98.1 m/s^2 measurement range, −54 °C to 121 °C operating temperature and a 0.0012 m/s^2 r.m.s. broadband resolution
1 x Measurement laptop	LMS Test.Lab 11A Turbine Testing software

The total measurement setup comprised of three LMS SCADAS which were used in a master-slave setup to allow for data acquisition in multiple locations and the simultaneous measurement of thirty-six accelerometers and eight strain gauges. The software used for continuous measurements was LMS Test.Lab 11A Turbine Testing. The eight PCB DC accelerometers (Model number 3711B1110G) were used to measure the linear acceleration of the SAAII. DC signal conditioners were custom designed, built and tested by members of the Sound and Vibration Research Group (SVRG). The accelerometers were calibrated in-house by the SVRG on a Svantek SV 111 Vibration Calibrator, designed according to ISO 8041, via the r.m.s. method (refer to Appendix D).

The LMS SCADAS have built in digital anti-aliasing with a cut-off frequency at 80 % of the bandwidth. The SCADAS has a 24-bit analogue to digital conversion and a 150 db dynamic range.

The software was set up to measure, for the duration of the 76 day voyage, save measured data every five minutes at a sample rate of 2048 Hz. However the system is not robust and the software crashed approximately every five days. To prevent a huge loss of data the measurement system was checked twice daily.

A sample rate of 2048 Hz was chosen because a minimum sample rate of 900 Hz was needed to satisfy the tolerances of the whole body weighting requirements described by Rimell and Mansfield (2007). The measurement duration of 300 s was selected for the following reasons;

- A confidence level greater than 90 % for a lower limiting frequency of 0.5 Hz assuming the data is random stationary (ISO 2631-1, 1997).

- For comparison with the data measured on the Central Measurement Computer (CMU), which stores data every five minutes (Soal, 2014).

5.3 Measurement setup

Eight uni-axial DC accelerometers were spread out in an array consisting of five different measurement locations across the SAAII as seen in Figure 5.2. Points 0, 1 and 2 were selected to comply with the modified six accelerometer array defined in Chapter 6. Points 3 and 4 are redundant accelerometers in this array and were used solely for the verification of the modified six accelerometer array.

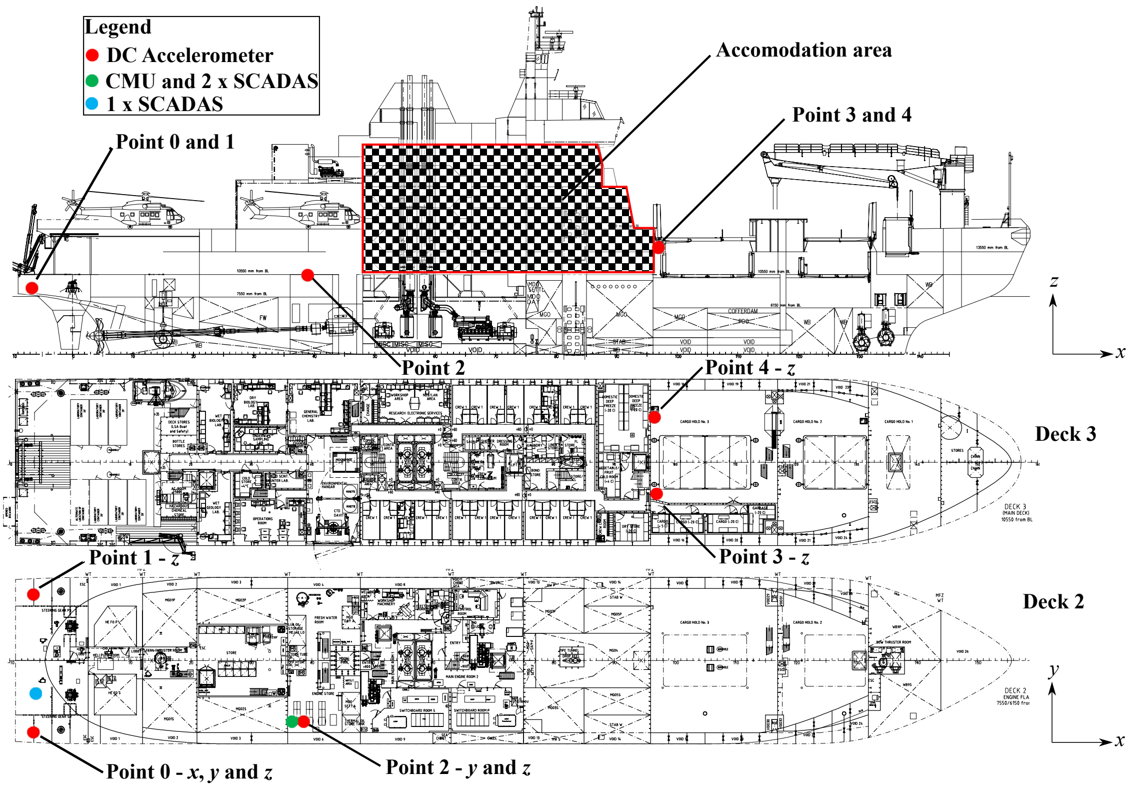

Figure 5.2: Measurement setup - Antarctica 2014/2015

Figure 5.3 shows the measurement positions on the SAAII. Each accelerometer was mounted on an aluminium mounting block with super glue, which was mounted to the hull and super structure of the ship using super glue. This was to minimize or eliminate any local deformation between 0 and 1 Hz. Mounting positions were selected to minimize human contact and interference (such as footsteps), such as the girders of the roof or in hard to get places on the floor, cargo hold, engine store room, port and starboard stern thruster room.

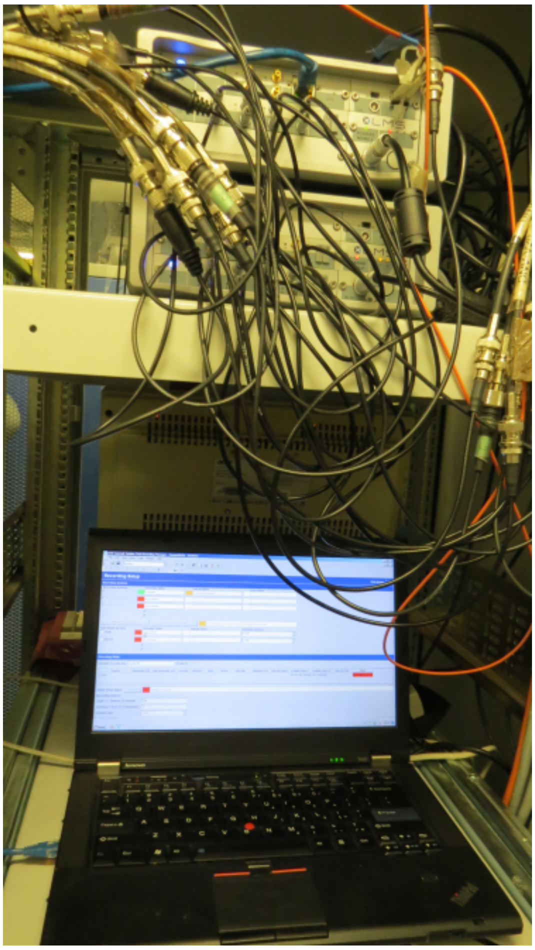

(a) Measurement laptop

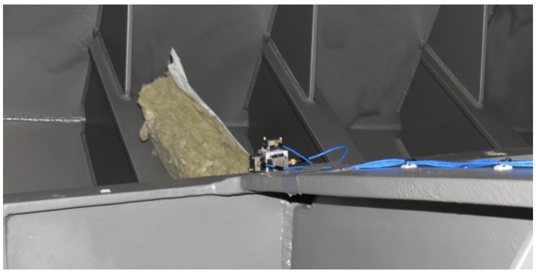

(b) Point 0 (x, y and z) - Starboard steering gear room

(c) Point 1 (z) - Port steering gear room

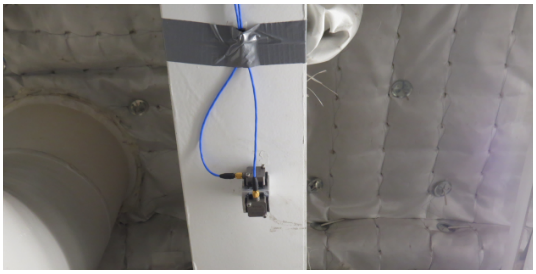

(d) Point 2 (y and z) - Engine store room

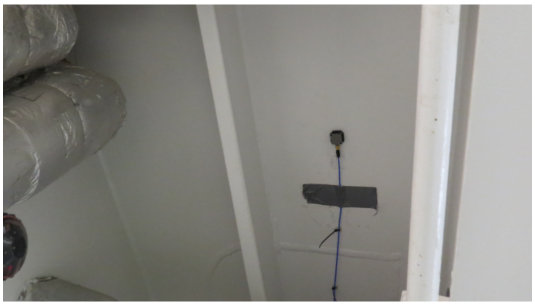

(e) Point 3 (z) - Starboard cargo hold

(f) Point 4 (z) - Port cargo hold

Figure 5.3: Measurement locations - Antatrica 2014/2015

5.4 Vibration analysis

The daily Crest Factor (CF) and weighted r.m.s. acceleration for the most popular locations, found in Chapter 3, D6 to D8 (z-axis only) are shown in Figures 5.4 to 5.5. Appendix D presents the CF and weighted r.m.s acceleration for each channel. The largest r.m.s. acceleration levels recorded at locations D6 ($0.532\,\mathrm{m/s^2}$) and D7 ($0.586\,\mathrm{m/s^2}$) was on the 13th of January, while the ship was in rough seas (sea state 9 on the Beaufort scale, 4 m-6 m swell). The crest factors tend to be less than 9 during the open water stages of the voyage. According to ISO 2631-1 (1997) if the crest factor is below 9 the acceleration time history is not considered impulsive and r.m.s. can be used (for comfort). The crest factors are higher in ice than in open water. During the ice legs of the voyage the weighted r.m.s. acceleration levels are almost negligible.

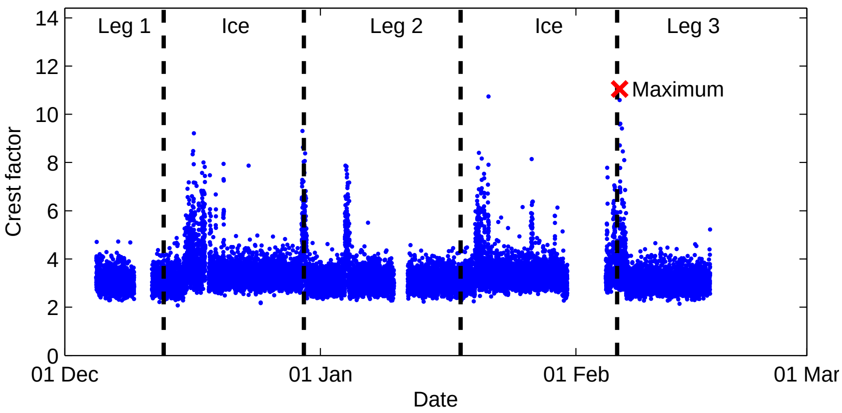

Figure 5.4: Crest factor (D6) - Antarctica 2014/2015

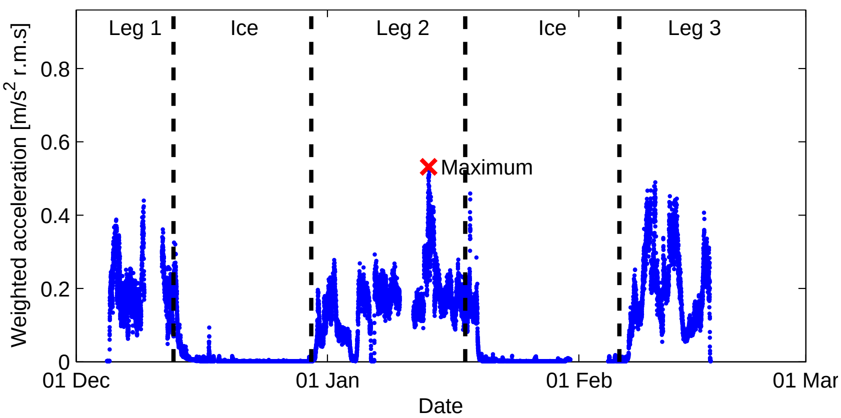

Figure 5.5: Weighted r.m.s. (D6) - Antarctica 2014/2015

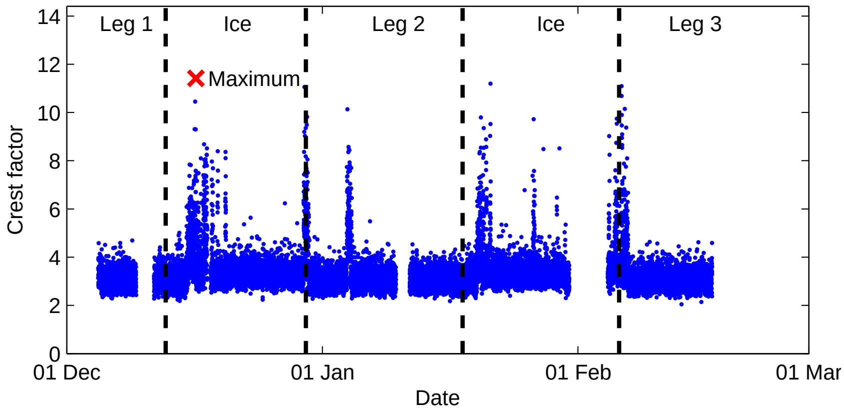

Figure 5.6: Crest factor (D7) - Antarctica 2014/2015

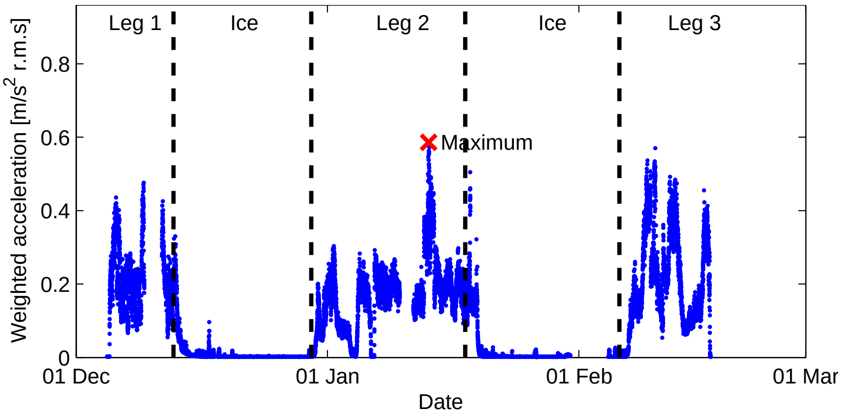

Figure 5.7: Weighted r.m.s. (D7) - Antarctica 2014/2015

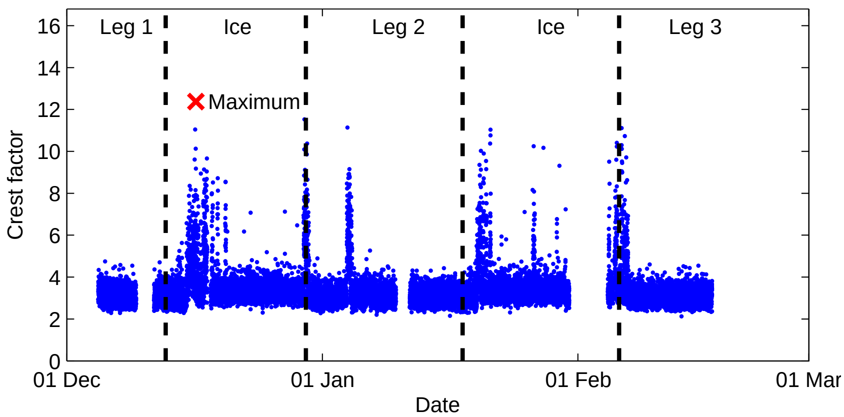

Figure 5.8: Crest factor (D8) - Antarctica 2014/2015

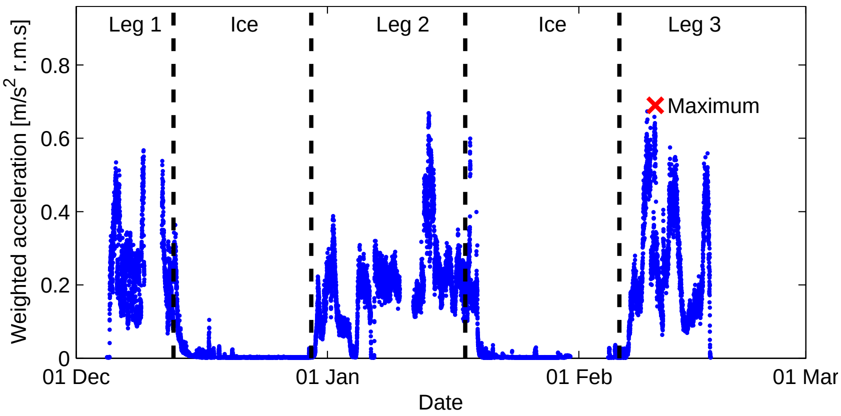

Figure 5.9: Weighted r.m.s. (D8) - Antarctica 2014/2015

Chapter 6

Rigid body motion of the SAAII

The six accelerometer array used to measure the rigid body motion of the SA Agulhas II (SAAII) in Chapter 5 did not satisfy the requirements of the six accelerometer array defined in Chapter 2. Hence, a modified six accelerometer array was developed. The development and testing of this modified six accelerometer array follows in this Chapter.

6.1 Modified six accelerometer array

The modified six accelerometer array in Figure 6.1 applies to the full-scale measurement array used on the SA Agulhas II during the 2014-2015 Antarctica voyage. The difference between this particular array and the six accelerometer array by Padgaonkar *et al.* (1975) is that Point 2 is neither required to be co-planar or orthogonal to Points 1 and 0.

The Cartesian coordinates for Points 0, 1 and 2 are;

$$\boldsymbol{r}_1 = 0\mathbf{i} + r_{y1}\mathbf{j} + 0\mathbf{k} \tag{6.1}$$

$$\boldsymbol{r}_2 = r_{x2}\mathbf{i} + r_{y2}\mathbf{j} + 0\mathbf{k} \tag{6.2}$$

$$\boldsymbol{r}_0 = 0\mathbf{i} + 0\mathbf{j} + 0\mathbf{k} \tag{6.3}$$

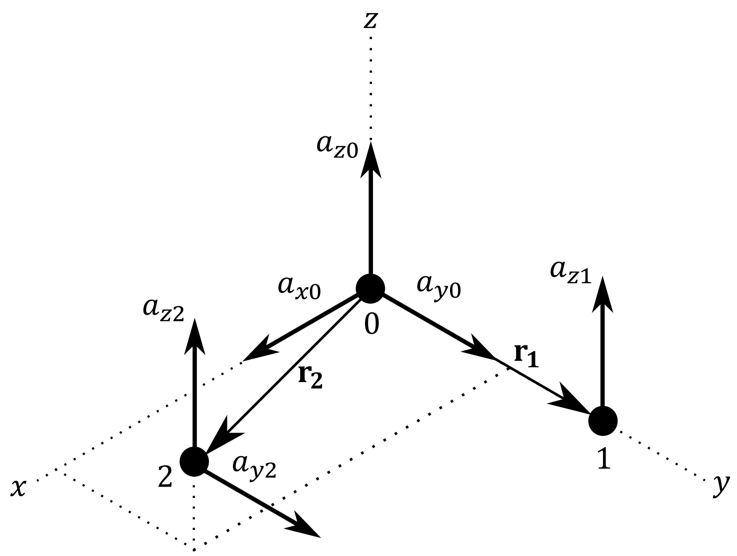

Figure 6.1: Modified six accelerometer array

Equations 6.1 to 6.3 combined with 2.21 reduces 2.20 to;

$$\alpha_x = (a_{z1} - a_{z0})/r_{y1} - \omega_y\omega_z \tag{6.4}$$

$$\alpha_y = -[a_{z2} - a_{z0} - \alpha_x r_{y2} - \omega_z(\omega_x r_{x2} + \omega_y r_{y2}) + r_{z2}(\omega_x^2 + \omega_y^2)]/r_{x2} \tag{6.5}$$

$$\alpha_z = [a_{y2} - a_{y0} - \alpha_x r_{z2} - \omega_y(\omega_z r_{z2} + \omega_x r_{x2}) + r_{y2}(\omega_x^2 + \omega_z^2)]/r_{x2} \tag{6.6}$$

6.2 Determining the rigid body motion of the modified six accelerometer array

As mentioned previously in this chapter solving for $\boldsymbol{\alpha}$ requires a stepwise numerical iterative scheme. A flow diagram of the Matlab code used to numerically solve for $\boldsymbol{\omega}$, $\boldsymbol{\alpha}$ and $\boldsymbol{A}_p$ follows in Figure 6.3, of which the code (`modified6_acc_array.m`) can be found in Appendix E.

6.2.1 Detrending, decimating and low pass filtering the data

Prior to loading (`aXXXXXXXa.mat`, a 300 second data recording on the SAAII) the acceleration data was detrended, decimated then low-pass filtered. Matlab's detrend function (`detrend.m`) removes the best linear fit (of the data) from the data. The purpose of (`detrend.m`) is to eliminate any DC offsets and eliminate drift (assuming that it is linear). The acceleration data was then down sampled from a sample rate of 2048 Hz to 32 Hz. An 8$^{\text{th}}$ order Butterworth low-pass filter with a cut-off frequency of 1 Hz was applied to the data. Various orders of the Butterworth filter are compared in Figure 6.2. The final low-pass filter was selected for the following reasons;

- Matlab offers various other filter such as; Chebyshev (Type-I and Type-II) and elliptic, but the Butterworth filter was preferred as it has reduced pass- and stop-band ripples (Ronald and Mills, 2004).
- It was assumed by Pisula *et al.* (2012) that rigid body motion of the ship occurred below 1 Hz, thus a cut-off frequency of 1 Hz was chosen.
- The first bending mode of the SAAII was found to be 1.94 Hz by Soal (2014) via Operational Modal Analysis (OMA). Thus it is reasonable to assume that rigid body motion occurs below 1 Hz.
- A eighth order Butterworth filter ensured that the frequency content below 1 Hz was unaffected by the filter and any frequency content above 1 Hz is reduced to a negligible amplitude.

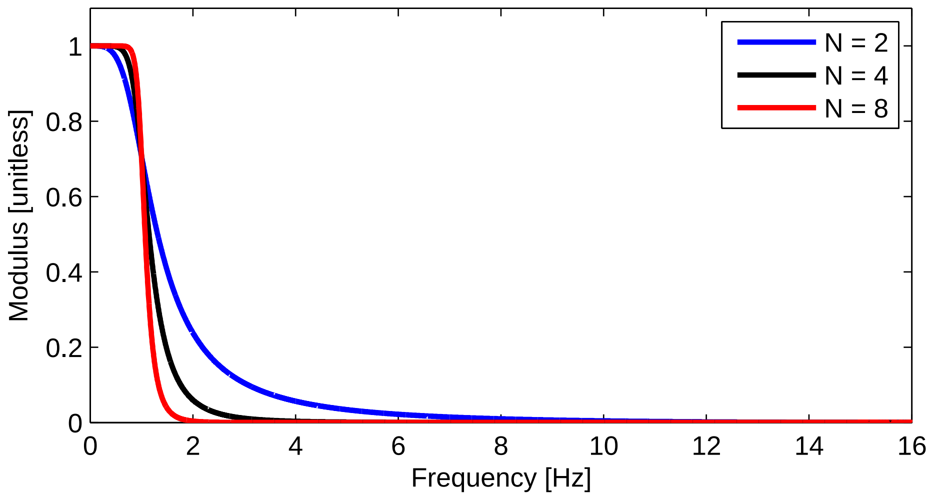

Figure 6.2: Second, fourth and eighth order low-pass Butterworth filters with a cutoff frequency of 1 Hz

6.2.2 Flow diagram

Firstly a .mat file (`aXXXXXXXa.mat`) is loaded which includes acceleration data of Points 0 to 4 namely; a_{0x}, a_{0y}, a_{0z}, a_{1z}, a_{2y}, a_{2z}, a_{3z} and a_{4z}. Simultaneously the Cartesian coordinates ($\boldsymbol{r}_0$, $\boldsymbol{r}_1$, $\boldsymbol{r}_2$, $\boldsymbol{r}_3$ and $\boldsymbol{r}_4$) are of Points 0 to 4 are loaded. The inputs to `modified6_acc_array.m`, are the measured accelerations from Points 0, 1 and 2, the Cartesian coordinates of Points 1 and 2 as well as the time step (`dt`) and number of iterations (`niter`). The Cartesian coordinates were determined by digitizing a technical drawing of the SAAII with marked sensor locations.

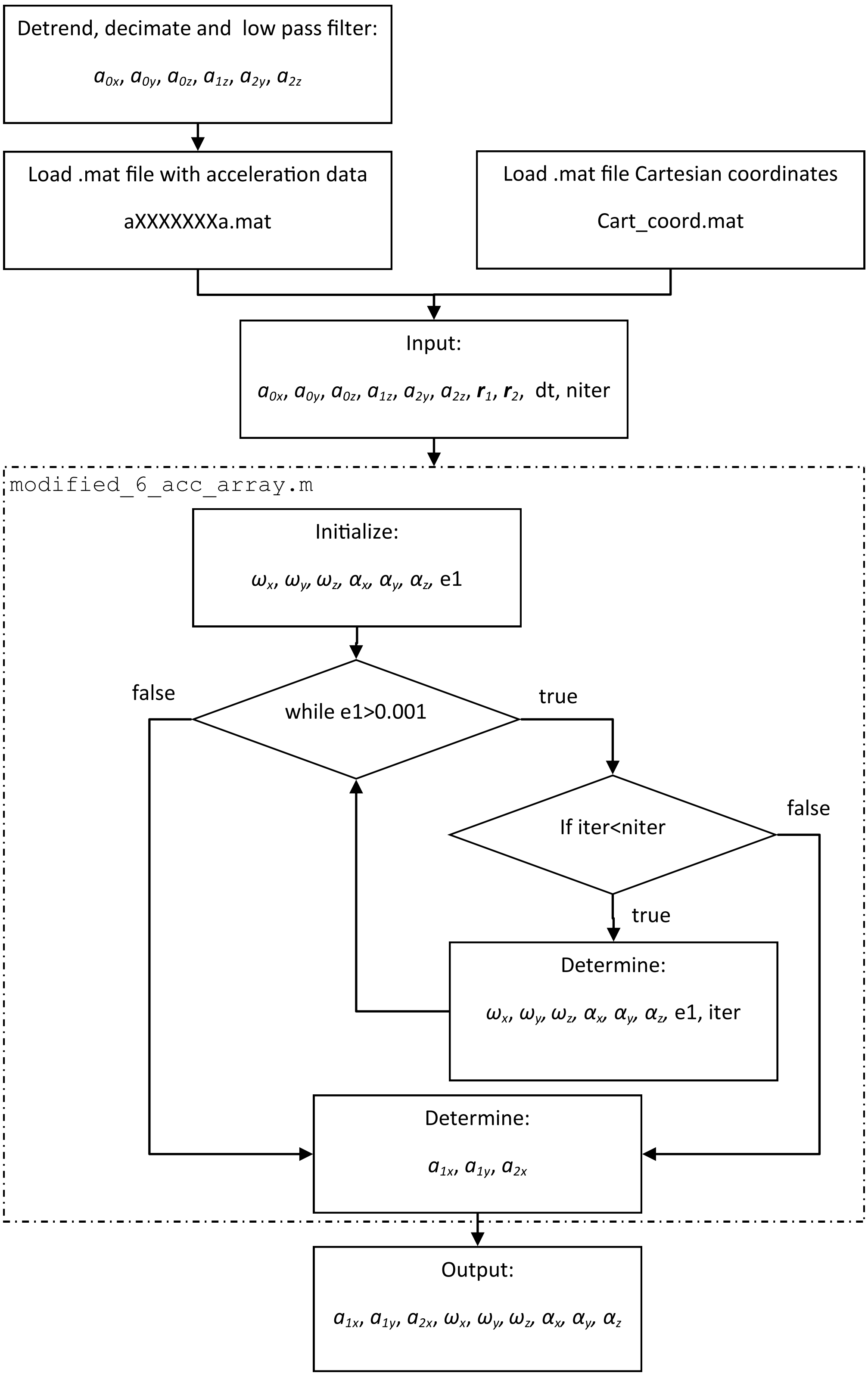

Figure 6.3: Flow diagram for determining rigid body motion

Within `modified6_acc_array.m` $\boldsymbol{\omega}$ and $\boldsymbol{\alpha}$ are initialized to zero, $\boldsymbol{\alpha}$ is then determined using equations 6.4 to 6.6 and substituting the initial values of $\boldsymbol{\omega}$. By integrating $\boldsymbol{\alpha}$, $\boldsymbol{\omega}$ is determined, these new values of $\boldsymbol{\omega}$ are then substituted back into $\boldsymbol{\alpha}$. This process repeats itself until either the maximum number of 100 iterations (`niter`) is reached or an error tolerance (`e1`) is satisfied. The error between previous and current iteration steps is determined by using the root mean squared error method. Once $\boldsymbol{\omega}$ and $\boldsymbol{\alpha}$ are known, then the acceleration of any Point p can be determined using equation 2.20.

6.3 Validation of the modified six accelerometer array

To demonstrate the reliability of the six accelerometer array a two-step validation procedure was used. The same two-step validation procedure was used by Padgaonkar *et al.* (1975). The procedure requires the validation by means of hypothetical and experimental data.

6.3.1 Validation by hypothetical data

Since the SAAII is unconstrained in its motion about all degrees of freedom, a set of hypothetical data was generated with angular acceleration about all three axes as well as translational acceleration $\ddot{\boldsymbol{R}}$ in all three directions. A set of hypothetical acceleration data was generated. The set was sinusoidal and was the same order of magnitudes based off ship motion measured by Lawther and Griffin (1986). The hypothetical Cartesian coordinates used for Points 1 and 2 were the same as the measurement setup of the SAAII in Figure 5.2.

A flow diagram depicting the process of determining the process of validating the modified six accelerometer array is shown in Figure 6.4. First sinusoidal data for ω_x, ω_y, ω_z, α_x, α_y and α_z is generated at a frequency of 0.1 Hz and a duration of 300 s. Table 6.1 summarises the magnitudes used for ω_x, ω_y, ω_z, α_x, α_y and α_z. The coordinates for Point 1 and Point 2 are $\boldsymbol{r}_1 = [0\mathbf{i}, 18.39\mathbf{j}, 0\mathbf{k}]$ m and $\boldsymbol{r}_2 = [36.36\mathbf{i}, 0.58\mathbf{j}, 1.71\mathbf{k}]$ m with respect to Point 0 (Point 0 is taken as the origin of the vessel).

ω_x, ω_y, ω_z, α_x, α_y, α_z, $\boldsymbol{r}_1$ and $\boldsymbol{r}_2$ are used to determine a_{1z}, a_{2y} and a_{2z} using equation 2.20. The Matlab function `modified6_acc_array.m` is used to predict ω_x, ω_y, ω_z, α_x, α_y and α_z using a_{0x}, a_{0y}, a_{0z}, a_{1z}, a_{2y}, a_{2z}, $\boldsymbol{r}_1$ and $\boldsymbol{r}_2$ as inputs. Refer to Appendix E for implementation of this process in Matlab.

Figures 6.5 and 6.6 demonstrate, for the first 18 s, that both the hypothetically generated data and the predicted data overlap with a maximum root mean square error of 9.1×10^{-19} rad/s.

Table 6.1: Amplitude of angular acceleration and velocity

Parameter	Amplitude
ω_x	$1.50e10^{-4}$ rad/s
ω_y	$3.50e10^{-4}$ rad/s
ω_z	$0.50e10^{-5}$ rad/s
α_x	$9.42e10^{-5}$ rad/s^2
α_y	$2.20e10^{-4}$ rad/s^2
α_z	$3.14e10^{-6}$ rad/s^2

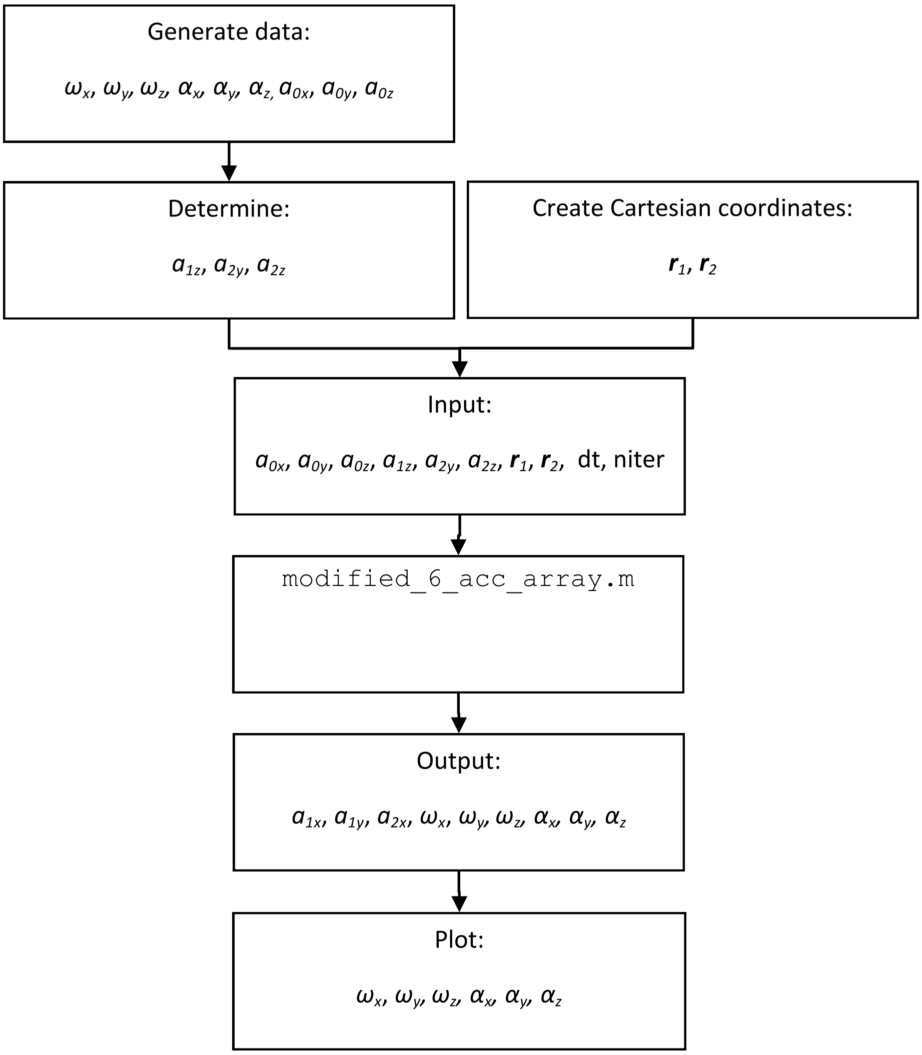

Figure 6.4: Flow diagram for generating and comparing hypothetical data

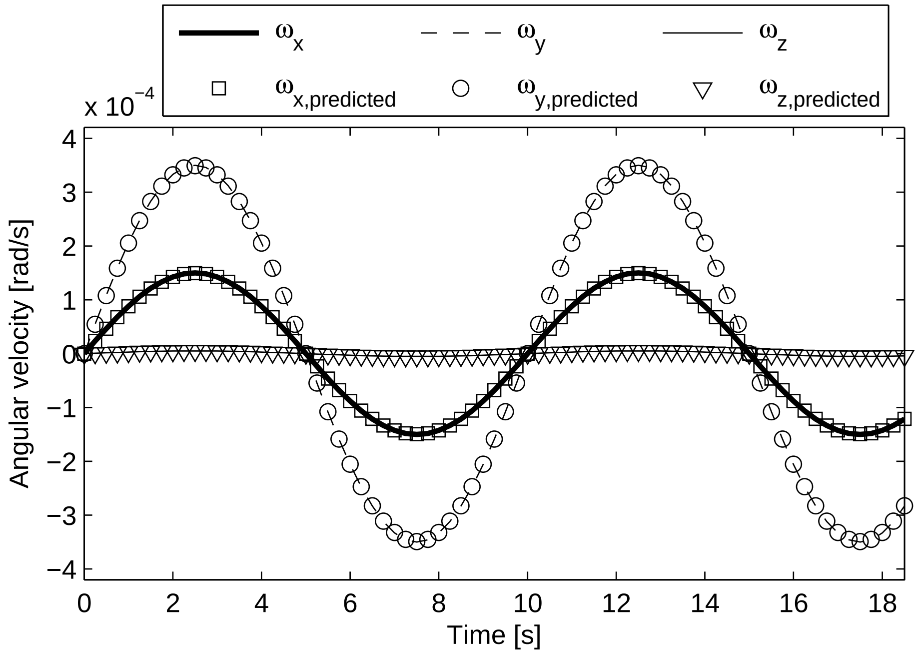

Figure 6.5: Predicted versus hypothetical angular velocity

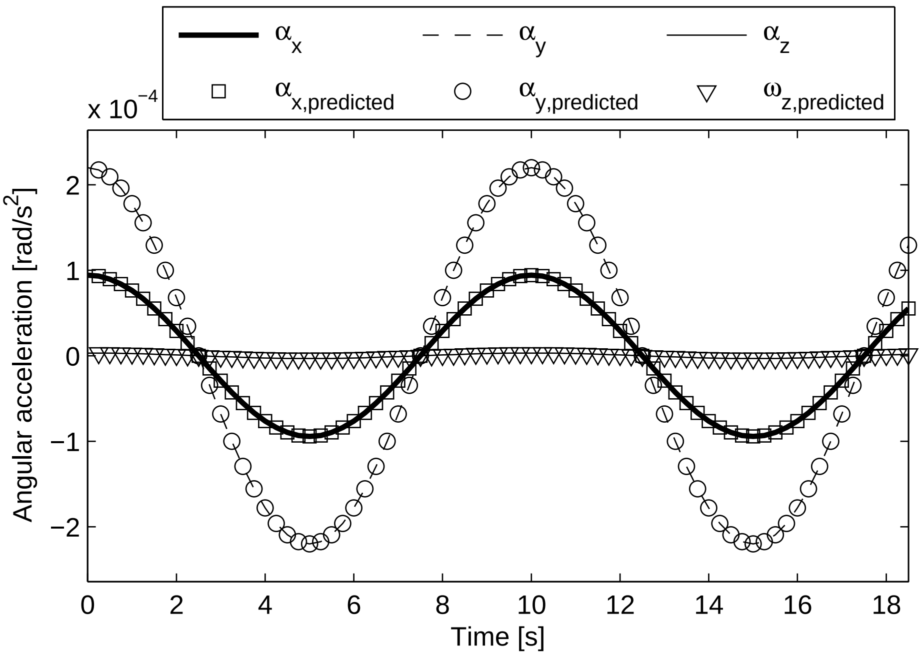

Figure 6.6: Predicted versus hypothetical angular acceleration

6.3.2 Validation by measured data on board the SA Agulhas II

For the validation of the measured data a 300 s data file was randomly selected. The measurement was taken at 12:58:07 Coordinated Universal Time (UTC) on the sixth of December 2014 (with a sea state of 4 on the Beaufort scale and an average swell height of 2 m). The predicted and measured vertical acceleration at Points 3 and 4 are shown in Figure 6.7 with root mean square errors of 0.0079 m/s^2 and 0.0076 m/s^2 respectively. The angular velocity and acceleration are presented in Figure 6.8 are of a similar order of magnitude found in Lawther and Griffin (1986).

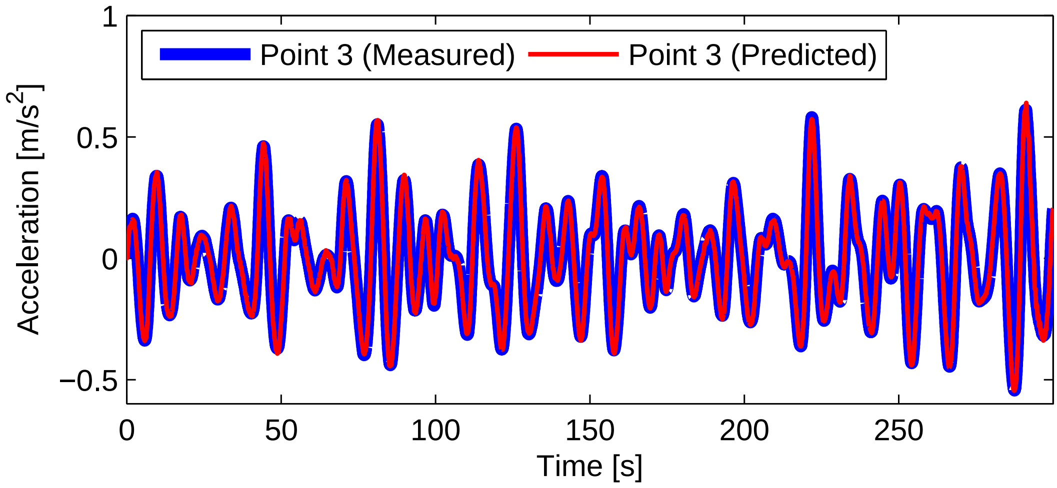

(a) Point 3

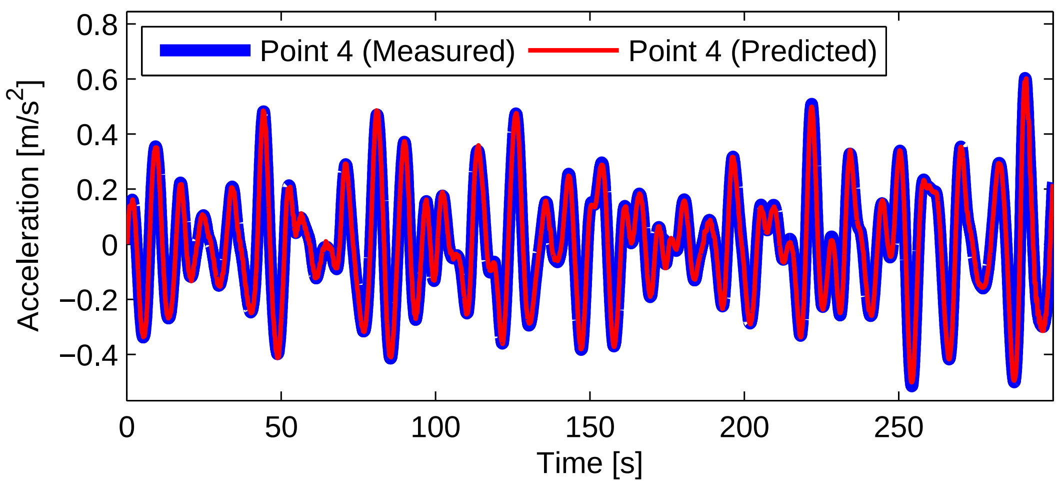

(b) Point 4

Figure 6.7: Predicted acceleration of (a) Point 3 and (b) Point 4

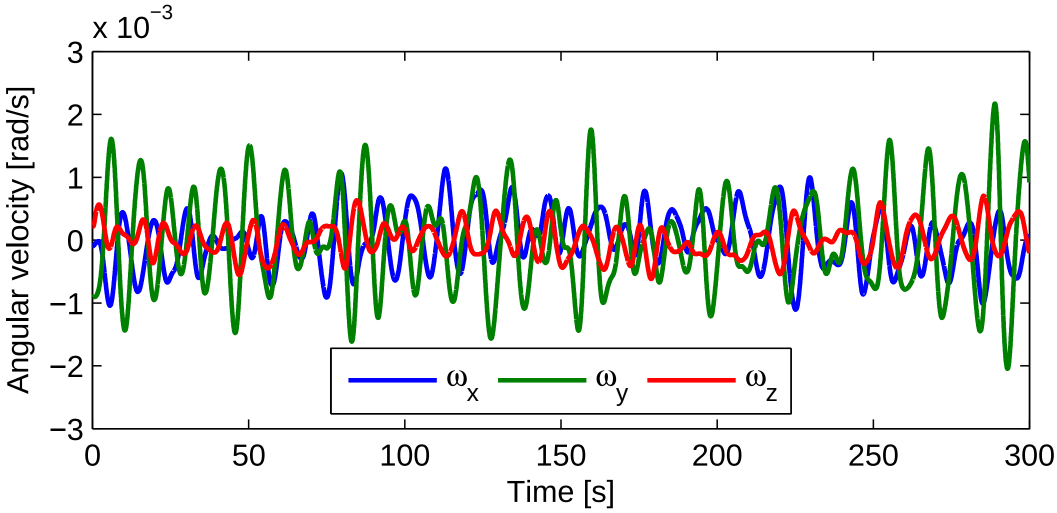

(a) Angular velocity

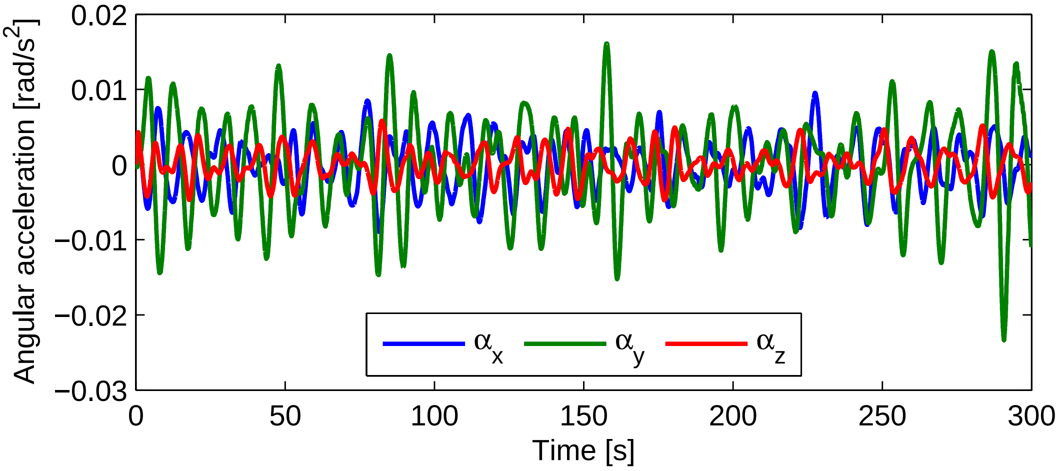

(b) Angular acceleration

Figure 6.8: (a) Predicted angular velocity and (b) acceleration from a 300 s measurement on the SA Agulhas II

6.4 Ship motion

The variation of acceleration of the ship is presented in Figures 6.9a, to 6.9c for the same 300 s data record used in Section 6.3.2. The lowest levels of r.m.s. acceleration were found to be in the accommodation area. Should the z-axis and x axis be dominant the lower decks in the accomodation areas would be preferable.

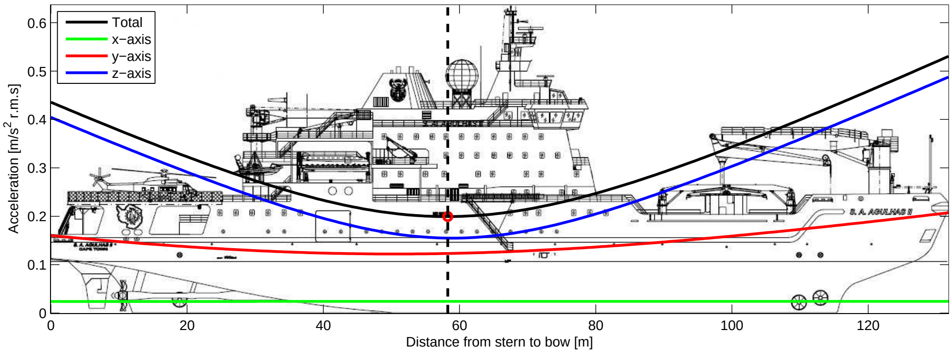

(a) Length

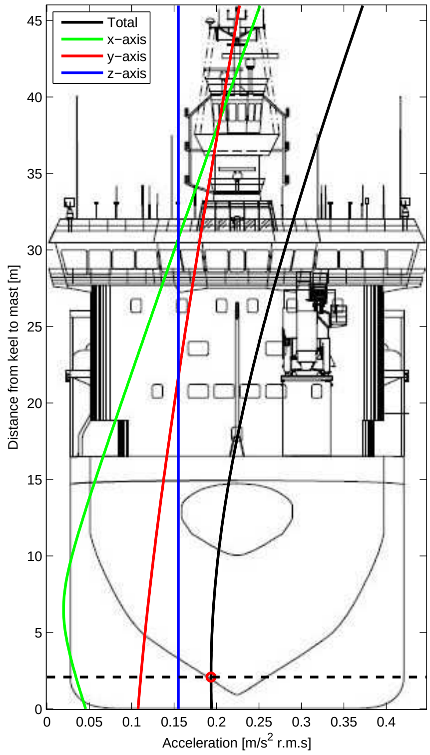

(b) Height

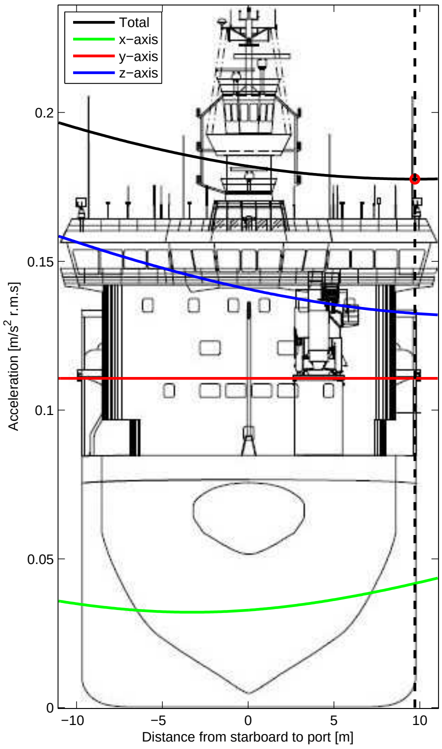

(c) Width

Figure 6.9: Variation in the magnitude of r.m.s. translational acceleration of the SA Agulhas II

The following findings were made about the length, width and height of the vessel with regards to the variation of the magnitude of r.m.s. acceleration;

- The magnitude of the x-axis acceleration remained constant along the length of the vessel while vertical acceleration (z-axis) varied due to pitch. The peak vertical acceleration was found at the bow of the vessel and a minimum vertical magnitude of acceleration at 53.64 m (which falls into accommodation area of the vessel) from the stern. The magnitude of the y-axis acceleration varied along the length of the vessel, but not to the same extent of the z-axis.

- Along the width of the vessel the magnitude of the z-axis r.m.s. acceleration varied due to roll, with the roll centre towards the port side of the vessel. This behaviour occurs in oblique seas and is demonstrated by Riola *et al.* (2001) when they determined the motion sickness incidence on a deck of a ship. The x-axis acceleration remained constant along the width of the vessel as it is not a function of roll. The y-axis acceleration varied along the width of the vessel due to roll.

- The magnitude of z-axis r.m.s. acceleration did not vary along the height of the vessel due to roll.

Similar findings were found by Pisula *et al.* (2012) save for the variation along the width of the ship.

Chapter 7

Regression analysis and Kendall's ranked correlations

During the seventy-six day voyage to Antarctica a total of thirty-two daily observations ($N = 32$) were made for Illness Rating (IR) and Motion Sickness (MS), with vomiting only occurring on six of these days. IR, MS and Percentage Vomiting (PV) shall be described from now on as motion sickness factors. This chapter finds relationships between; the motion sickness factors, location and direction. All statistical techniques used were conducted using Statistica. Techniques such as;

- Shapiro-Wilk's W-test (test for normality) is used to determine the distribution of motion sickness factors (Haward *et al.*, 2009).
- The Kendall's ranked correlation coefficient (a non-parametric statistical technique) is used to determine the correlations between non-normally distributed dependant and independent variables (Haward *et al.*, 2009).
- Linear and multiple regression analysis are used to identify the effects location on board the SA Agulhas II (SAAII) and direction of motion has on IR (Lawther and Griffin, 1986).

7.1 Terminology

Gujarati (2003) describes various statistical techniques and terminology, particularly for multiple regression analysis. The multiple coefficient of determination (R^2) is used to determine the goodness of fit. However, the R^2 does not take into account the number of variables in the model. The $R^2_{adjusted}$ is the adjusted R^2 value which takes into account the number of variables in the model, which means that two different models can be compared. The F-test is another way to determine which model best fits the independent variable. The higher F is the more significant the regression model.

7.2 Multiple regression analysis

Multiple regression analysis is often used in behavioural science disciplines and econometrics (Gujarati, 2003; Nathans *et al.*, 2012). The three-variable regression model (found in equations 7.1) is the simplest multiple regression model, consisting of one dependent (response variable) variable and two independent (predictor) variables.

$$Y_{response} = \beta_0 + \beta_1 X_1 + \beta_2 X_2 + u_i \tag{7.1}$$

$$Y_{response} = Y_{predicted} + u_i \tag{7.2}$$

where $Y_{response}$ is the response variable, $Y_{predicted}$ is the predicted variable, u_i is the error term (residual), β_0 is the intercept and β_1 to β_2 are the partial regression coefficients. Partial regression coefficients are often relied upon in order to assess the importance of the predictor variables (Gujarati, 2003). However in multiple regression analysis the predictor variables are usually intercorrelated (Nathans *et al.*, 2012). This intercorrelation is known as collinearity or multicollinearity.

Consequences of multicollinearity are (Gujarati, 2003); one or more of the partial regression coefficients are insignificant. Although, the partial regression coefficients are insignificant the R^2 values are high. The standard errors are large in relation to the coefficients themselves. Large standard errors mean that the coefficients cannot be estimated accurately and precisely. Multicollinearity can be detected by high R^2 values with few significant partial regression coefficients, high correlations between the independent variables (roughly 0.8) and auxiliary regression analysis. Multicollinearity can be reduced by dropping independent variables, transformation of the independent and dependent variables (choosing a new model) or adding more samples (N).

7.3 Motion sickness factors

A Shapiro-Wilk's W-test was used to determine whether the motion sickness factors were normally distributed or not (Haward *et al.*, 2009). It was found that the motion sickness factors were non-normally distributed, which meant that non-parametric statistical techniques had to be used (Haward *et al.*, 2009). Once such technique is the Kendall rank correlation coefficient.

The Kendall's rank correlation coefficient (T, presented in Table 7.1) was used to determine the correlation between the motion sickness factors. The highest correlation between the motion sickness factors was found to be between IR and MS. PV had the lowest correlation among all the motion sickness factors.

Table 7.1: Kendall correlation coefficient (T) between the motion sickness factor ($p < 0.05$)

	IR	PV	MS
IR	1	0.436	0.815
PV	0.436	1	0.446
MS	0.815	0.446	1

Linear relationships were established between the motion sickness factors via linear regression analysis. These relationships are shown in Table 7.2 with their associated the F, R^2 and $R^2_{adjusted}$ values.

MS and IR had the highest R^2 value of 0.920. Should any of the motion sickness factors be known these relationships could be used to predict any of the other motion sickness factors (PV, IR or MS).

Table 7.2: Linear relationships between motion sickness factors

Relationship	R^2	$R^2_{adjusted}$	F
$PV = 11.3IR - 1.0$	0.600	0.582	45.65
$MS = 72.4IR$	0.920	0.920	369.04
$PV = 0.2MS - 1.2$	0.623	0.610	51.13

Figure 7.1 plots the relationships determined in Table 7.2 of the motion sickness factors.

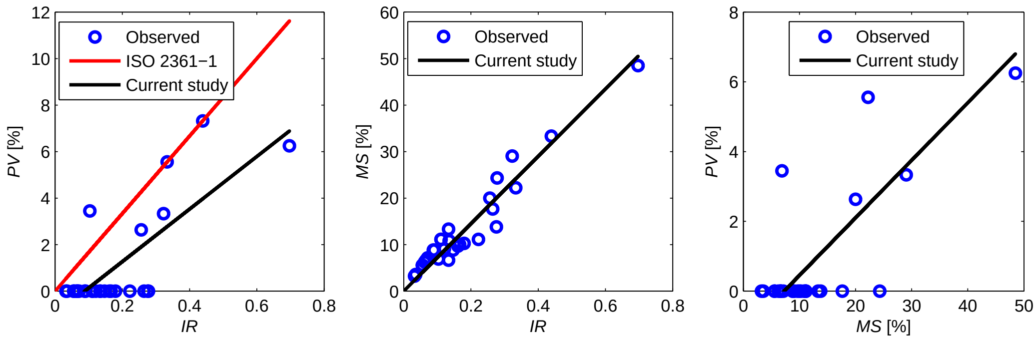

(a) PV vs IR (b) MS vs IR (c) PV vs MS

Figure 7.1: Relationship between motion sickness factors

It was observed from Table 7.2 and Figure 7.1 that the relationship established between PV and IR indicated that above $IR = 0.088$ (x-intercept) passengers get motion sick. Passengers start vomiting after 7.27 % (x-intercept) of the passengers are motion sick

7.4 Motion sickness and location

Kendall's rank correlation coefficients (T) were determined between the motion sickness factors and the Motion Sickness Dose Value (MSDV)'s for each direction ($MSDV_{x,6h}$, $MSDV_{y,6h}$ and $MSDV_{z,6h}$) at each zone (A1 to F13). The MSDV's for x- and y-axis are $MSDV_{x,6h}$ and $MSDV_{y,6h}$ weighted using W_{dg}. Each of the 78 zones had different correlation coefficients for each direction, the variation in these correlation coefficients are summarised in Table 7.3. PV was found to be insignificantly correlated the y-axis at all zones. Zones A7, B7, C7, D7, E7 and F7 were found to be insignificantly correlated with the z-axis.

Table 7.3: Kendall correlation coefficient (T) for the maximum daily 6 h MSDV ($p < 0.05$) for all 78 (A1 to F13) ship zones found in Figure 3.5

	$MSDV_{x,6h}$	$MSDV_{y,6h}$	$MSDV_{z,6h}$
IR	0.525-0.603	0.340-0.387	0.505-0.583
PV	0.285-0.326	0.148-0.230*	0.230* (0.251-0.278)
MS	0.452-0.542	0.251-0.312	0.444-0.504
* $p > 0.05$			

The correlation coefficients (T) are all positive which implies that an increase in the MSDV in any direction leads to an increase in the motion sickness factors. The correlation coefficients between the y-axis and motion sickness factors were found to be the lowest, it was also found that PV had the lowest correlation with direction. The correlation coefficients do not indicate the amount that each direction contributes to illness rating, therefore multiple linear regression is required.

It was determined, in Chapter 3, that passengers spent most of their time in the accommodation area. The effects of these zones in predicting motion sickness is shown in Table 7.4 and Figures 7.2 to 7.3. The linear model used to describe the relationship between $MSDV_{z,6h}$ and IR is described in equation 7.3.

$$IR_{predicted} = k \times MSDV_{z,6h} \tag{7.3}$$

where k is the gradient between IR and $MSDV_{z,6h}$. A summary of the gradient k is found in Table 7.4.

Table 7.4: Relationship between zones (E1, E4, D5, D8 and B8) and $MSDV_{z,6h}$

Zone	k	R^2	$R^2_{adjusted}$	F
E1	0.00254	0.539	0.539	36.22
E4	0.00450	0.473	0.473	27.85
D5	0.00471	0.453	0.453	25.72
D8	0.00371	0.474	0.474	27.96
B8	0.00371	0.474	0.474	27.97

The most provocative zone of those described in Table 7.4 was determined to be D5. D5 was found to be 46.07 % more provocative that E1, 21.23 % more provocative than both D8 and B8. Other observations include;

- Both D8 and B8 have the same gradients with the same x (length) and y-coordinates (width), but different z-coordinates (height).
- E1 and E4 have different gradients with the same y- and z-coordinates, but different x-coordinates. The same observation can be made for D5 and D8.
- D5 and E4 have similar gradients with the same y-coordinates, but different x- and z-coordinates. Both zones are in close proximity to each other which could explain the similar gradients.

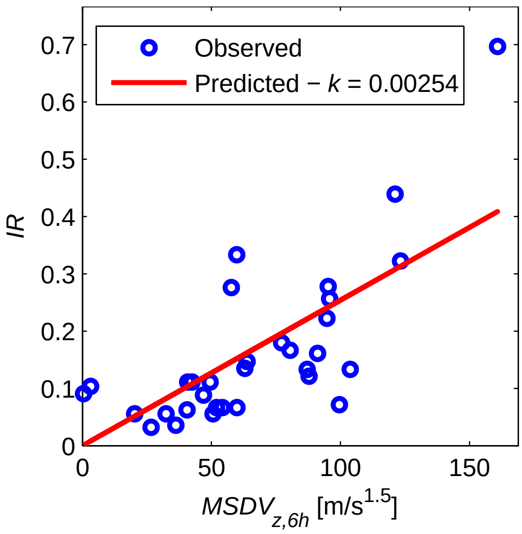

(a) Zone E1

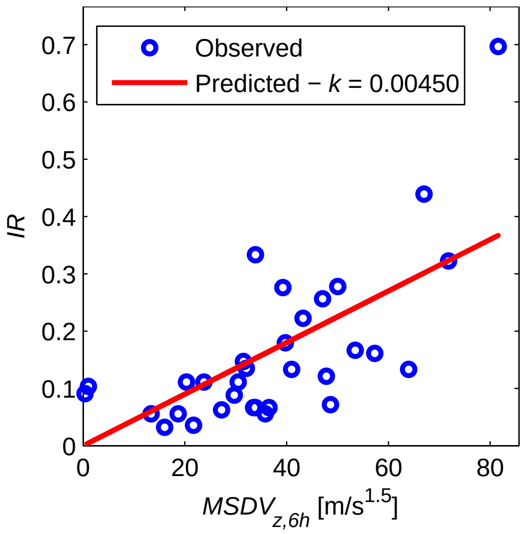

(b) Zone E4

Figure 7.2: Effects of location on illness rating (Part 1)

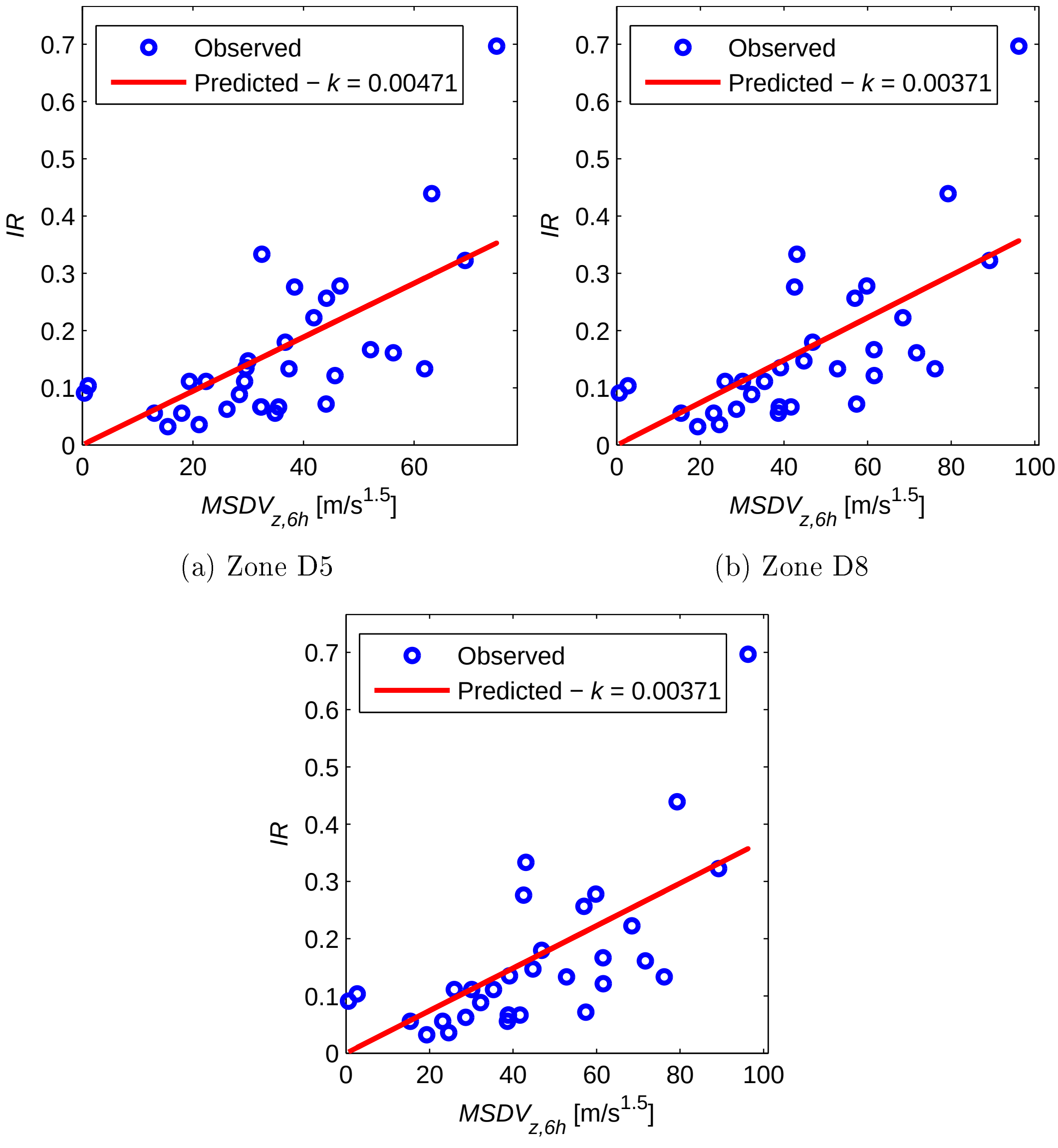

(a) Zone D5

(b) Zone D8

(c) Zone B8

Figure 7.3: Effects of location on illness rating (Part 2)

7.5 Motion sickness and direction

In order to determine the relationship between direction and motion sickness one ship zone was selected in order to simplify the process. Zone D7 was selected because it was one of the ten most frequented zones on the SAAII. Furthermore, D7 is a central area in the accommodation area. The correlation matrix between IR and $MSDV_{x,6h}$, $MSDV_{y,6h}$ and $MSDV_{z,6h}$ for zone D7 is located in Table 7.5.

Table 7.5: Kendall correlation coefficient (T) for the maximum daily 6 h MSDV ($p < 0.05$) for zone D7 found in Figure 3.5

	$MSDV_{x,6h}$	$MSDV_{y,6h}$	$MSDV_{z,6h}$
IR	0.583	0.358	0.521
PV	0.299	0.196*	0.230*
MS	0.512	0.296	0.452
* $p > 0.05$			

7.5.1 Initial prediction equation

Equation 7.4 presents the non-linear regression model was selected to describe the effects of direction ($MSDV_{x,6h}$, $MSDV_{y,6h}$ and $MSDV_{z,6h}$) have on IR. This model was selected due to its similarity of combining the different axes of vibration together to determine the vibration total value (see 2.3.5).

$$IR_{predicted} = \sqrt{\beta_1 MSDV_{x,6h}^2 + \beta_2 MSDV_{y,6h}^2 + \beta_3 MSDV_{z,6h}^2} \tag{7.4}$$

where the β_i coefficients ($i = 0, 1, 2, ..., n$) are found in Table 7.6. Both $MSDV_{y,6h}$ and $MSDV_{z,6h}$ were deemed insignificant ($p > 0.05$) and their β coefficients were negative, contrary to having positive correlations with illness rating (as shown in Table 7.5). It is suspected that multicollinearity is present in the model, since two of the predictor variables were found to be insignificant and the standard errors have the same order of magnitude in relation to the coefficients. More insight is needed in order to determine that there is multicollinearity (Gujarati, 2003). Hence the need determine the intercorrelation between lateral and vertical motion as to perform auxiliary regression.

Table 7.6: Multiple non-linear regression - initial model

Dependent variable: IR

Variable	Coefficient	Standard error	p
$MSDV_{x,6h}$	647.7e-6	172.7e-6	0.000
$MSDV_{y,6h}$	-33.9e-6	21.0e-6	0.117
$MSDV_{z,6h}$	-7.0e-6	17.1e-6	0.688
$R^2 = 0.648$, $R^2_{adjusted} = 0.624$, $F = 17.79$			

7.5.2 Intercorrelation between lateral and vertical motion

Table 7.7 presents the Kendall rank incorrelation matrix between $MSDV_{x,6h}$, $MSDV_{y,6h}$ and $MSDV_{z,6h}$. The highest correlations was found to be between $MSDV_{x,6h}$ and $MSDV_{z,6h}$. These high correlations suggest that there could be a multicollinearity problem when combining $MSDV_{x,6h}$, $MSDV_{y,6h}$ and $MSDV_{z,6h}$ to predict IR.

Table 7.7: Kendall rank intercorrelation matrix (T) for the maximum daily 6 h MSDV ($p < 0.05$) at Zone D7 found in Figure 3.5

	$MSDV_{x,6h}$	$MSDV_{y,6h}$	$MSDV_{z,6h}$
$MSDV_{x,6h}$	1	0.597	0.798
$MSDV_{y,6h}$	0.597	1	0.661
$MSDV_{z,6h}$	0.798	0.661	1

7.5.3 Auxiliary regression

Auxiliary regression is the regression of each variable ($MSDV_{x,6h}$, $MSDV_{y,6h}$ or $MSDV_{z,6h}$) as a combination of the remaining variables (Gujarati, 2003). A summary of the analysis can be found in Table 7.8.

Table 7.8: R^2 values from auxiliary regression analysis

Dependent variable	Independent variables	R^2
$MSDV_{x,6h}$	$MSDV_{y,6h}$ and $MSDV_{z,6h}$	0.874
$MSDV_{y,6h}$	$MSDV_{x,6h}$ and $MSDV_{z,6h}$	0.701
$MSDV_{z,6h}$	$MSDV_{x,6h}$ and $MSDV_{y,6h}$	0.910

The R^2 values are all high except with the possibility of $MSDV_{y,6h}$. These R^2 values are all higher than the R^2 value obtained for the initial model described in equation 7.4 and Table 7.6.

7.5.4 Prediction equations

Based on the findings in sections 7.5.1 to 7.5.3 it was determined that there was multicollinearity problem. It was decided to mitigate the problem by either eliminating various independent variables or combining the independent variables or transforming regression model. Models 2 through 4 were based on equation 7.4 to 7.7 respectively. These models was selected as they resemble the prediction model of. While models 5 to 7 were based off equation 7.4, lastly model 8 is based off equation 7.8. The models along with the initial equation, model 1, are presented and compared in Table 7.9.

$$IR_{predicted} = \beta_0 + \beta_1 MSDV_{x,6h} \tag{7.5}$$

$$IR_{predicted} = \beta_0 + \beta_2 MSDV_{y,6h} \tag{7.6}$$

$$IR_{predicted} = \beta_0 + \beta_3 MSDV_{z,6h} \tag{7.7}$$

$$IR_{predicted} = \beta_0 + \beta_1 \sqrt{MSDV_{x,6h}^2 + MSDV_{y,6h}^2 + MSDV_{z,6h}^2} \tag{7.8}$$

Table 7.9: Illness rating models

Dependent variable: IR

Model	Independent variables	R^2	$R^2_{adjusted}$	F
1	$MSDV_{x,6h}$, $MSDV_{y,6h}$ and $MSDV_{z,6h}$	0.648	0.624	17.79
2	$MSDV_{x,6h}$	0.561	0.547	38.38
3	$MSDV_{y,6h}$	0.230	0.204	8.96
4	$MSDV_{z,6h}$	0.457	0.438	25.21
5	$MSDV_{x,6h}$ and $MSDV_{y,6h}$	0.646	0.634	27.36
6	$MSDV_{x,6h}$ and $MSDV_{z,6h}$	0.616	0.603	24.08
7	$MSDV_{y,6h}$ and $MSDV_{z,6h}$	0.477	0.460	13.89
8	$MSDV_{x,6h}$, $MSDV_{y,6h}$ and $MSDV_{z,6h}$	0.417	0.398	21.47

The β coefficients for each model are defined in Table 7.10. The significant coefficients (hence significant independent variables) were identified based off their p-values ($p < 0.05$).

Table 7.10: Illness rating models - coefficients

Model	β_0	β_1	β_2	β_3
1	0	647.70e-6	-33.78e-6*	-7.0e-3*
2	-20.57e-3*	9.64e-3	0	0
3	33.90e-3*	0	2.99e-3	0
4	-23.93e-3*	0	0	4.13e-3
5	0	589.10e-6	-38.39e-6	0
6	0	664.08e-6	0	-22.4e-6*
7	0	0	-38.47e-6*	46.17e-6
8	-22.53e-3*	3.86e-3	0	0
* $p > 0.05$				

It was hypothesised that the combination of lateral and vertical motion played a role affected the motion sickness factors. The purpose of this regression analysis was to identify the effects of direction on IR and thus the most dominant direction. However multicolliniearity was identified in models 1, 5, 6 and 7 which made this impossible to do hence they were rejected. Which leaves models 2, 3, 4 and 8. Based off the R^2, $R^2_{adjusted}$ and F values the y direction was deemed insignificant (model 3). Model 2 was the best model based off the F value. Models 2 to 4 are shown in Figure 7.4. ISO 2631-1 (1997) over predicted the maximum IR by 228 %.

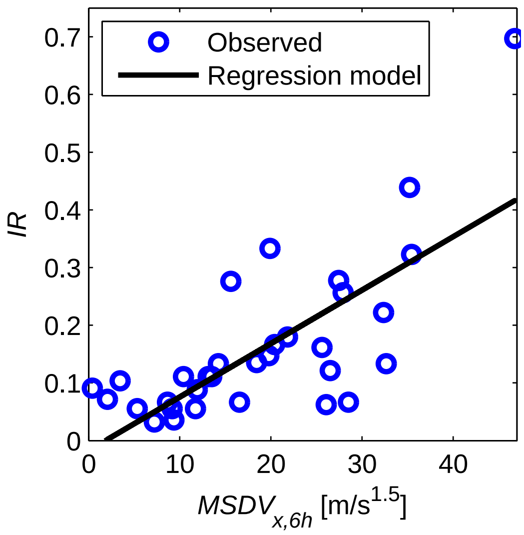

(a) Model 2

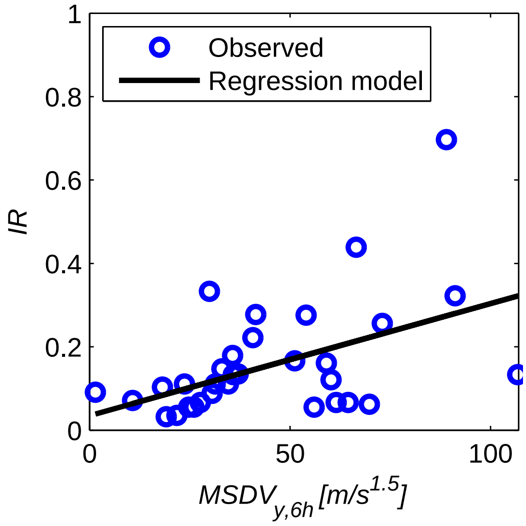

(b) Model 3

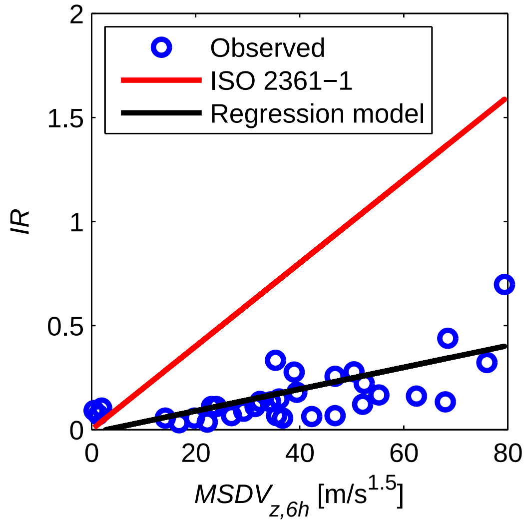

(c) Model 4

Figure 7.4: Regression models for the prediction of IR

Chapter 8

Conclusions and recommendations

8.1 Conclusions

Full scale measurements were conducted on the SA Agulhas II (SAAII) to determine the effects location (on board the SAAII) and direction had motion sickness. The full scale measurements were conducted on two voyages namely the Marion Island 2014 and Antarctica 2014/2015 voyage. Each measurement had a six accelerometer array which was used to predict the acceleration levels at any location on board the SAAII. Each voyage had a survey consisting of numerous questionnaires which measured the subjective response of the participants towards motion sickness. The questionnaires were also designed to determine the inter- and intra-subject variability of participants towards motion sickness.

The Marion Island 2014 questionnaire had a poor response rate starting at 43 % on Day 1 and dropping to 9.23 % by Day 10 with confidence intervals of and 11 % to 27.9 % respectively. These confidence intervals were unacceptable, therefore the subjective responses from this voyage were ignored. Factors that could have an influence on the low response rate, could be due to the fact that no researcher from the Sound and Vibration Research Group (SVRG) was on board the SAAII during the voyage to administer the questionnaire. Administration of the questionnaire would include; encouraging the passengers to fill in the questionnaires, motivating and explaining the questionnaires to the participants. Other factors influencing the response rate could be due to having a three page long daily diary.

The questionnaires from Antarctica 2014/2015 voyage were more successful than the Marion Island 2014 voyage. The response rate was as high as 72 % and dropped as low as 29 % with confidence intervals ranging from 0 % to 13 %. Females were reported to be more susceptible towards motion sick. It was also reported that the older males were less susceptible towards motion sickness than the younger males. Participants spent the majority of their time in the accommodation area of the vessel, particularly centred around the lounges on Deck 6 and 7. The accommodation areas were the also found to be the most frequently used zones of the vessel.

A modified six accelerometer array was developed and tested (for the Antarctica 2014/2015 voyage) successfully with hypothetically generated data and measured data. The minimum r.m.s. acceleration levels in the vertical direction (z-axis) along the length of the SAAII were determined to be 53.64 m from the stern. The vertical r.m.s. acceleration was found to be independent of height, but varied along the width of the vessel. The lowest levels of r.m.s. acceleration were found to be in the accommodation area. The z-axis and x axis found to be dominant, which meant that the lower decks in the accommodation areas would be preferable to reducing the chances of getting motion sickness.

There were 32 observations of motion sickness factors such as IR and MS, whereas there were only 6 days of reported vomiting (PV). The motion sickness factors (IR, MS and PV) were correlated and a linear regression model was determined between PV and IR, MS and IR, PV and MS. Of the motion sickness factors the highest correlation was found to be between MS and IR. It was found that ISO 2631-1 (1997) over predicted the maximum IR 228 %.

The Kendall correlation coefficient (T) was determined between the motion sickness factors and direction of motion. To take direction into account the maximum daily 6 h Motion Sickness Dose Value (MSDV) for the x-, y- and z-axis was determined at all 78 ship zones. All motion sickness factors were positively correlated with motion in the x-, y- and z-axis. The x- and z-axis were both highly correlated with IR and MS. The correlation between the y-axis and PV suggested that acceleration in y-axis is insignificant. IR had the highest correlation with the direction of motion.

In order to determine the relationship between location and motion sickness, the $MSDV_{z,6h}$ was determined at the accommodation zones. Prediction equations were developed between IR and $MSDV_{z,6h}$ via linear regression analysis. Based on the prediction equations, it was found that height on the vessel does not change the severity of motion sickness. The severity of motion sickness changed along the length of the vessel. Zone E1 was found to be the most provocative. The least provocative zones were B8 and D8 (in the accomodation area).

To identify the relationship between direction and motion sickness the maximum daily 6 h MSDV ($MSDV_{x,6h}$, $MSDV_{y,6h}$ and $MSDV_{z,6h}$) at zone D7 was were determined. Zone D7 was one of the ten most frequented zones and is a central location in the accommodation area. Multiple linear and non-linear regression analysis was performed to determine the most significant direction of motion sickness and how much each axis contributes to motion sickness. It was discovered that there was multicollinearity between $MSDV_{x,6h}$, $MSDV_{y,6h}$ and $MSDV_{z,6h}$ for both the linear and non-linear regression models. Hence, the contribution and significance of each axis could not be identified. The reasons for multicollinearity are most probably due to the small number of observation ($N = 32$).

8.2 Recommendations

It is recommended to improve the response rate as this will improve confidence intervals. To do this participants are to be regularly encouraged to fill in their questionnaires. Responses to incorrectly filled in questions are rejected, since it was found that passengers do not fill in the location part of the *personal details questionnaire* correctly it is suggested to improve that question. To improve the question it may be necessary to replace it with an image of the SAAII divided up into various zones and the passengers are asked to circle their top three zones. It is also recommended to add a questionnaire that takes the passengers susceptibility into account. To increase the number of samples it is suggested to perform full scale measurements, on motion sickness, on vessels which do multiple short voyages a day. This more than one sample (N) can be obtained a day. More samples could potentially solve the multicollinearity problem. It is also recommended to create an analytical model which combines rigid body and dynamic motion. This model could be used as a tool to test the data analysis algorithm.

List of references

Alexander, S., Cotzin, M., Klee, J. and Wendt, G. (1947). Studies of motion sickness: XVI. The effects upon sickness rates of waves of various frequencies but identical acceleration. *The Journal of Experimental Psychology*, vol. 37, pp. 440–448.

Bos, J., Damala, D., Lewis, C., Ganguly, A. and Turan, O. (2007). Susceptibility to seasickness. *Ergonomics*, vol. 50, no. 6, pp. 890–901.

Donohew, B. and Griffin, M. (2004). Motion sickness: Effect of the frequency of lateral oscillation. *Aviation, Space, and Environmental Medicine*, vol. 75, no. 8, pp. 649–656.

Förstberg, J. (2000). Motion-related comfort in tilting trains: Human responses and motion enviroments in a train experiment. Tech. Rep., Swedish National Road and Transport Institute.

Gahlinger, P. (2000). Cabin location and the likelihood of motion sickness in cruise ship passengers. *Journal of Travel Medicine*, vol. 7, no. 3, pp. 120–124.

Golding, J. (2006 oct). Motion sickness susceptibility. *Autonomic Neuroscience: Basic & Clinical*, vol. 129, no. 1-2, pp. 67–76.

Griffin, M. (1990). *Handbook of Human Vibration*. Elsevier Academic Press, London.

Griffin, M. and Howarth, H. (2000). Motion sickness history questionnaire. Tech. Rep., Institute of sound and vibration. University of Southampton.

Gujarati, D. (2003). *Basic econometrics*. 4th edn. McGraw-Hill, New York.

Haward, B., Lewis, C. and Griffin, M. (2009). Motions and crew responses on an offshore oil production and storage vessel. *Applied Ergonomics*, vol. 40, no. 5, pp. 904–914.

Howarth, H. and Griffin, M. (2009). Human exposure to low frequency horizontal motion in buildings and offshore structures: An assessment of guidance in BS 6611 and ISO 6897. In: *Euronoise 2009*. Edinburgh, Scotland.

ISO 2631-1 (1997). Mechanical vibration and shock - Evaluation of human exposure to whole-body vibration Part 1 : General Requirements.

Johnson, D. (2005). Introduction to and review of simulator sickness research. Tech. Rep., U.S. Army Research Institute.

Joseph, J. and Griffin, M. (2007). Motion sickness from combined lateral and roll oscillation: Effect of varying phase relationships. *Aviation, Space, and Environmental Medicine*, vol. 78, no. 10, pp. 944–950.

Khalid, H., Turan, O., Bos, J. and Incecik, A. (2011). Application of the subjective vertical-horizontal-conflict physiological motion sickness model to the field trials of contemporary vessels. *Ocean Engineering*, vol. 38, no. 1, pp. 22–33.

Lawther, A. and Griffin, M. (1986). The motion of a ship at sea and the consequent motion sickness amongst passengers. *Ergonomics*, vol. 29, no. 4, pp. 535–552.

Lawther, A. and Griffin, M. (1987). Prediction of the incidence of motion sickness from the magnitude, frequency, and duration of vertical oscillation. *The Journal of the Acoustical Society of America*, vol. 82, no. 3, pp. 957–966.

Lawther, A. and Griffin, M. (1988). Motion sickness and motion characteristics of vessels at sea. *Ergonomics*, vol. 31, no. 10, pp. 1373–1394.

Lewis, C. and Griffin, M. (1997). Evaluating the motions of a semi-submersible platform with respect to human response. *Applied Ergonomics*, vol. 28, no. 3, pp. 193–201.

McCauley, M., O'Hanlon, J., Royal, J., Wackie, R. and Wylie, C. (1976). Motion sickness incidence: Exploratory studies of habituation, pitch and roll, and the refinment of a mathematical model. Tech. Rep., Human Factors Research, Incorporated.

Mcmahon, K. (2014). *Whole-body vibration comfort measurement aboard the S.A. Agulhas II and just noticeable difference threshold testing in the laboratory*. Master's thesis, Stellenbosch University.

Meriam, J. and Kraige, L. (2008). *Engineering Mechanics - Dynamics*. 6th edn. John Wiley & Sons, Inc, Hoboken.

Nathans, L., Oswald, F. and Nimon, K. (2012). Interpreting multiple linear regression: A guidebook of variable importance. *Practical Assesment Research & Evaluation*, vol. 17, no. 9, p. 19. ISSN 1531-7714, 1531-7714.

O'Hanlon, J. and McCauley, M. (1973). Motion sickness incidence as a funciton of the vertical frequency and acceleration of vertical sinusoidal motion. Tech. Rep. September, Human Factors Research, Incorporated, California.

Padgaonkar, A., Krieger, K. and King, A. (1975). Measurement of angular acceleration of a rigid body using linear accelerometers. *Journal of Applied Mechanics*, vol. 42, no. 3, pp. 552–556.

Persson, R. (2008). Motion sickness on tilting trains: Description and analysis of the present knowledge - Literature study. Tech. Rep., VTI, Sweden.

Pisula, P., Lewis, C. and Bridger, R. (2012). Vessel motion thresholds for maintaining physical and cognitive performance : A study of naval personnel at sea. *Ergonomics*, vol. 55, no. 6, pp. 636–649.

Riccio, G. and Stoffregen, T. (1991). An ecological Theory of Motion Sickness and Postural Instability.

Rimell, A. and Mansfield, N. (2007). Design of digital filters for frequency weightings required for risk assessments of workers exposed to vibration. *Industrial health*, vol. 45, no. 4, pp. 512–519.

Rimell, A. and Mansfield, N. (2010). Design of digital filters for frequency weightings required for risk assessments of workers exposed to vibration - Corrigendum. *Industrial Health*, vol. 48, no. 5, p. 743.

Riola, J., Esteban, S., Girón-Sierra, J. and Aranda, J. (2001). Motion and seasickness of fast warships. In: *RTO AVT Symposium on "Habitability of Combat and Transport Vehicles: Noise, Vibration and Motion"*, pp. 1–9. Prague, Czech Republic.

Riola, J. and García de Arboleya, M. (2006). Habitability and personal space in seakeeping behaviour. *Journal of Maritime Research*, vol. 3, no. 1, pp. 41–54.

Ronald, A. and Mills, D. (2004). *Signal analysis - Time, frequency, scale and structure.* John Wiley & Sons, Inc.

Soal, K. (2014). *Vibration response of the polar supply and research vessel the S.A. Agulhas II in Antarctica and the Southern Ocean.* Master's thesis, Stellenbosch University.

STX Finland (2010). FINNSAP Modal analysis of NB1369.

Walton, D., Lamb, S. and Kwok, K. (2011). A review of two theories of motion sickness and their implications for tall building motion sway. *Wind and Structures An International Journal*, vol. 14, no. 6, pp. 499–515.

Appendix A

Acceleration and velocity in a moving reference frame

A.1 Derivation of velocity and acceleration using a moving reference frame

Figure 2.9 is reproduced as Figure A.1 for ease of reference during the derivation of acceleration of Point P.

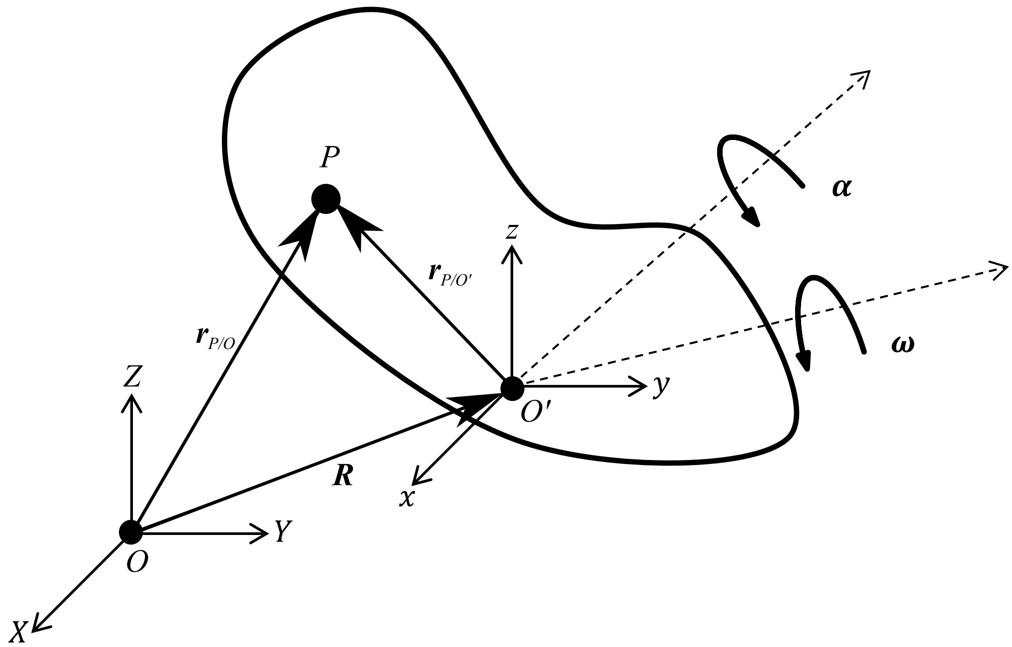

Figure A.1: Relative motion and moving reference frame

Since the fixed-body frame (xyz) is free to rotate and translate the unit vectors are no longer fixed in direction. As a result of this the derivation of any arbitrary vector $\boldsymbol{A}$ (equation A.1) is not longer simple.

$$\boldsymbol{A} = A_1\mathbf{e}_1 + A_2\mathbf{e}_2 + A_3\mathbf{e}_3 \tag{A.1}$$

Deriving $\boldsymbol{A}$ once with respect to time gives equation A.2 as a result of the product rule. For linear acceleration the time derivatives of the unit vectors $\dot{\mathbf{e}}_i$ (where $i = 1, 2, 3$) are equal to zero.

$$\dot{\boldsymbol{A}} = \dot{A}_1\mathbf{e}_1 + \dot{A}_2\mathbf{e}_2 + \dot{A}_3\mathbf{e}_3 + A_1\dot{\mathbf{e}}_1 + A_2\dot{\mathbf{e}}_2 + A_3\dot{\mathbf{e}}_3 \tag{A.2}$$

where

$$\dot{\mathbf{e}}_i = \boldsymbol{\omega} \times \mathbf{e}_i \tag{A.3}$$

Therefore

$$\dot{\boldsymbol{A}} = (\dot{\boldsymbol{A}})_r + \boldsymbol{\omega} \times \boldsymbol{A} \tag{A.4}$$

Where $(\dot{\boldsymbol{A}})_r$ is the derivative of $\boldsymbol{A}$, as measured in a rotating frame in which unit vectors are fixed. In other words $(\dot{\boldsymbol{A}})_r$ could be seen as either the relative linear velocity or acceleration between two or more points on a fixed-body, these terms are zero should the distance between points remain constant. Now the position of Point P relative to O (refer to Figure A.1) is given by

$$\boldsymbol{r}_{P/O} = \boldsymbol{R} + \boldsymbol{r}_{P/O'} \tag{A.5}$$

Differentiation of equation A.5 gives the velocity of Point P relative to O

$$\boldsymbol{v}_{P/O} = \dot{\boldsymbol{r}}_{P/O} = \dot{\boldsymbol{R}} + \dot{\boldsymbol{r}}_{P/O'} \tag{A.6}$$

now using equation A.4, equation A.7 is obtained

$$\dot{\boldsymbol{r}}_{P/O'} = (\dot{\boldsymbol{r}}_{P/O'})_r + \boldsymbol{\omega} \times \boldsymbol{r}_{P/O'} \tag{A.7}$$

where $(\boldsymbol{v}_{P/O'})_r = (\dot{\boldsymbol{r}}_{P/O'})_r$ and the equation describing the velocity $\boldsymbol{v}_{P/O}$ is finally determined by

$$\boldsymbol{v}_{P/O} = \dot{\boldsymbol{R}} + (\boldsymbol{v}_{P/O'})_r + \boldsymbol{\omega} \times \boldsymbol{r}_{P/O'} \tag{A.8}$$

Differentiating $(\boldsymbol{v}_{P/O'})_r$ with respect to time yields equation A.9.

$$\frac{d}{dt}(\boldsymbol{v}_{P/O'})_r = (\dot{\boldsymbol{v}}_{P/O'})_r + \boldsymbol{\omega} \times (\boldsymbol{v}_{P/O'})_r \tag{A.9}$$

The acceleration of Point P relative to O is determined by deriving equation A.8

$$\dot{\boldsymbol{v}}_{P/O} = \ddot{\boldsymbol{R}} + (\dot{\boldsymbol{v}}_{P/O'})_r + \boldsymbol{\omega} \times (\boldsymbol{v}_{P/O'})_r + \boldsymbol{\omega} \times (\dot{\boldsymbol{r}}_{P/O'}) + \dot{\boldsymbol{\omega}} \times \boldsymbol{r}_{P/O'} \tag{A.10}$$

Substiting $\boldsymbol{a}_{P/O} = \dot{\boldsymbol{v}}_{P/O}$, $(\boldsymbol{a}_{P/O'})_r = (\dot{\boldsymbol{v}}_{P/O'})_r$, $\boldsymbol{\alpha} = \dot{\boldsymbol{\omega}}$ as well as equation A.6 into A.10 the equation describing $\boldsymbol{a}_{P/O}$ is obtained

$$\boldsymbol{a}_{P/O} = \ddot{\boldsymbol{R}} + (\boldsymbol{a}_{P/O'})_r + 2\boldsymbol{\omega} \times (\boldsymbol{v}_{P/O'})_r + \boldsymbol{\omega} \times (\boldsymbol{\omega} \times \boldsymbol{r}_{P/O'}) + \boldsymbol{\alpha} \times \boldsymbol{r}_{P/O'} \quad \text{(A.11)}$$

Equation A.11 can be simplified by making the following assumptions; Point O is stationary $(\boldsymbol{a}_O)$ and the position vector $\boldsymbol{r}_{O'} = 0\mathbf{i} + 0\mathbf{j} + 0\mathbf{k}$. The position vector and acceleration of Point P are defined as follows;

$$\boldsymbol{r}_P = \boldsymbol{r}_O + \boldsymbol{r}_{P/O} \quad \text{(A.12)}$$

$$\boldsymbol{a}_P = \boldsymbol{a}_O + \boldsymbol{a}_{P/O} \quad \text{(A.13)}$$

Hence

$$\boldsymbol{r}_P = \boldsymbol{r}_{P/O} \quad \text{(A.14)}$$

$$\boldsymbol{a}_P = \boldsymbol{a}_{P/O} \quad \text{(A.15)}$$

Finally the absolute acceleration of Point P is described by the following

$$\boldsymbol{a}_P = \ddot{\boldsymbol{R}} + (\boldsymbol{a}_{P/O'})_r + 2\boldsymbol{\omega} \times (\boldsymbol{v}_{P/O'})_r + \boldsymbol{\omega} \times (\boldsymbol{\omega} \times \boldsymbol{r}_P) + \boldsymbol{\alpha} \times \boldsymbol{r}_P \quad \text{(A.16)}$$

Assuming a body is rigid the distance between Point P and O' remain constant. Hence, $(\boldsymbol{a}_{P/O'})_r$ and $(\boldsymbol{v}_{P/O'})_r$ are equal to zero and equation A.16 simplifies to

$$\boldsymbol{a}_P = \ddot{\boldsymbol{R}} + \boldsymbol{\omega} \times (\boldsymbol{\omega} \times \boldsymbol{r}_P) + \boldsymbol{\alpha} \times \boldsymbol{r}_P \quad \text{(A.17)}$$

A.2 Derivation of the angular acceleration in a six accelerometer array

In order to derive equations 2.25 to 2.27 equation A.17 is needed. The layout of six accelerometer array is also reproduced here (Figure A.2) for ease of reference.

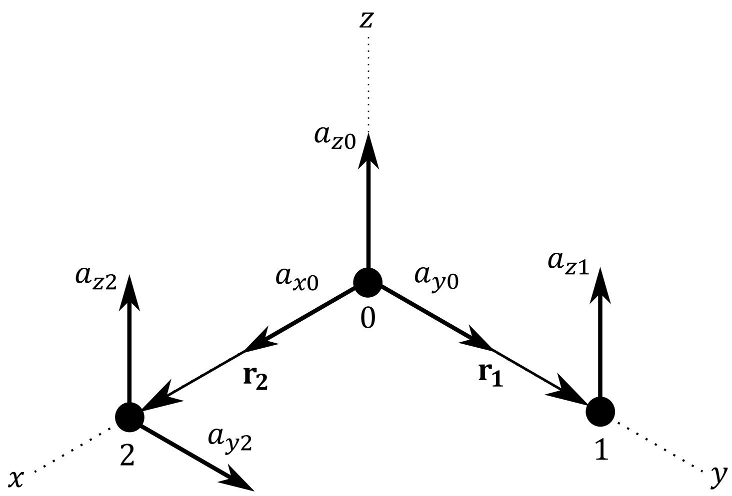

Figure A.2: Six accelerometer array

Since $P = 0, 1, 2, ..., n$ the equations describing the acceleration of Points 0, 1 and 2 are described as follows;

$$\boldsymbol{a}_0 = \ddot{\boldsymbol{R}} + \boldsymbol{\omega} \times (\boldsymbol{\omega} \times \boldsymbol{r}_0) + \boldsymbol{\alpha} \times \boldsymbol{r}_0 \tag{A.18}$$

$$\boldsymbol{a}_1 = \ddot{\boldsymbol{R}} + \boldsymbol{\omega} \times (\boldsymbol{\omega} \times \boldsymbol{r}_1) + \boldsymbol{\alpha} \times \boldsymbol{r}_1 \tag{A.19}$$

$$\boldsymbol{a}_2 = \ddot{\boldsymbol{R}} + \boldsymbol{\omega} \times (\boldsymbol{\omega} \times \boldsymbol{r}_2) + \boldsymbol{\alpha} \times \boldsymbol{r}_2 \tag{A.20}$$

The Cartesian coordinates of Points 0, 1 and 2 are;

$$\boldsymbol{r}_0 = 0\mathbf{i} + 0\mathbf{j} + 0\mathbf{k} \tag{A.21}$$

$$\boldsymbol{r}_1 = 0\mathbf{i} + r_{y1}\mathbf{j} + 0\mathbf{k} \tag{A.22}$$

$$\boldsymbol{r}_2 = r_{x2}\mathbf{i} + 0\mathbf{j} + 0\mathbf{k} \tag{A.23}$$

And the equations describing the angular velocity and angular acceleration are presented as;

$$\boldsymbol{\omega} = \omega_x\mathbf{i} + \omega_y\mathbf{j} + \omega_z\mathbf{k} \tag{A.24}$$

$$\boldsymbol{\alpha} = \alpha_x\mathbf{i} + \alpha_y\mathbf{j} + \alpha_z\mathbf{k} \tag{A.25}$$

Substituting equation A.21 into A.18 it is found that

$$\boldsymbol{a}_0 = \ddot{\boldsymbol{R}} \tag{A.26}$$

Hence

$$\boldsymbol{a}_1 = \boldsymbol{A}_0 + \boldsymbol{\omega} \times (\boldsymbol{\omega} \times \boldsymbol{r}_1) + \boldsymbol{\alpha} \times \boldsymbol{r}_1 \tag{A.27}$$

$$\boldsymbol{a}_2 = \boldsymbol{A}_0 + \boldsymbol{\omega} \times (\boldsymbol{\omega} \times \boldsymbol{r}_2) + \boldsymbol{\alpha} \times \boldsymbol{r}_2 \tag{A.28}$$

Where

$$\boldsymbol{a}_0 = a_{x0}\mathbf{i} + a_{y0}\mathbf{j} + a_{z0}\mathbf{k} \tag{A.29}$$

$$\boldsymbol{a}_1 = a_{x1}\mathbf{i} + a_{y1}\mathbf{j} + a_{z1}\mathbf{k} \tag{A.30}$$

$$\boldsymbol{a}_2 = a_{x2}\mathbf{i} + a_{y2}\mathbf{j} + a_{z2}\mathbf{k} \tag{A.31}$$

Solving for the cross products of equation A.27

$$\boldsymbol{\omega} \times \boldsymbol{r}_1 = \begin{vmatrix} \mathbf{i} & \mathbf{j} & \mathbf{k} \\ \omega_x & \omega_y & \omega_z \\ 0 & r_{y1} & 0 \end{vmatrix} = -\omega_z r_{y1}\mathbf{i} + 0\mathbf{j} + \omega_x r_{y1}\mathbf{k} \tag{A.32}$$

$$\boldsymbol{\alpha} \times \boldsymbol{r}_1 = \begin{vmatrix} \mathbf{i} & \mathbf{j} & \mathbf{k} \\ \alpha_x & \alpha_y & \alpha_z \\ 0 & r_{y1} & 0 \end{vmatrix} = -\alpha_z r_{y1}\mathbf{i} + 0\mathbf{j} + \alpha_x r_{y1}\mathbf{k} \tag{A.33}$$

$$\boldsymbol{\omega} \times (\boldsymbol{\omega} \times \boldsymbol{r}_1) = \begin{vmatrix} \mathbf{i} & \mathbf{j} & \mathbf{k} \\ \omega_x & \omega_y & \omega_z \\ -\omega_z r_{y1} & 0 & \omega_x r_{y1} \end{vmatrix} \tag{A.34}$$

$$\boldsymbol{\omega} \times (\boldsymbol{\omega} \times \boldsymbol{r}_1) = \omega_x\omega_y r_{y1}\mathbf{i} + (\omega_z^2 - \omega_x^2) r_{y1}\mathbf{j} + \omega_y\omega_z r_{y1}\mathbf{k} \tag{A.35}$$

Substituting equations A.29, A.30, A.32, A.33 and A.35 into A.27

$$\begin{bmatrix} a_{x1}\mathbf{i} \\ a_{y1}\mathbf{j} \\ a_{z1}\mathbf{k} \end{bmatrix} = \begin{bmatrix} a_{x0}\mathbf{i} \\ a_{y0}\mathbf{j} \\ a_{z0}\mathbf{k} \end{bmatrix} + \begin{bmatrix} \omega_x\omega_y r_{y1}\mathbf{i} \\ (\omega_z^2 - \omega_x^2) r_{y1}\mathbf{j} \\ \omega_y\omega_z r_{y1}\mathbf{k} \end{bmatrix} + \begin{bmatrix} -\alpha_z r_{y1}\mathbf{i} \\ 0\mathbf{j} \\ \alpha_x r_{y1}\mathbf{k} \end{bmatrix} \tag{A.36}$$

Finally solving for α_x using the acceleration in the $\mathbf{k}$ direction

$$a_{z1} = a_{z0} + \omega_y\omega_z r_{y1} + \alpha_x r_{y1} \tag{A.37}$$

$$\alpha_x r_{y1} = a_{z1} - a_{z0} - \omega_y\omega_z r_{y1} \tag{A.38}$$

$$\alpha_x = (a_{z1} - a_{z0})/r_{y1} - \omega_y\omega_z \tag{A.39}$$

Solving for the cross products of equation A.28

$$\boldsymbol{\omega} \times \boldsymbol{r}_2 = \begin{vmatrix} \mathbf{i} & \mathbf{j} & \mathbf{k} \\ \omega_x & \omega_y & \omega_z \\ r_{x2} & 0 & 0 \end{vmatrix} = 0\mathbf{i} + \omega_z r_{x2}\mathbf{j} - \omega_y r_{x2}\mathbf{k} \tag{A.40}$$

$$\boldsymbol{\alpha} \times \boldsymbol{r}_2 = \begin{vmatrix} \mathbf{i} & \mathbf{j} & \mathbf{k} \\ \alpha_x & \alpha_y & \alpha_z \\ r_{x2} & 0 & 0 \end{vmatrix} = 0\mathbf{i} + \alpha_z r_{x2}\mathbf{j} - \alpha_y r_{x2}\mathbf{k} \tag{A.41}$$

$$\boldsymbol{\omega} \times (\boldsymbol{\omega} \times \boldsymbol{r}_2) = \begin{vmatrix} \mathbf{i} & \mathbf{j} & \mathbf{k} \\ \omega_x & \omega_y & \omega_z \\ 0 & \omega_z r_{x2} & -\omega_y r_{x2} \end{vmatrix} \tag{A.42}$$

$$\boldsymbol{\omega} \times (\boldsymbol{\omega} \times \boldsymbol{r}_2) = -(\omega_y^2 + \omega_z^2) r_{x2}\mathbf{i} + \omega_x\omega_y r_{x2}\mathbf{j} + \omega_x\omega_z r_{x2}\mathbf{k} \tag{A.43}$$

kk Substituting equations A.29, A.31, A.40, A.41 and A.43 into A.28

$$\begin{bmatrix} a_{x2}\mathbf{i} \\ a_{y2}\mathbf{j} \\ a_{z2}\mathbf{k} \end{bmatrix} = \begin{bmatrix} a_{x0}\mathbf{i} \\ a_{y0}\mathbf{j} \\ a_{z0}\mathbf{k} \end{bmatrix} + \begin{bmatrix} -(\omega_y^2 + \omega_z^2) r_{x2}\mathbf{i} \\ \omega_x\omega_y r_{x2}\mathbf{j} \\ \omega_x\omega_z r_{x2}\mathbf{k} \end{bmatrix} + \begin{bmatrix} 0\mathbf{i} \\ \alpha_z r_{x2}\mathbf{j} \\ -\alpha_y r_{x2}\mathbf{k} \end{bmatrix} \tag{A.44}$$

Finally solving for α_y and α_z using the acceleration in the $\mathbf{k}$ and $\mathbf{j}$ directions respectively.

$$a_{z2} = a_{z0} + \omega_x\omega_z r_{x2} - \alpha_y r_{x2} \tag{A.45}$$

$$-\alpha_y r_{x2} = a_{z2} - a_{z0} - \omega_x\omega_z r_{x2} \tag{A.46}$$

$$\alpha_y = -(a_{z2} - a_{z0})/r_{x2} + \omega_x\omega_z \tag{A.47}$$

$$a_{y2} = a_{y0} + \omega_x\omega_y r_{x2} + \alpha_z r_{x2} \tag{A.48}$$

$$\alpha_z r_{x2} = a_{y2} - a_{y0} - \omega_x\omega_y r_{x2} \tag{A.49}$$

$$\alpha_z = (a_{y2} - a_{y0})/r_{x2} - \omega_x\omega_y \tag{A.50}$$

Appendix B

Motion sickness questionnaires

This Appendix contains the three questionnaires used during the Marion 2014 voyage, the personal details questionnaire, the motion sickness susceptibility questionnaire and the daily diary questionnaire.

B.1 Marion personal details questionnaire

1.	***Date boarded***		(dd/mm/yy)	2.	**Date disembarked**		(dd/mm/yy)
3.	***Age***			4.	**Gender**	Male	Female
5.	***Body weight***			6.	**Stature**		
7.	***Voyage experience***						
a.	**Number of voyages**	1	2	3	4	5	6+
b.	**Sea time**	Months	Years				
8.	***Motion sickness medication***						
a.	***Do you take any motion sickness medication or use bands?***	Yes	No				
b.	*If yes what kind do you use and what dosage do you take?*						
	Type		***Dosage***				

B.2 Marion motion sickness susceptability questionnaire

Motion sickness susceptibility questionnaire

This questionnaire is designed to determine: (i) which modes of transport are most effective at causing motion sickness and, (ii) how susceptible people are to motion sickness.

Please read each questionnaire carefully and answer all of the by ticking the box that describes you.

All information given is confidential and will be used for research purposes only.

Thank you for your time and patience.

1. In the past **year**, how many times have you travelled **as a passenger** in the following types of transport?

	Never	1	2-3	4-15	16-63	64-255	256+
Cars							
Buses							
Coaches							
Small boats							
Ships							
Aeroplanes							
Trains							

2. In the past **year**, how many times have you felt **ill** whilst travelling **as a passenger** in the following types of transport?

	Never	1	2	3	4-7	8-15	16+
Cars							
Buses							
Coaches							
Small boats							
Ships							
Aeroplanes							
Trains							

3. In the past **year**, how many times have you felt **vomited** whilst travelling **as a passenger** in the following types of transport?

	Never	1	2	3	4-7	8-15	16+
Cars							
Buses							
Coaches							
Small boats							
Ships							
Aeroplanes							
Trains							

4. Do you ever feel **hot** or **sweat** whilst travelling **as a passenger** in the following types of transport?

	Never	Occasionally	Often	Always
Cars				
Buses				
Coaches				
Small boats				
Ships				
Aeroplanes				
Trains				

5. Do you ever suffer from loss/change of skin colour (**go pale**) whilst travelling **as a passenger** in the following types of transport?

	Never	Occasionally	Often	Always
Cars				
Buses				
Coaches				
Small boats				
Ships				
Aeroplanes				
Trains				

6. Do you ever suffer from **headaches** whilst travelling **as a passenger** in the following types of transport?

	Never	Occasionally	Often	Always
Cars				
Buses				
Coaches				
Small boats				
Ships				
Aeroplanes				
Trains				

7. Do you ever suffer from **mouth-watering** whilst travelling **as a passenger** in the following types of transport?

	Never	Occasionally	Often	Always
Cars				
Buses				
Coaches				
Small boats				
Ships				
Aeroplanes				
Trains				

8. Do you ever feel from **dizzy** whilst travelling **as a passenger** in the following types of transport?

	Never	Occasionally	Often	Always
Cars				
Buses				
Coaches				
Small boats				
Ships				
Aeroplanes				
Trains				

9. Do you ever feel from **drowsy** whilst travelling **as a passenger** in the following types of transport?

	Never	Occasionally	Often	Always
Cars				
Buses				
Coaches				
Small boats				
Ships				
Aeroplanes				
Trains				

10. Do you ever suffer from **nausea** whilst travelling **as a passenger** in the following types of transport?

	Never	Occasionally	Often	Always
Cars				
Buses				
Coaches				
Small boats				
Ships				
Aeroplanes				
Trains				

11. Have you ever **vomited** whilst travelling **as a passenger** in the following types of transport?

	Yes	No	Do not know
Cars			
Buses			
Coaches			
Small boats			
Ships			
Aeroplanes			
Trains			

12. Would you ever avoid any of the following types of transport because of motion sickness?

	Never	Occasionally	Often	Always
Cars				
Buses				
Coaches				
Small boats				
Ships				
Aeroplanes				
Trains				

13. Which of the following best describes you susceptibility to motion sickness?

Much less than average	
Less than average	
Average	
More than average	
Much more than average	

14. Have you ever suffered from any serious illness or injury?

Yes	No

B.3 Marion daily diary questionnaire

April 2014

Mo	Tu	We	Th	Fr	Sa	Su
	1	**2**	3	4	5	6
7	8	9	10	**11**	12	13
14	15	**16**	17	**18**	19	20
21	**22**	23	**24**	25	26	**27**
28	29	30				

May 2014

Mo	Tu	We	Th	Fr	Sa	Su
			1	2	3	4
5	**6**	**7**	8	9	10	11

Daily Diary for motion sickness

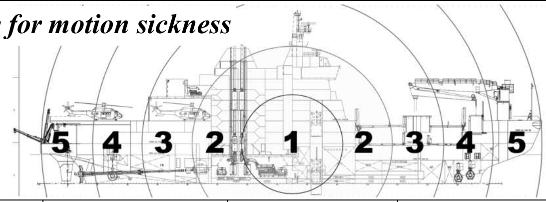

1.	***Date started***		(dd/mm/yy)	2.	***Time started***		(e.g.00:00 – 24:00)
	Date ended		(dd/mm/yy)		***Time ended***		(e.g.00:00 – 24:00)

2\. ***Task performance (Work tasks / leisure activities)***

Please list maximum of 6 main work tasks or leisure activities and their locations in the vessel in the last 24 hours (refer diagram). Also specify the approximate percentage of time spent. Proceed to circle a number which most closely relates to any performance problems listed, according to any difficulties experienced, using codes 0 - 4 as follows: 0 = none, 1 = slight, 2 = some, 3 = great, 4 = severe.

Use the provision for "Other Activities" if more than one work task of a similar category is performed in another location on the vessel.

Work task / leisure activity	***Location in vessel***	***% time***	***Balance / Moving***	***Carrying/ Lifting***	***Hand / eye co-ordination***	***Vision***	***Attention / concentration***	***Task completion time***	
Physical work (lifting, lab work, etc.)			0 1 2 3 4	0 1 2 3 4	0 1 2 3 4	0 1 2 3 4	0 1 2 3 4	Same time	More time
Typing / Writing			0 1 2 3 4	0 1 2 3 4	0 1 2 3 4	0 1 2 3 4	0 1 2 3 4	Same time	More time
Using Electronic Equipment			0 1 2 3 4	0 1 2 3 4	0 1 2 3 4	0 1 2 3 4	0 1 2 3 4	Same time	More time
Operating machinery (crane, lifter, etc.)			0 1 2 3 4	0 1 2 3 4	0 1 2 3 4	0 1 2 3 4	0 1 2 3 4	Same time	More time
Visual activities (Watching TV / Reading)			0 1 2 3 4	0 1 2 3 4	0 1 2 3 4	0 1 2 3 4	0 1 2 3 4	Same time	More time
Eating/ walking/sitting			0 1 2 3 4	0 1 2 3 4	0 1 2 3 4	0 1 2 3 4	0 1 2 3 4	Same time	More time
Other Activities (Please specify)									
_______________			0 1 2 3 4	0 1 2 3 4	0 1 2 3 4	0 1 2 3 4	0 1 2 3 4	Same time	More time
_______________			0 1 2 3 4	0 1 2 3 4	0 1 2 3 4	0 1 2 3 4	0 1 2 3 4	Same time	More time

3\. ***Symptoms***

(Please record any symptoms experienced during the last 24-hour period for work and leisure activities using the following headings).

	Work Tasks					***Leisure Activities***				
Symptoms	***None***	***Slight***	***Some***	***Great***	***Severe***	***None***	***Slight***	***Some***	***Great***	***Severe***
Stomach awareness	☐	☐	☐	☐	☐	☐	☐	☐	☐	☐
Nausea	☐	☐	☐	☐	☐	☐	☐	☐	☐	☐
Vomiting / retching	☐	☐	☐	☐	☐	☐	☐	☐	☐	☐
Lack of motivation	☐	☐	☐	☐	☐	☐	☐	☐	☐	☐
Depression	☐	☐	☐	☐	☐	☐	☐	☐	☐	☐
Tension / anxiety	☐	☐	☐	☐	☐	☐	☐	☐	☐	☐
Yawning / drowsiness	☐	☐	☐	☐	☐	☐	☐	☐	☐	☐
Dizziness	☐	☐	☐	☐	☐	☐	☐	☐	☐	☐
Faintness	☐	☐	☐	☐	☐	☐	☐	☐	☐	☐
Feelings of vertigo	☐	☐	☐	☐	☐	☐	☐	☐	☐	☐
Headaches	☐	☐	☐	☐	☐	☐	☐	☐	☐	☐
Irregularities in breathing	☐	☐	☐	☐	☐	☐	☐	☐	☐	☐
Sensations of warmth	☐	☐	☐	☐	☐	☐	☐	☐	☐	☐
Sweating	☐	☐	☐	☐	☐	☐	☐	☐	☐	☐
Aches and pains	☐	☐	☐	☐	☐	☐	☐	☐	☐	☐
Low back pain	☐	☐	☐	☐	☐	☐	☐	☐	☐	☐
Infections	☐	☐	☐	☐	☐	☐	☐	☐	☐	☐
Others (please specify)										
__________________	☐	☐	☐	☐	☐	☐	☐	☐	☐	☐

4.	***Motion sickness medication***						
a.	*Did you take any motion sickness medication or use bands to combat motion sickness in the last 24 hours?*				Yes		No
b.	*If yes what kind do you use and what dosage do you take?*						
	Type				***Dosage***		
5.	***Environmental Factors*** *(Please record any problems experienced during the last 24 -hour period using codes 0 -4 below.* *0 = none, 1 = slight, 2 = some, 3 = great, 4 = severe)*						
		0	1	2	3	4	
	Mental tiredness	☐	☐	☐	☐	☐	
	Noise	☐	☐	☐	☐	☐	
	Vibration	☐	☐	☐	☐	☐	
	Temperature	☐	☐	☐	☐	☐	
	Lighting	☐	☐	☐	☐	☐	
	Air quality	☐	☐	☐	☐	☐	
	Other (please specify)						
	____________________	☐	☐	☐	☐	☐	
6.	***Tiredness and sleep*** *(Please record any problems experienced during the last 24 hour period using the codes 0 – 4 below: 0 = none, 1 = slight, 2 = some, 3 = great, 4 = severe)*						
	Tiredness & Sleep	0	1	2	3	4	
	Mental tiredness	☐	☐	☐	☐	☐	
	Physical tiredness	☐	☐	☐	☐	☐	
	Sleepy feelings	☐	☐	☐	☐	☐	
	Poor sleep quality	☐	☐	☐	☐	☐	
	Not enough sleep	☐	☐	☐	☐	☐	
	Sleep interruptions	☐	☐	☐	☐	☐	
	(Please specify causes)						
	________________________________						
	Hours of sleep	☐	☐	☐	☐		
		<4	5 - 8	9 - 12	>12 Hours		

Daily Diary for Slamming

1. Did you encounter any slamming incidents in the past 24-hours? Yes ☐ No ☐

If 'No' ignore the remaining questions on this page

2 How frequent were the slamming incidents?

Once or twice ☐ Occasionally ☐ Regularly ☐ Always ☐

3.a How would you rate the worst slamming incident on the scale of 1 to 10?

1 ☐ 2 ☐ 3 ☐ 4 ☐ 5 ☐ 6 ☐ 7 ☐ 8 ☐ 9 ☐ 10 ☐

Just noticeable Mild Heavy Severe Bouncing

b. What part of this slamming incident seems to make it worst? (you can choose more than one option)

Noise ☐ Vibration ☐ Shock Impact ☐ Other ☐ ________________

c. What was your location in the vessel at the time of the worst slamming incident? (Please refer diagram) ______

4. Do you consider these slamming to be unpredictable? ***Yes*** ☐ ***No***☐

If yes, do you feel this factor contributes towards making slamming uncomfortable? ***Yes*** ☐ ***No***☐

5. ***Human Performance***

Which of the following tasks were you performing during the last 24-hours when slamming occurred and how were they affected?

Please select the appropriate tasks and for each, please circle a number which most closely relates to any performance problems listed, according to any difficulties experienced, using codes 0 - 4 as follows: 0 = none, 1 = slight, 2 = some, 3 = great, 4 = severe (Task wasn't completed)

	Task / Activity	***Location***	***Balance / Moving***	***Carrying/ Lifting***	***Hand / eye co-ordination***	***Vision***	***Attention / concentration***	***Task delay?***	
☐	Physical work (lifting, lab work, etc.)		0 1 2 3 4	0 1 2 3 4	0 1 2 3 4	0 1 2 3 4	0 1 2 3 4	Same time	More time
☐	Typing / Writing		0 1 2 3 4	0 1 2 3 4	0 1 2 3 4	0 1 2 3 4	0 1 2 3 4	Same time	More time
☐	Using Electronic Equipment		0 1 2 3 4	0 1 2 3 4	0 1 2 3 4	0 1 2 3 4	0 1 2 3 4	Same time	More time
☐	Operating machinery (crane, lifter, etc.)		0 1 2 3 4	0 1 2 3 4	0 1 2 3 4	0 1 2 3 4	0 1 2 3 4	Same time	More time
☐	Visual activities (Watching TV / Reading)		0 1 2 3 4	0 1 2 3 4	0 1 2 3 4	0 1 2 3 4	0 1 2 3 4	Same time	More time
☐	Eating/ walking/sitting		0 1 2 3 4	0 1 2 3 4	0 1 2 3 4	0 1 2 3 4	0 1 2 3 4	Same time	More time
	Other Activities (Please specify)								
☐	___________		0 1 2 3 4	0 1 2 3 4	0 1 2 3 4	0 1 2 3 4	0 1 2 3 4	Same time	More time
☐	___________		0 1 2 3 4	0 1 2 3 4	0 1 2 3 4	0 1 2 3 4	0 1 2 3 4	Same time	More time

6. **Equipment Performance**

a. Did slamming affect the functioning of your instrument/equipment? Please describe the experience.

No☐ Physical damage ☐ Malfunctioning ☐ Knocked out ☐ Cannot operate ☐ Others ☐ ___________

Description: ____

7. **Symptoms**

(Please record any symptoms experienced during the last 24-hour period due to slamming for activities using the following headings).

	Symptoms	***None***	***Slight***	***Some***	***Great***	***Severe***
a.	Headache	☐	☐	☐	☐	☐
b.	Tension / Anxiety	☐	☐	☐	☐	☐
c.	Aches and pains	☐	☐	☐	☐	☐
d.	Low Back pain	☐	☐	☐	☐	☐
e.	Depression	☐	☐	☐	☐	☐
f.	Other: Please specify ___________	☐	☐	☐	☐	☐

8. **Sleep**

a. Did slamming incidents interfere with your sleep last night?

No☐ Slight unease ☐ Sleep interruptions ☐ Kept you up for some time ☐ Others ☐ ___________

Appendix C

Equipment details

The channel identity, sensitivity and point number on the measurement setups for each accelerometer are summarised for both the Marion Island 2014 and Antarctica 2014/2015 voyages in Tables C.1 and C.2. Tables C.1 and C.2 also summarized the other equipment used during the voyages.

Table C.1: Marion Island 2014 equipment

Equipment	Model number	Serial number	Point	Channel ID	Sensitivity [mV/(m/s^2)]
DC accelerometer (PCB)	3711B1110G	LW6305	a_{0x}	Point 21	19.84
DC accelerometer (PCB)	3711B1110G	LW6310	a_{0y}	Point 22	19.60
DC accelerometer (PCB)	3711B1110G	LW6301	a_{0z}	Point 23	19.64
DC accelerometer (PCB)	3711B1110G	LW6300	a_{1z}	Point 7	20.23
DC accelerometer (PCB)	3711B1110G	LW6309	a_{2y}	Point 5	19.97
DC accelerometer (PCB)	3711B1110G	LW6302	a_{2z}	Point 6	19.73
DC accelerometer (PCB)	3711B1110G	LW6303	a_{3z}	Point 24	20.67
SCADAS (LMS)	SCM02	52112007	-	-	-
SCADAS (LMS)	SCM03S	52122505	-	-	-
SCADAS (LMS)	SCM03S	52122506	-	-	-
Laptop (Lenovo)	-	-	-	-	-
DC signal conditioner (SVRG - US)	-	-	-	-	-

Table C.2: Antarctica 2014/2015 equipment

Equipment	Model number	Serial number	Point	Channel ID	Sensitivity [mV/(m/s^2)]
DC accelerometer (PCB)	3711B1110G	LW6305	a_{0x}	Point 37	19.84
DC accelerometer (PCB)	3711B1110G	LW6310	a_{0y}	Point 38	19.60
DC accelerometer (PCB)	3711B1110G	LW6301	a_{0z}	Point 39	19.64
DC accelerometer (PCB)	3711B1110G	LW6300	a_{2y}	Point 19	20.23
DC accelerometer (PCB)	3711B1110G	LW6309	a_{2z}	Point 18	19.97
DC accelerometer (PCB)	3711B1110G	LW6302	a_{1z}	Point 40	19.73
DC accelerometer (PCB)	3711B1110G	LW6303	a_{3z}	Point 15	20.67
DC accelerometer (PCB)	3711B1110G	LW6308	a_{4z}	Point 16	20.64
SCADAS (LMS)	SCM02	52112007	-	-	-
SCADAS (LMS)	SCM03S	52122505	-	-	-
SCADAS (LMS)	SCM03S	52122506	-	-	-
Laptop (Lenovo)	-	-	-	-	-
DC signal conditioner (SVRG - US)	-	-	-	-	-

Appendix D

Vibration evaluation

The weighted r.m.s. acceleration levels and crest factors for the various each measurement channels on the Marion Island 2014 and Antarctica 2014/2015 voyage are summarised in this Appendix.

D.1 Weighted r.m.s. acceleration - Marion 2014

The weighted r.m.s. levels for each 5 min measurement file was determined for Points 0, 1 and 2. These weighted r.m.s. levels are found in Figures D.1 to D.2.

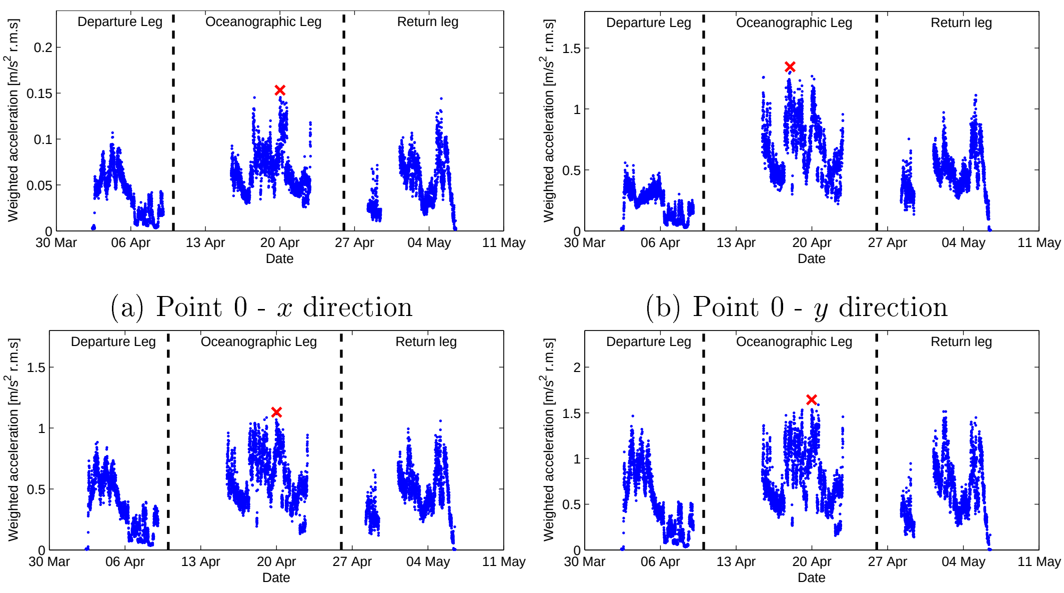

(a) Point 0 - x direction

(b) Point 0 - y direction

(c) Point 0 - z direction

(d) Point 1 - z direction

Figure D.1: Weighted r.m.s. acceleration - Marion 2014 (Part 1)

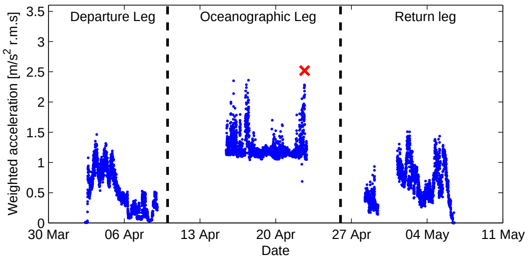

(a) Point 2 - z direction

Figure D.2: Weighted r.m.s. acceleration - Marion 2014 (Part 2)

D.2 Crest factor - Marion 2014

Crest factors (found in Figure D.2) were determined for each 5 min measurement file at Points 0, 1 and 2 of the Marion accelerometer array.

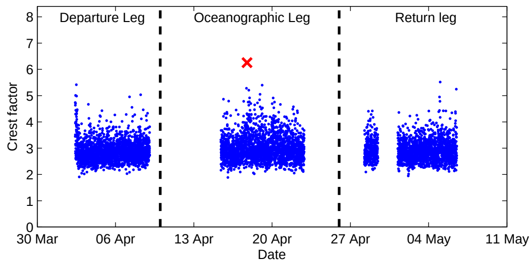

(a) Point 0 - x direction

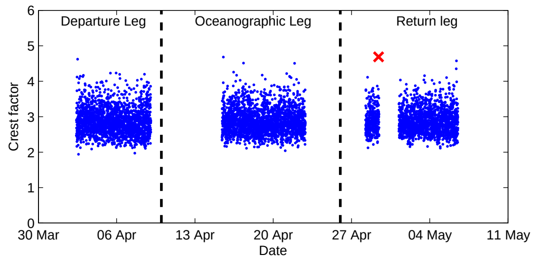

(b) Point 0 - y direction

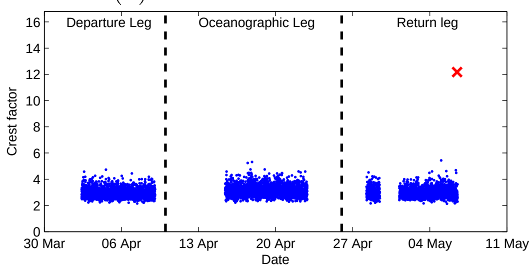

(c) Point 0 - z direction

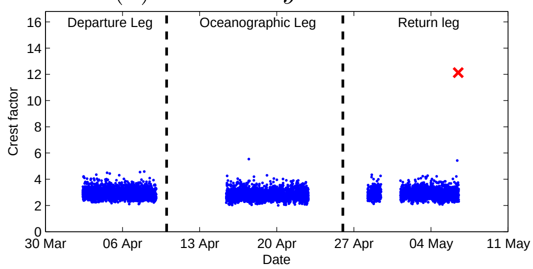

(d) Point 1 - z direction

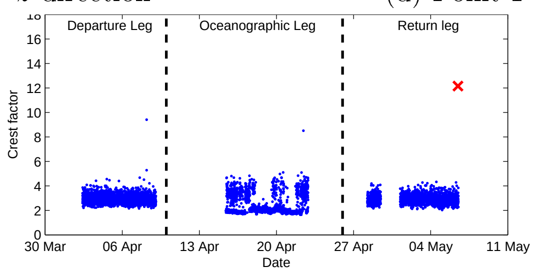

(e) Point 2 - z direction

Figure D.3: Crest factor - Marion 2014

D.3 Weighted r.m.s. acceleration - Antarctica 2014/2015

The weighted r.m.s. acceleration levels were determined, for every 5 min measurement, for all eight accelerometers used during the Antarctica 2014/2015 voyage are found in Figure D.4. The peak levels of r.m.s. acceleration were found during Legs 2 and 3.

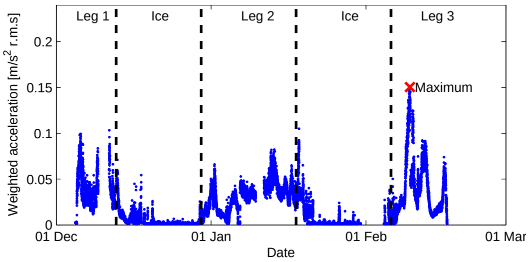

(a) Point 0 - x direction

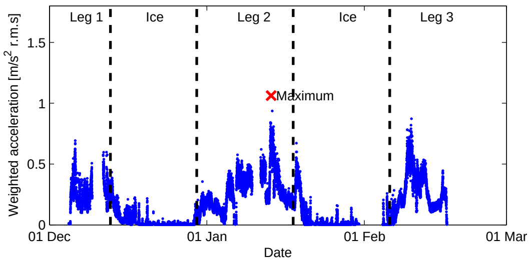

(b) Point 0 - y direction

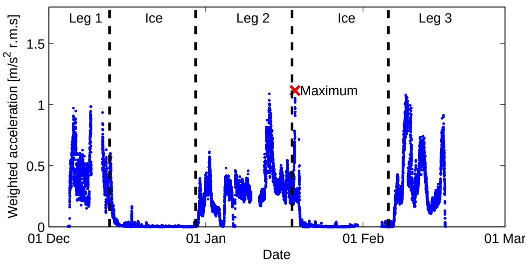

(c) Point 0 - z direction

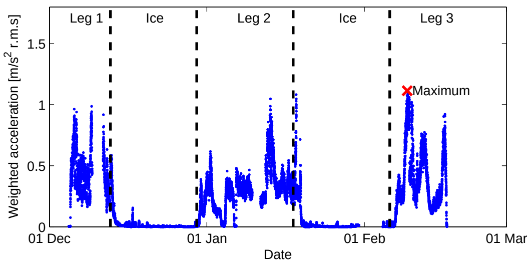

(d) Point 1 - z direction

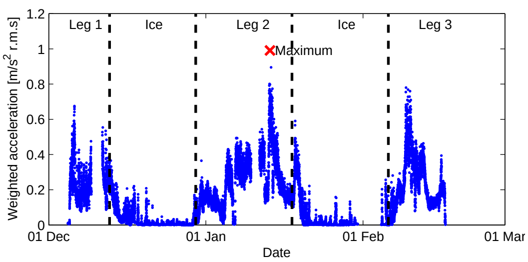

(e) Point 2 - y direction

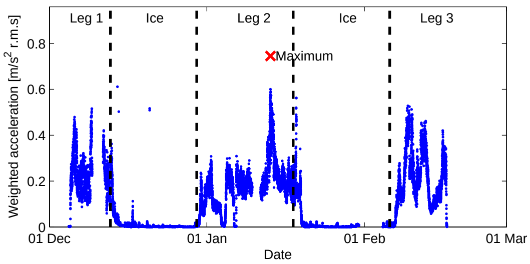

(f) Point 2 - z direction

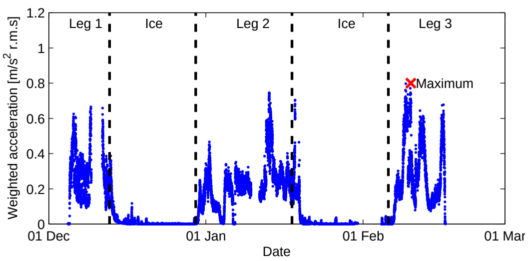

(g) Point 3 - z direction

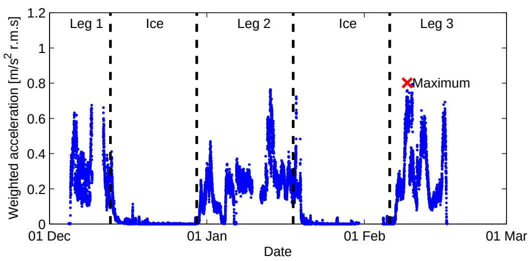

(h) Point 4 - z direction

Figure D.4: Weighted r.m.s. acceleration - Antartica 2014/2015

D.4 Crest factor - Antartica 2014/2015

Figure D.5 presents the crest factors for the Antarctica 2014/2015 voyage for each 5 min measurement. The crest factors peaked during the ice legs of the voyage and remained relatively constant during Legs 1 to 3.

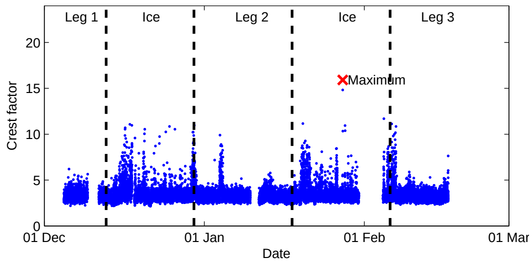

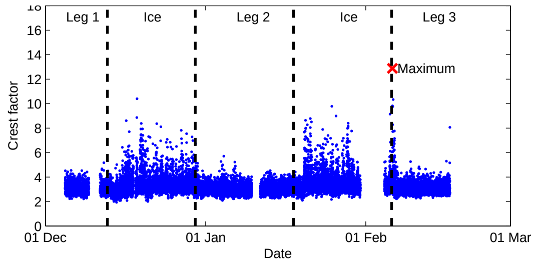

(a) Point 0 - x direction (b) Point 0 - y direction

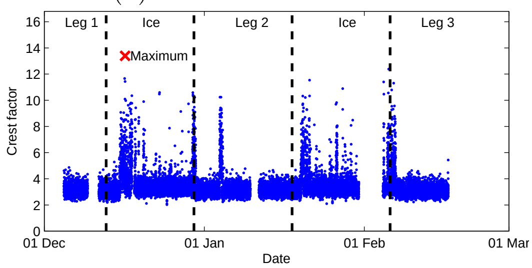

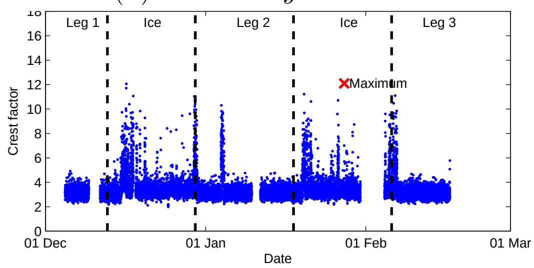

(c) Point 0 - z direction (d) Point 1 - z direction

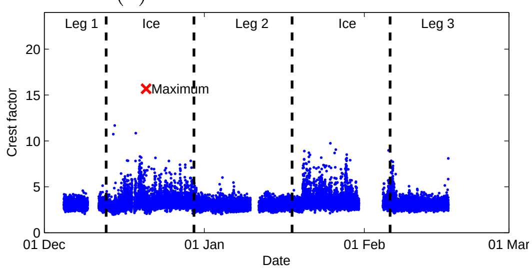

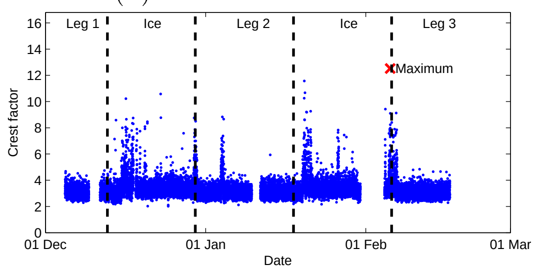

(e) Point 2 - y direction (f) Point 2 - z direction

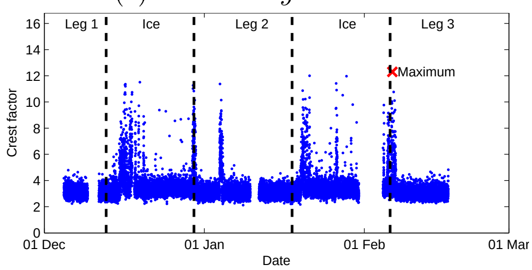

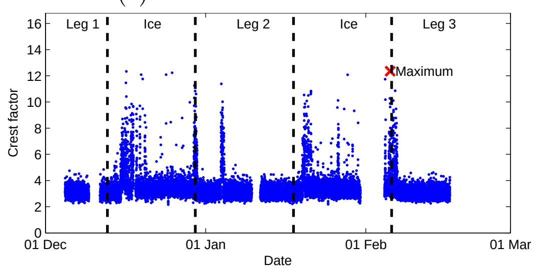

(g) Point 3 - z direction (h) Point 4 - z direction

Figure D.5: Crest factor - Antartica 2014/2015

Appendix E

Matlab code

Key Matlab functions used to determine the Rigid Body Motion (RBM) of the SA Agulhas II (SAAII) as well as the Infinite Impulse Response (IIR) filter are presented in this Appendix.

E.1 IIR Weighting filter

iirFilterISO.m

```
function X = iirFilterISO(x,k,fs)
% Developed by Brendan Guy Boulle (15609804)
% Stellenbosch University
% Department of Mechanical and Mechatronic Engineering
% Sound and Vibration Research Group
% 2014
%
% Weights the input acceleration "x" according to ISO 2631-1 (1997)
% and Donohew and Griffin (2004). Outputs the weighted acceleration
% "X" according to the filter selected "k".
%
% References:
% AN. Rimell, NJ. Mansfield. 2007. Digital Filters for Frequency
% Weightings Required for Risk Assessments of Workers Exposed to
% Vibration. Industrial Health 2007, 45, 512-519.
%
% BS ISO 2631-1:1997. Mechanical vibration and shock - Evaluation
% of human exposure to whole-body vibration. Part 1: General
% Requirements. BSI Standards Publication.
%
% Donohew BE, Griffin MJ. 2004. Motion sickness: Effect of the
% frequency of lateral oscillation
%
% Weighting | k | Input     | Direction   | Frequency range ( Hz) |
% --------- | - | --------- | ----------- | --------------------- |
% Wc        | 1 | Back      | x           | 0.5 - 80              |
```

```
% Wd          | 2 | Seat     | x & y        | 0.5 - 80        |
%             |   | Standing | x & y        |                 |
%             |   | Laying   | y & z        |                 |
%             |   | Back     | y & z        |                 |
% We          | 3 | Seat     | rx, ry & rz  | 0.5 - 80        |
% Wf          | 4 | MS       | z            | 0.1 - 0.5       |
% Wj          | 5 | Laying   | z (head)     | 0.5 - 80        |
% Wb / Wk     | 6 | Seat     | z            | 0.5 - 80        |
%             |   | Feet     | x, y & z     |                 |
%             |   | Standing | z            |                 |
%             |   | Laying   | x            |                 |
% Wm          | 7 | -        | -            | -               |
% *Wdg        | 8 | MS       | x & y        | 0.5 - 80        |
%
% MS = Motion sickness
% *Donohew (2004)

fs_min = [900 900 900 6.93 800 900 900 6.93];

%% Coefficients
% High pass filter
w1 = 2*tan([0.4 0.4 0.4 0.08 0.4 0.4 0.7943 0.02]*pi/fs);
Q1 = [1 1 1 1 1 1 1 1]/sqrt(2);
% Low pass filter
w2 = 2*tan([100 100 100 0.63 100 100 100 0.63]*pi/fs);
Q2 = [1 1 1 1 1 1 1 1]/sqrt(2);
% Acceleration-velocity transition filter
w3 = 2*tan([8 2 1 inf 0 12.5 5.68 0]*pi/fs);
w4 = 2*tan([8 2 1 0.25 0 12.5 5.684 0.25]*pi/fs);
Q4 = [0.63 0.63 0.63 0.86 0 0.63 0.5 0.86];
% Upward step filter
w5 = 2*tan([0 0 0 0.0625 3.75 2.37 0 0]*pi/fs);
Q5 = [0 0 0 0.8 0.91 0.91 0 1];
w6 = 2*tan([0 0 0 0.1 5.3 3.35 0 0]*pi/fs);
Q6 = [0 0 0 0.8 0.91 0.91 0 1];

%% IIR filters with coefficients
% Coefficients for Hh
aHh = [ Q1(k)*w1(k)^2 + 2*w1(k) + 4*Q1(k), 2*Q1(k)*w1(k)^2 - ...
    8*Q1(k), Q1(k)*w1(k)^2 - 2*w1(k) + 4*Q1(k)];
bHh = [ 4*Q1(k), -8*Q1(k), 4*Q1(k)];
% Coefficients for Hl
aHl = [ Q2(k)*w2(k)^2 + 2*w2(k) + 4*Q2(k), 2*Q2(k)*w2(k)^2 - ...
    8*Q2(k), Q2(k)*w2(k)^2 - 2*w2(k) + 4*Q2(k)];
bHl = [ Q2(k)*w2(k)^2, 2*Q2(k)*w2(k)^2, Q2(k)*w2(k)^2 ];
% Coefficients for Ht - Wf and Wf_l
aHtf = [ Q4(k)*w4(k)^2 + 2*w4(k) + 4*Q4(k), 2*Q4(k)*w4(k)^2 - ...
    8*Q4(k), Q4(k)*w4(k)^2 - 2*w4(k) + 4*Q4(k)];
bHtf = [ Q4(k)*w4(k)^2, 2*Q4(k)*w4(k)^2, Q4(k)*w4(k)^2];
% Coefficients for Ht - Wk
aHtk = [ Q4(k)*w3(k)*w4(k)^2 + 2*w3(k)*w4(k) + 4*Q4(k)*w3(k),...
    2*Q4(k)*w3(k)*w4(k)^2 - 8*Q4(k)*w3(k),...
```

```
    Q4(k)*w3(k)*w4(k)^2 - 2*w3(k)*w4(k) + 4*Q4(k)*w3(k)];
bHtk = [ 2*Q4(k)*w4(k)^2 + Q4(k)*w3(k)*w4(k)^2, ...
    2*Q4(k)*w3(k)*w4(k)^2, Q4(k)*w3(k)*w4(k)^2 - 2*Q4(k)*w4(k)^2];
% Coefficients for Hs
aHs = [ Q5(k)*Q6(k)*w6(k)^2 + 2*Q5(k)*w6(k) + 4*Q5(k)*Q6(k),...
    2*Q5(k)*Q6(k)*w6(k)^2 - 8*Q5(k)*Q6(k),...
    Q5(k)*Q6(k)*w6(k)^2 - 2*Q5(k)*w6(k) + 4*Q5(k)*Q6(k)];
bHs = [ Q5(k)*Q6(k)*w5(k)^2 + 2*Q6(k)*w5(k) + 4*Q5(k)*Q6(k),...
    2*Q5(k)*Q6(k)*w5(k)^2 - 8*Q5(k)*Q6(k),...
    Q5(k)*Q6(k)*w5(k)^2 - 2*Q6(k)*w5(k) + 4*Q5(k)*Q6(k)];

%% Irr filters
    if fs >= fs_min(k)
        if k >= 1 && k <= 8
            if k == 1 || k == 2 || k == 3 || k == 7
                xHh = filter(bHh,aHh,x);
                xHl = filter(bHl,aHl,xHh);
                X = filter(bHtk,aHtk,xHl);
            elseif k == 4
                xHh = filter(bHh,aHh,x);
                xHl = filter(bHl,aHl,xHh);
                xHt = filter(bHtf,aHtf,xHl);
                X = filter(bHs,aHs,xHt);
            elseif k == 5
                xHh = filter(bHh,aHh,x);
                xHl = filter(bHl,aHl,xHh);
                X = filter(bHs,aHs,xHl);
            elseif k == 6
                xHh = filter(bHh,aHh,x);
                xHl = filter(bHl,aHl,xHh);
                xHt = filter(bHtk,aHtk,xHl);
                X = filter(bHs,aHs,xHt);
            elseif k == 8
                xHh = filter(bHh,aHh,x);
                xHl = filter(bHl,aHl,xHh);
                X = filter(bHtf,aHtf,xHl);
            end
        else
           fprintf('Enter a valid k value\n')
        end
    else
        fprintf('Your sample frequency is too low\n')
    end
end
```

E.2 Modified six accelerometer array

modified_6_acc_array.m

```
function [ax2,ax1,ay1,wx,wy,wz,wdx,wdy,wdz,e1] = ...
    modified_6_acc_array(ax0,ay0,az0,ay2,az2,az1,r1,r2,niter,dt)
% rbm_SAAII

% Initializes wx, wy, wz, wdx, wdy, wdz
wx = zeros(1,length(ax0));
wy = zeros(1,length(ax0));
wz = zeros(1,length(ax0));
wdx = zeros(1,length(ax0));
wdy = zeros(1,length(ax0));
wdz = zeros(1,length(ax0));

iter = 0;
e1 = 1000;
err = 1000;

while err>1e-12
    if iter<niter
        wdx = (az1-az0)/r1(2)-wy.*wz;
        wdy = -(az2-az0-wdx*r2(2)-wz.*(wx*r2(1)+wy*r2(2))+...
            r2(3)*(wx.^2+wy.^2))/r2(1);
        wdz = (ay2-ay0+wdx*r2(3)-wy.*(wz*r2(3)+wx*r2(1))+...
            r2(2)*(wz.^2+wx.^2))/r2(1);

        Wx = wx;
        Wy = wy;
        Wz = wz;
        E1 = e1;
        wx = cumtrapz(detrend(wdx))*dt;
        wy = cumtrapz(detrend(wdy))*dt;
        wz = cumtrapz(detrend(wdz))*dt;

        wx = detrend(wx);
        wy = detrend(wy);
        wz = detrend(wz);

        iter = iter + 1;
        err1 = sqrt(mean((Wx-wx).^2));
        err2 = sqrt(mean((Wy-wy).^2));
        err3 = sqrt(mean((Wz-wz).^2));
        e1 = max([err1 err2 err3]);
        fprintf('Iteration number: %d',iter)
        disp(e1)
        err = abs(E1-e1);
    else
        break
    end
end

ax2 = ax0-wdy*r2(3)+wdz*r2(2)-wx.*(wy*r2(2)+wz*r2(3))+...
    r2(1)*(wy.^2+wz.^2);
ax1 = ax0+wdz*r1(2)-wx.*wy*r1(2);
```

```
ay1 = ay0+r1(2)*(wz.^2+wx.^2);

end
```

E.3 Rigid body motion

rbm.m

```
function [axp,ayp,azp] = rbm(ax0,ay0,az0,wx,wy,wz,wdx,wdy,wdz,rp)
% Developed by Brendan Guy Boulle (15609804)
% Stellenbosch University
% Department of Mechanical and Mechatronic Engineering
% Sound and Vibration Research Group
% 2015
%
% Determines the unknown linear acceleration at Point p with the
% following inputs;
%   Angular velocity (wx, wy and wz)
%   Angular acceleration (wdx, wdy and wdz)
%   Linear acceleration of Point 0 (ax0,ay0 and az0)
%   Cartesian coordinates of Point p relative to Point 0 (rp)
%   The angular velocity and acceleration are determined using
%   "modified_6_acc_array.m"

axp = ax0+wdy*rp(3)-wdz.*rp(2)+wx.*(wy*rp(2)+wz*rp(3))-...
    rp(1)*(wy.^2+wz.^2);
ayp = ay0+wdz*rp(1)-wdx.*rp(3)+wy.*(wz*rp(3)+wx*rp(1))-...
    rp(2)*(wz.^2+wx.^2);
azp = az0+wdx*rp(2)-wdy.*rp(1)+wz.*(wx*rp(1)+wy*rp(2))-...
    rp(3)*(wx.^2+wy.^2);

end
```